

Cover Page



Universiteit Leiden



The handle <http://hdl.handle.net/1887/44777> holds various files of this Leiden University dissertation.

Author: Dissel, M.D. van

Title: Exploring and exploiting the mechanism of mycelial pellet formation by *Streptomyces*

Issue Date: 2016-12-12

Exploring and exploiting the mechanism of mycelial pellet formation by *Streptomyces*

*Cover Image: **The Human Aggregate.** Dino van Dissel, 2016*

Cover & layout design: Dino van Dissel

Printed by: Ridderprint BV, Ridderkerk, the Netherlands



Funding Statement: This research was supported by the Dutch Technology Foundation STW, which is part of the Netherlands Organisation for Scientific Research (NWO) and partly funded by the Ministry of Economic Affairs (project number 10379)

Exploring and exploiting the mechanism of mycelial pellet formation by *Streptomyces*

Proefschrift

ter verkrijging van

de graad van Doctor aan de Universiteit Leiden,

op gezag van Rector Magnificus prof.mr. C.J.J.M. Stolker,

volgens besluit van het College voor Promoties

ter verdediging op 12 december 2016

klokke 11:15 uur

door

Marius Dino van Dissel

Geboren te Amsterdam, Nederland

5 maart 1985

Promotor:

Prof. dr. G.P. van Wezel

Promotiecommissie:

Prof. dr. H.P. Spaink

Prof. dr. A.H. Meijer

Prof. dr. ir. M.C.M. van Loosdrecht

Prof. dr. J. Anné

Prof. dr. P.J. Punt

Contents

| | | |
|------------------|---|-----|
| Chapter 1 | General Introduction | 9 |
| Chapter 2 | Morphogenesis of <i>Streptomyces</i> in submerged cultures | 15 |
| Chapter 3 | A novel locus for mycelial aggregation forms a gateway to improved <i>Streptomyces</i> cell factories | 41 |
| Chapter 4 | Hyphal aggregation and surface attachment of <i>Streptomyces</i> is governed by extracellular poly- β -1,6- <i>N</i> -acetylglucosamine | 59 |
| Chapter 5 | Control of pellet morphology by altering the timing of <i>matAB</i> transcription | 79 |
| Chapter 6 | Morphology-driven downscaling of <i>Streptomyces lividans</i> to micro cultivation | 95 |
| Chapter 7 | General discussion | 107 |
| | Nederlandse samenvatting | 115 |
| | References | 123 |
| | Curriculum Vitae | 153 |
| | Publications | 155 |

1

General Introduction

FROM NATURE'S CHEMISTS TO INDUSTRIAL WORKHORSES

Although these days the *Streptomyces* genus is mainly studied for its diverse natural products, when these multicellular soil bacteria were first isolated from nature, people were mostly interested in their particular morphology (Hopwood, 2007). As the visual characteristics were like miniature filamentous fungus people thought that these organisms could represent a group phylogenetically positioned between bacteria and fungi (Figure 1, left). This idea is reflected in their name which literally translates as “twisted fungi”.

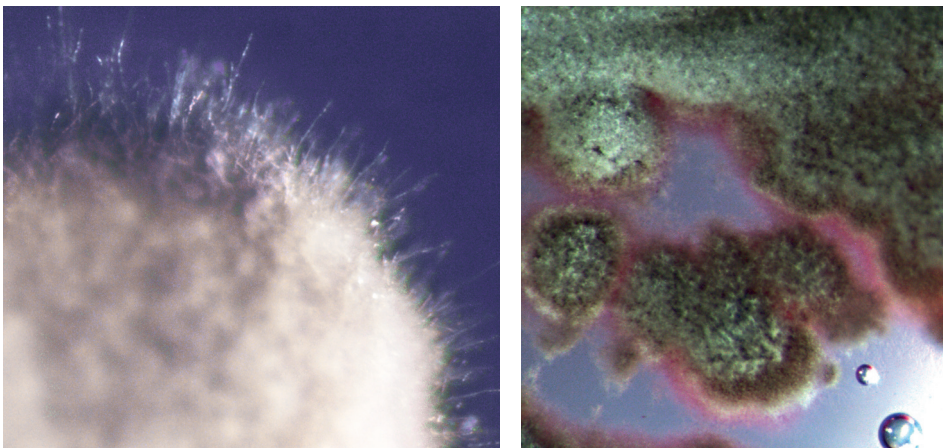


Figure 1. *Streptomyces coelicolor* growing on a soyflour manitol agar medium. The hair like treads of the spore forming hyphae can be clearly visual protruding from the colony (left). *S. coelicolor* produces pigmented antibiotics which can be seen difusing into the media (right).

Streptomyces, and other filamentous members of the *Actinomycetales* order don't grow like most bacteria by dividing in the middle, but instead grow by the combination of tip extension and lateral branching, forming a multicellular tread-like network in the soil. The multinucleoid hyphae are compartmentalized by cross-walls and form spores as an ultimate strategy for survival. The vegetative mycelium secretes a wide range of proteo- and cellulolytic enzymes allowing assimilation of plant matter and is capable of producing a wide range of antibiotics to fight off competitors (Figure 1, right). Established as a bacterium in the 19th century, it took until 1943, with the discovery of the antibiotic streptomycin as a drug for the treatment of tuberculosis, that research into these bacteria really took off (Schatz *et al.*, 1944). It was soon realized that no other group of organisms produces so many biologically active compounds as the streptomycetes, which includes over 50% of all known antibiotics, as well as many natural products with anticancer, antifungal and immunosuppressant activity. In addition, these bacteria produce a multitude of industrial enzymes, used among others as additive to washing detergent or for the production of bioethanol (Vrancken & Anne, 2009).

A COMPLEX MORPHOLOGY DURING SUBMERGED GROWTH

Despite their relevance, industry does not prefer *Streptomyces* as biotechnological production platform. Industrial production occurs most efficiently in large bioreactors, during which these organisms are cultivated in liquid media. The filamentous life style of streptomycetes challenges the fermentation process. The long hyphae are at risk of breaking in the turbulent mixing environment, causing cell lysis. Entanglement of the individual hyphae leads to large increases in viscosity, lowering maximal productivity (Figure 2, left). And in some cases the mycelial network can aggregate into dense self-immobilized granules, often called pellets (Figure 2, right). These biofilm-like structures

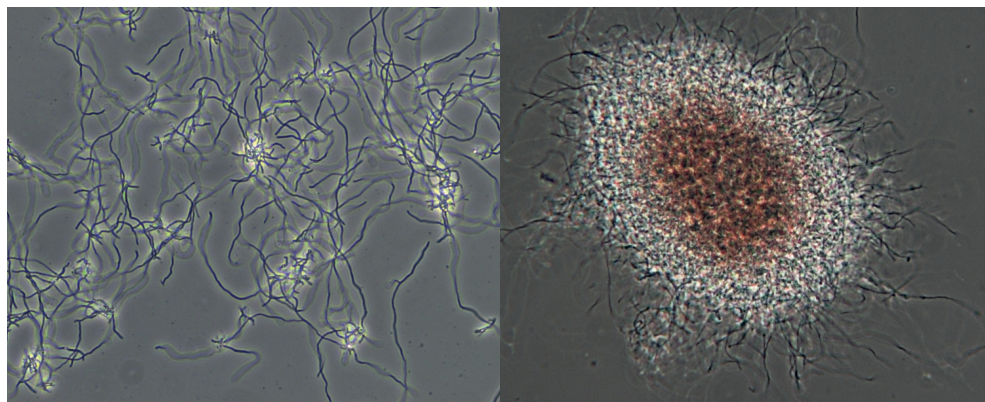


Figure 2. *S. clavuligerus* growing dispersed as a mycelial mat (left) versus *S. coelicolor* growing as pellet (Right). In general dispersed growth results in faster growth, but pellets could induce the developmental cycle and antibiotic production, indicated by the red pigmented antibiotic undecylprodigiosin which seems to originate from the core of a pellet.



limit mass transfer to the interior of the pellet, which decreases the average growth rate and elongates the fermentation time. Not only does the morphology of filamentous microorganisms negatively affect process dynamics, but also product formation depends on the morphology in a so far poorly understood fashion. In general terms, for the production of proteins it seems best to have a non-aggregating, dispersed morphology (van Wezel *et al.*, 2006, van Dissel *et al.*, 2015), but for the production of antibiotics pellets can be beneficial (Martin & Bushell, 1996, López *et al.*, 2005). Because product formation and morphology are tightly linked it is key to gain control over their morphology, both in order to improve our understanding about this link and to enable morphology-driven product optimization. This thesis provides new insights and methods to control *Streptomyces* morphology with the purpose of increasing the fermentability and productivity of these bacteria.

An overview of the current knowledge of the link between morphology and productivity and how morphology is controlled by a combination of environmental factors and the genetic components that affects morphology is reviewed in detail in **Chapter 2**.

REVERSE ENGINEERING OF MORPHOGENESIS

To improve growth of streptomycetes in an industrial setting it is desirable to get more control over their morphology. To achieve this, random strain improvement is still applied regularly, as it can efficiently create favorable phenotypes without the requirement of an understanding of the system. Although this requires little upfront knowledge, it is labor intensive, time consuming and nontransferable to other strains. Unravelling the genetic mechanism of such mutants, helped by increasingly affordable next-generation sequencing techniques, is a great way to discover the genomic changes that lie at the heart of a given phenotype. **Chapter 3** presents the results of the reverse engineering the genetics of a mutant with improved growth characteristics in a bioreactor, leading to the discovery of *matA* and *matB*, a two gene loci required for pellet formation. Removal of these genes in wild-type *Streptomyces lividans* yielded a strain that no longer formed pellets and was superior in terms of growth rate and heterologous enzyme production.

ELUCIDATING A BACTERIAL GLUE

After the discovery of the *matAB* locus we investigated the underlying mechanism by which these genes contribute to pellet formation. Bioinformatics analysis of the MatB protein suggested that it produced an extracellular polysaccharide. Extracellular polysaccharides are well known mediators of adhesion in biofilm systems, where they can take up 90% of the biomass (Branda *et al.*, 2005). A biofilm is a multicellular community that is 'glued' to a (a)biotic surface via a self-produced extracellular matrix. Polysaccharides, often charged, are an essential component to keep the biofilm community together. Although *Streptomyces* pellets do not follow the definition of a biofilm as a "surface-attached multicellular community", many similarities exist, as underlined by the dependence of hyphal attachment

on extracellular polysaccharides. With a variety of techniques, we demonstrated that the MatB protein catalyzes the formation of poly-N-acetylglucosamine (PNAG), which functions as a bacterial glue connecting neighboring hyphae. Earlier work had already identified that CslA and GlxA are cooperatively involved in the formation of a cellulose-like glycan, which is also required for pellet formation (de Jong *et al.*, 2009b, Xu *et al.*, 2008, Chaplin *et al.*, 2015). Now we show that the glycan produced by CslA and GlxA is mainly involved in mediating hydrophobic interactions, while the PNAG polymer is more tailored towards hydrophilic interactions. Finally, it was also shown that the introduction of the *mat* genes is sufficient to induce pellet formation in species that lack these genes, demonstrating the applicability to other *Streptomyces* species. The results of this study can be found in **Chapter 4**.

FURTHER STEPS TOWARDS SYNTHETIC MORPHOLOGY

As described in **Chapter 3**, the dispersed morphology of the *matAB* null mutant dramatically increases the growth rate compared to the pelleting wild-type strain. This is counterbalanced by a steep rise in viscosity, resulting from entangling of dispersed hyphae. High viscosity reduces mixing rates, lowering oxygen and heat transfer and elongating mixing times, all of which are negative for productivity. Production of PNAG by MatAB can be harnessed to modify the mycelial morphology during growth. In **Chapter 5** we describe the application of altered *mat* gene expression in order to balance growth rate and rheology. By placing the *mat* locus under the control of promoters that are activated just before the culture enters the stationary growth phase we could alter the morphological profile in a growth phase depended manner. This gave strains that maintained a maximal growth rate equal to that of the *matAB* null mutant, but which aggregated late in the exponential growth phase, limiting the rise in viscosity.

MORPHOLOGY-DRIVEN DOWNSCALING BY ENVIRONMENTAL CONTROL

As stated above, morphology is the result of both the genetic makeup of a strain and its environment. The effect of the environment on morphology, in the form of agitation intensity, is presented in **Chapter 6**. Here we attempted to control the morphology in 100 μ L micro-cultures. Growth in such small volumes is often desirable from a (high throughput) screening perspective, but at the same time often problematic when growing filamentous actinomycetes, due to their complex mycelia and the dependence of product formation on morphology. For example, the search for new antibiotics, which requires screening of thousands of strains under many different conditions, which would be greatly facilitated by small culture volumes, reducing space and costs.

With the help of whole-slide imaging combined with automated image analysis, morphologically relevant parameters could be quantified and compared. We show that fine-tuning the agitation intensity is essential to mimic the morphology obtained in shake flasks

and also show that good levels of production of heterologous enzymes and antibiotics can be achieved in 100 μ L cultures.

Finally, the results described in this thesis and their implications for industrial application of *Streptomyces* as production platform are discussed in **Chapter 7**.



2

Morphogenesis of *Streptomyces* in submerged cultures

This chapter was published as:

van Dissel, D., Claessen, D., & van Wezel, G. P. (2014). *Adv. Appl. Microbiol.*, 89, 1-45.

ABSTRACT

Members of the genus *Streptomyces* are mycelial bacteria that undergo a complex multicellular life cycle and propagate via sporulation. Streptomycetes are important industrial microorganisms, as they produce a plethora of medically relevant natural products, including the majority of clinically important antibiotics, as well as a wide range of enzymes with industrial application. While development of *Streptomyces* in surface-grown cultures is well studied, relatively little is known of the parameters that determine morphogenesis in submerged cultures. Here, growth is characterized by the formation of mycelial networks and pellets. From the perspective of industrial fermentations, such mycelial growth is unattractive, as it is associated with slow growth, heterogeneous cultures and high viscosity. Here, we review the current insights into the genetic and environmental factors that determine mycelial growth and morphology in liquid-grown cultures. The genetic factors include cell-matrix proteins and extracellular polymers, morphoproteins with specific roles in liquid culture morphogenesis, with the SsgA-like proteins as well-studied examples, and programmed cell death. Environmental factors refer in particular to those dictated by process engineering, such as growth media and reactor set-up. These insights are then integrated to provide perspectives as to how this knowledge can be applied to improve streptomycetes for industrial applications.



1. INTRODUCTION

Streptomycetes are filamentous bacteria that belong to the phylum of actinobacteria. These medically and industrially highly relevant microorganisms are producers of over half of the antibiotics used in the clinic today as well as of a plethora of other natural products, such as anticancer, immunosuppressive, antifungal and antihelminthic agents (Baltz, 2007, Baltz, 2008, Olano *et al.*, 2009, Hopwood, 2007). Furthermore, streptomycetes are saprophytic bacteria that grow on almost any natural polymer, and as such are a rich source of industrial enzymes (Bhosale *et al.*, 1996, Tokiwa & Calabia, 2004, Vrancken & Anne, 2009, Yikmis & Steinbüchel, 2012). Unlike most other bacteria, streptomycetes are non-planktonic and grow as a mycelium consisting of a network of closely interwoven hyphae. Exponential growth is thereby achieved by a combination of tip extension and branching. The multigenomic hyphae are divided by occasional cross-walls, which makes *Streptomyces* a rare example of a multicellular prokaryote (Claessen *et al.*, 2014). When nutrient availability becomes limiting, streptomycetes initiate a complex developmental program, which leads to morphological and chemical differentiation (Chater & Losick, 1997, Flärdh & Buttner, 2009). At this stage, aerial hyphae are formed that are coated with water-repellent proteins to allow them to break through the aqueous soil surface and grow into the air (Wösten & Willey, 2000, Claessen *et al.*, 2006). Eventually the aerial hyphae differentiate into chains of unigenomic spores, following a spectacular cell division process whereby some one hundred septa are produced in a very short time span (Schwedock *et al.*, 1997, Jakimowicz & van Wezel, 2012). Genes that are involved in the onset of aerial mycelium formation are designated bald (*bld*) genes, characterized by the bald appearance of mutants due to their failure to produce the fluffy aerial hyphae (Merrick, 1976), and those that are essential for the formation of grey-pigmented spores are called white (*whi*) genes, characterized by the white appearance of mutants due to the lack of the WhiE spore pigment (Chater, 1972). It is important to note that most of the developmental regulators function by controlling transcription or translation. In this review, we primarily focus on the genes that control morphogenesis in submerged culture. For detailed information on the genes that control aerial hyphae formation and sporulation in surface-grown cultures we refer to excellent reviews elsewhere (Chater & Losick, 1997, Kelemen & Buttner, 1998, Flärdh & Buttner, 2009).

The timing of antibiotic production is tightly controlled with the life cycle, and many antibiotics are produced at a time correlated to the onset of morphological differentiation (Bibb, 2005, van Wezel & McDowall, 2011, Liu *et al.*, 2013a). Mutants that are blocked in development (so-called *bld* mutants) therefore typically fail to produce antibiotics (Bibb, 2005). The onset of development and antibiotic production coincides with the autolytic dismantling of the vegetative mycelium, necessary to provide nutrients as building blocks for the aerial mycelium, in a process strongly resembling programmed cell death (Fernández & Sánchez, 2002, Manteca *et al.*, 2006b).

Industry-level production of secondary metabolites and enzymes occurs in bioreactors, and industrial exploitation of streptomycetes is hampered by the formation of large mycelial

networks or clumps, which is unattractive from the perspective of process engineering (Braun & Vecht-Lifshitz, 1991, Hodgson, 2000, van Wezel *et al.*, 2009). Compared to fermentations with unicellular microorganisms such as *Saccharomyces cerevisiae*, *Escherichia coli* or *Bacillus subtilis*, the more complex morphology of streptomycetes puts constraints on the ability to maximize product yields (Wucherpennig *et al.*, 2010). Entanglement of mycelia increases the viscosity of the broth, which lowers the transfer rates of nutrients and gasses, and because many strains have the tendency to aggregate into pellets a part of the biomass might be shielded from the supply of nutrients altogether. To further complicate matters, optimal productivity is tied to morphology in a product-specific manner, meaning that often less favored conditions have to be accepted for optimal productivity (Martin & Bushell, 1996, Wardell *et al.*, 2002, van Wezel *et al.*, 2006, Anné *et al.*, 2014).

We are only beginning to unravel the mechanisms that control morphogenesis of streptomycetes, and this is particularly true for mycelial growth in submerged cultures. At the same time, understanding the correlation between morphogenesis and productivity is of critical importance for the exploitation of streptomycetes in the industrial domain. In this review we present an overview of the current literature on the morphogenesis of streptomycetes in liquid-grown cultures and look at how this may be translated to better match morphology and productivity during industrial fermentations.

2. MORPHOGENESIS IN SUBMERGED CULTURES

2.1 Hyphal growth

Active growth of streptomycetes typically starts with spore germination. The spore is not only a means for dispersal but also serves as a way to survive a period of adverse environmental conditions. Once the conditions become favorable for growth, spores typically establish two germ tubes at the polar sides, which grow out to become young vegetative hyphae. The molecular steps responsible for the emergence of germ tubes have not yet been identified, and surprisingly little is known about this germination process. One reason may be that it is difficult to differentiate between early signaling events for the onset of germination and essential metabolic and housekeeping activities that relate to early growth. Spore germination is controlled by the cyclic-AMP receptor protein Crp (Derouaux *et al.*, 2004, Piette *et al.*, 2005), but Crp also controls antibiotic production (Gao *et al.*, 2012). A major consequence of the absence of Crp was the production of a very thick spore wall, which was identified as a likely cause for the germination delay (Piette *et al.*, 2005). The correlation between cell-wall hydrolysis and the speed of germination was further supported by the delayed germination in the absence of the cell-wall hydrolase RpfA (Haiser *et al.*, 2009). Another cell wall-associated protein that relates to germination is NepA, originally identified as a protein that localizes to the 'subapical stem', which connects vegetative with aerial hyphae during early development (Dalton *et al.*, 2007). Deletion of nepA results in altered germination, which in particular occurs in a more synchronized



manner (de Jong et al., 2009a).

After germination, the hyphae grow out to form a branched network of hyphae, the vegetative mycelium. Studies in streptomycetes with compounds that are incorporated into newly synthesized peptidoglycan, such as labelled vancomycin or N-acetylglucosamine, revealed that peptidoglycan synthesis primarily occurs at hyphal tips and - therefore by definition - also at emerging branches (Gray *et al.*, 1990, Daniel & Errington, 2003). Penicillins particularly target apical sites of the hyphae, and less the lateral walls, and the latter may therefore be regarded as a relatively inert murein. During normal growth of streptomycetes cross-walls are formed in the hyphae, which do not lead to cell fission, thus resulting in long multinucleoid compartments (Chater & Losick, 1997, Flårdh & van Wezel, 2003, Jakimowicz & van Wezel, 2012). Branches are formed at sites behind the tip, and

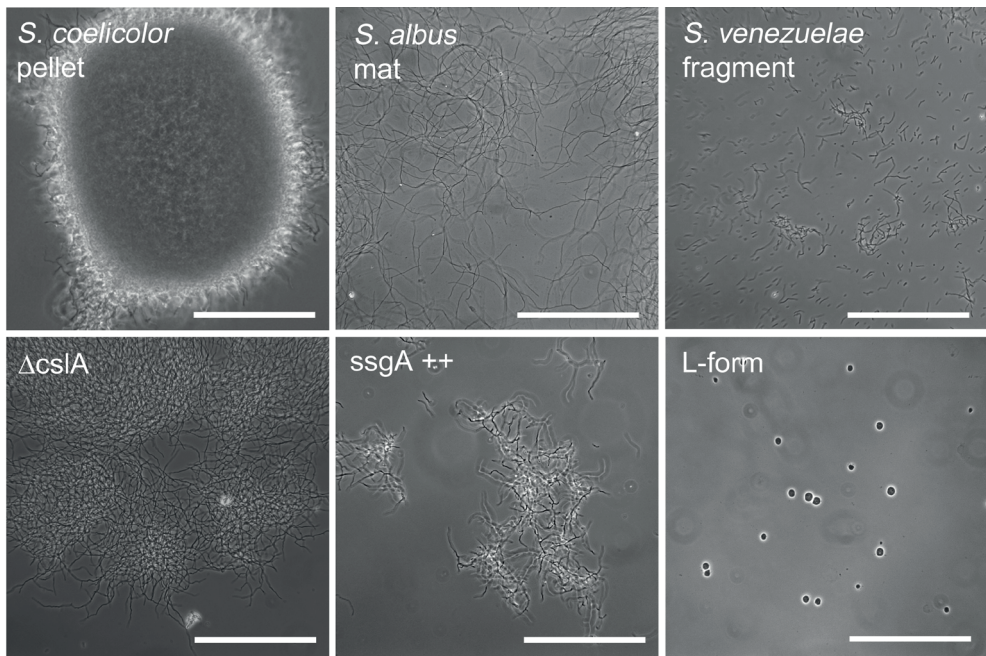


Figure 1. Distinct morphologies of *Streptomyces* species in submerged cultures. Top row: *Streptomyces* strains representing different morphologies, namely pellets (*S. coelicolor*), mycelial mats (*S. albus*) and fragments (*S. venezuelae*). Bottom row: changes in morphology due to genetic factors. Images show *cslA* null mutant (left) and *SsgA* overexpressing strains (middle) of *S. coelicolor*, and L-form cells derived from *S. viridifaciens*. Scale bar, 100 μ m.

frequently but not always adjacent to crosswalls, leading to the establishment of new cell poles, and the combination of apical growth and branching ensures exponential growth (Flårdh *et al.*, 2012).

Subsequent growth and morphology of the mycelial mass is in part species and strain-dependent. Three types of morphologies are generally distinguished in liquid-grown cultures; (1) freely dispersed mycelia, which predominantly behave like single cells with

high mass transfer properties; (2) open mycelial networks, also often called mycelial mats, which generally have good mass transfer characteristics, but increase the viscosity of the media; and (3) pellets that do not increase the viscosity significantly, but often contain a nutrient-deprived center (Paul & Thomas, 1998), Fig. 1). The wide range of morphological phenotypes, which often co-exist in the reactor, is due to the large number of variables that influence the ability of the mycelia to grow, branch, aggregate and fragment (see Section 5). The dominant type is genetically determined, and differs considerably between species and strains. For instance, *Streptomyces venezuelae* typically forms highly fragmented mycelia and sporulates in liquid cultures, *Streptomyces clavuligerus* forms mycelial mats, while *Streptomyces coelicolor* mostly forms large and dense pellets (Bewick *et al.*, 1975, van Wezel *et al.*, 2006). These differences already reveal that general predictions are difficult to make, although some genetic determinants influence morphology regardless of the strain (see below).

2.2. Submerged sporulation

Whereas major differences in mycelial architecture are observed between different streptomycetes, further complexity is caused by the capacity of some strains to form spores in liquid environments. The first report of submerged sporulation was made as early as in 1947 (Erikson, 1947). However, in 1983 Kendrick and Ensign provided a groundbreaking study on the morphology and on sporulation of *Streptomyces griseus* B-2682 in submerged culture (Kendrick & Ensign, 1983). This led to the identification of several streptomycetes that produce submerged spores, including *Streptomyces granaticolor*, *S. griseus*, *Streptomyces roseosporus* and *S. venezuelae* (Kendrick & Ensign, 1983, Daza *et al.*, 1989, Glazebrook *et al.*, 1990). These can be further subdivided into streptomycetes that only sporulate in nutrient-limiting media, such as *S. griseus* (Kendrick & Ensign, 1983), and those that produce submerged spores in nearly all media, such as *S. venezuelae* (Glazebrook *et al.*, 1990). Although until recently it was believed that the ability to produce spores in liquid cultures was something like a rarity, the possibility cannot be ruled out that in principle all streptomycetes can do so under specific conditions; indeed, a recent survey revealed that submerged sporulation is likely much more widespread than originally anticipated, with half of a random selection of over 50 streptomycetes sporulating in submerged culture at least under some growth conditions (Girard *et al.*, 2013). Interestingly, addition of high concentrations of calcium to liquid-grown cultures of *S. coelicolor* and *Streptomyces lividans* induces the occasional formation of spore-like compartments. Since phosphate starvation is an important trigger for submerged sporulation, this calcium effect was explained by the reduction of the phosphate pool (Kendrick & Ensign, 1983, Daza *et al.*, 1989, Glazebrook *et al.*, 1990), although further analysis is required to corroborate this.

There is a clear transition in the vegetative hyphae prior to submerged sporulation: the hyphae thicken, and widened club-like structures or 'pre-conidia' are produced at the apical sites of the hyphae (Biró *et al.*, 1980, Rueda *et al.*, 2001a). Comparison of thin sections



of aerial and submerged spores by transmission electron microscopy (TEM) showed that the cell walls of surface-grown spores are thicker than those of submerged spores, with a width of approximately 40 nm and 25 nm, respectively (Kendrick & Ensign, 1983). However, aerial and submerged sporogenic hyphae of *Streptomyces brazilensis* by TEM show strong similarity (Rueda *et al.*, 2001b), with the main difference in the appearance of the sheath around the hyphae, which was thinner and less structured in sporogenic vegetative hyphae, perhaps due to a difference in the rodlet layer (Gebbinck *et al.*, 2005).

While sporulation of streptomycetes is typically studied in surface-grown cultures, the study of sporulation in submerged cultures is an attractive alternative for several reasons. First of all, culturing time is much shorter, and synchronous sporulation can be more readily achieved. Sporulation of *S. griseus* is induced by transferring the strain from rich to nutrient-limited media, whereby sporogenic hyphae become evident within a few hours and then continue to elongate until septation occurs at approximately 10 h, with spores maturing over a subsequent period of 10-12 hours (Kwak & Kendrick, 1996).

In addition to the advantage of synchronization of cultures, submerged development also readily facilitates global expression profiling by systems biology approaches like transcriptome, proteome or metabolome analysis. This is exemplified by recent studies on developmental mutants in *S. venezuelae* (Bibb *et al.*, 2012, Bush *et al.*, 2013). Buttner and colleagues are currently developing *S. venezuelae* as model system for morphological differentiation for its ability to readily sporulate in both minimal and rich liquid media, and developmental (*bld*, *whi*) mutants that were studied previously in *S. coelicolor*, are being recreated in this interesting background to facilitate ‘-omics’ approaches (Mark Buttner and Maureen Bibb, pers. comm.). Submerged sporulation also allows discriminating between genes involved in the control of aerial hyphae formation and those required for sporulation-specific cell division. After all, the former is not relevant in submerged cultures, and presumably genes required for erection of aerial hyphae should not interfere with the ability to initiate sporulation-specific cell division, while the cell division process itself is likely very similar during submerged and solid culture sporulation. Thus, submerged sporulation should be a particularly good model system for studies on developmental cell division.

2.3. A special case: *Streptomyces* L-forms

Mycelial growth is a hallmark feature of streptomycetes. Production of secondary metabolites, such as antibiotics or antitumor agents, is often linked to the inherent capacity to form mycelial pellets. However, streptomycetes can also be forced to produce single cells. Treatment of mycelia with lysozyme results in the formation of protoplasts, which are identical-sized spherical cells without a cell wall used for cell fusion and plasmid transformation (Hopwood *et al.*, 1977, Bibb *et al.*, 1978)1977, Bibb<style face="italic"> et al.</style>, 1978. While protoplasts cannot propagate, streptomycetes can also form so-called L-forms (Innes & Allan, 2001). Selection of L-forms occurs by growth in the presence of lysozyme, which degrades the peptidoglycan, and penicillin, which inhibits *de novo*

peptidoglycan synthesis. Subsequent cultivations in osmotically balanced media can lead to the acquisition of mutations that allow these cells to propagate without their cell wall, even in the absence of the inducing agents (i.e. penicillin and lysozyme; (Innes & Allan, 2001, Leaver *et al.*, 2009, Mercier *et al.*, 2013). L-forms have been shown to associate with plants acting as biocontrol agents (Amijee *et al.*, 1992, Innes & Allan, 2001). The absence of a cell wall allows these pleomorphic cells to invade spaces that would otherwise be inaccessible, such as the extracellular space within plant tissue, or even inside plant cells (Paton & Innes, 1991). Biocontrol activity was shown for *Pseudomonas* and *Bacillus* species (Amijee *et al.*, 1992, Walker *et al.*, 2002, Waterhouse *et al.*, 1996), but could also be true for streptomycetes, which naturally produce a large arsenal of antifungal and antimicrobial compounds (Hopwood, 2007).

L-forms have been generated in a wide-range of unrelated bacterial species, including, amongst others, *Escherichia coli* (Glover *et al.*, 2009), *Bacillus subtilis* (Leaver & Errington, 2005), and *Listeria monocytogenes* (Dell'Era *et al.*, 2009), and also in several *Streptomyces* species, including *Streptomyces hygroscopicus*, *S. griseus*, *Streptomyces levoris* and *Streptomyces viridifaciens* (Gumpert, 1982, Gumpert, 1983, Innes & Allan, 2001; Fig. 1). L-form growth is largely driven by changes in the cell surface area to volume ratio of these cells, and is characterized by blebbing, tubulation, vesiculation and fission (Errington, 2013, Mercier *et al.*, 2013). Interestingly, division of phospholipid vesicles, which to some extent resemble empty L-forms, could merely be driven by changes in lipid composition (Peterlin *et al.*, 2009). Also, cell division of L-forms is stimulated by increased fatty acid synthesis (Mercier *et al.*, 2013), and does not require the canonical cell division machinery (Leaver *et al.*, 2009). As such, L-form proliferation could mimic how primordial cells propagated before the cell wall was invented.

The production of secondary metabolites by streptomycetes is often linked to the complex pattern of morphological development (van Wezel & McDowall, 2011). Surprisingly, stable L-forms of *S. viridifaciens* were still able to produce tetracycline, in addition to another uncharacterized green-pigmented metabolite (Innes & Allan, 2001). However, compared to the parental form the yields were relatively low. Nevertheless, the capacity of L-forms to produce secondary metabolites including antibiotics highlights their potential use as biocontrol agents.

3. MOLECULAR CONTROL OF LIQUID-CULTURE MORPHOGENESIS

3.1. The tip-organizing center and the cytoskeleton

During apical growth, DivIVA localizes close to the growing tip and its pivotal role in the control of apical growth is highlighted by the fact that it is essential for growth, while its overexpression leads to drastic changes in hyphal morphology including hyper-branching (Flårdh *et al.*, 2012, Hempel *et al.*, 2012). In *Bacillus subtilis*, DivIVA controls septum-site determination by interacting with the MinCD cell division inhibitor complex (Edwards &



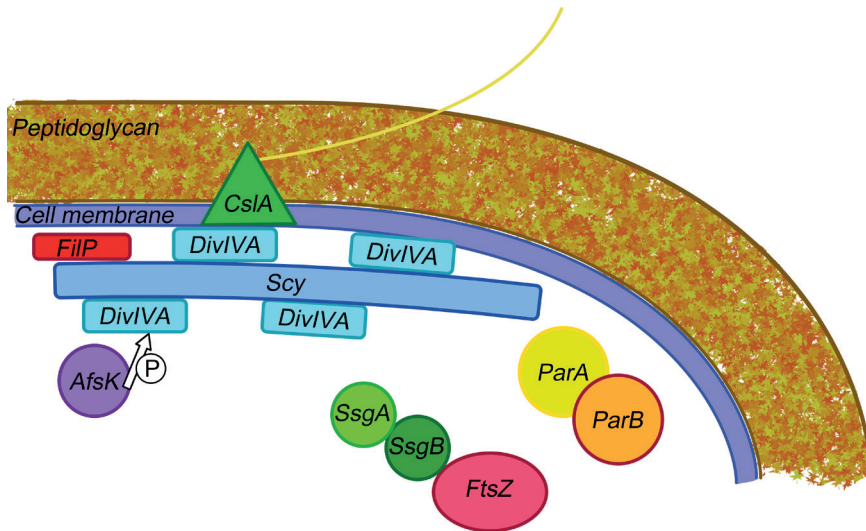


Figure 2. Components of the tip organizing center (TIPOC) of *S. coelicolor*. The TIPOC is a multi-protein complex that coordinates tip growth, cell wall synthesis, DNA replication and segregation, and cell division. DivIVA is required for peptidoglycan synthesis and interacts directly with the cytoskeletal protein Scy. The latter assists in assembly of the complex. Other members include the cellulose synthase-like protein CslA, the cytoskeletal element FiIP and SsgA, which controls processes requiring cell wall remodeling. The TIPOC interacts with the proteins involved in chromosome segregation (ParA and ParB), and probably with those involved in cell division (SsgA, SsgB and FtsZ). AfsK negatively controls the activity of DivIVA by phosphorylation. For further details and references see the text. Adapted from (Holmes *et al.*, 2013)

Errington, 1997). However, streptomycetes lack a Min system, and DivIVA has instead taken up a (yet not fully understood) role in apical growth.

DivIVA is part of a larger complex of proteins that collectively have been dubbed tip-organizing center (TIPOC; Fig. 2; (Holmes *et al.*, 2013). In recent years several proteins and protein complexes have been identified that play a role in tip growth and DNA replication. These include the *Streptomyces* cytoskeletal element Scy (Holmes *et al.*, 2013), the twin-arginine transport (Tat) secretion system (Willemse *et al.*, 2012), the cell-wall remodeling protein SsgA (Noens *et al.*, 2007) and the cellulose synthase-like protein CslA (Xu *et al.*, 2008). Furthermore, new chromosomes are also replicated close to but distinctly away from the tip in so-called replisomes (Wolánski *et al.*, 2011). The TIPOC likely ensures that all apical processes, such as DNA replication and cell wall synthesis, are carried out in coordinated fashion (Ditkowski *et al.*, 2013, Fuchino *et al.*, 2013) and that DNA is not damaged by the cell-wall synthetic machinery (K. Celler and GPvW, unpublished). The extracellular cellulose-like polymer synthesized by CslA might form an additional protective layer at the outside of the hyphal tips, thereby preventing cell damage (Chater *et al.*, 2010).

Recent evidence indicates that DivIVA is phosphorylated by the Ser/Thr protein kinase AfsK (Hempel *et al.*, 2012). The C-terminal part of DivIVA has multiple sites for phosphorylation, and the level of phosphorylation increases dramatically when cell-wall

synthesis is arrested (Hempel *et al.*, 2012). Increased phosphorylation coincided with the disappearance of DivIVA from the hyphal tips, followed by the emergence of new lateral branches. Under normal growth conditions, branches are formed by a so-called tip-splitting mechanism, in which new foci of DivIVA originate from existing foci (Richards *et al.*, 2012). Consistent with the observation that DivIVA is required for apical growth, it is recruited to branch sites to allow the start of apical growth.

The cytoskeleton of streptomycetes is highly complex, with likely over ten different cytostructural proteins (recently reviewed in (Celler *et al.*, 2013)). The Scy protein acts in close collaboration with DivIVA in establishing growth polarity (Holmes *et al.*, 2013). In contrast to *divIVA*, *scy* can be deleted, which has a pronounced effect of hyphal morphology. Notably, in the absence of Scy hyphal tips were often branching, leading to a tip-splitting phenotype and aberrant hyphal geometry. The Scy protein is a large 1326 amino acid (aa) protein with a high propensity to form coiled-coil structures. *In vitro* experiments indicated that this protein forms long filaments, which potentially act as a scaffold for the assembly of the TIPOC. Indeed, Scy not only interacts with DivIVA, but also with the chromosome-partitioning protein ParA (Ditkowski *et al.*, 2013) and with the intermediate filament-like protein FilP, encoded by a gene immediately downstream of *scy* (Bagchi *et al.*, 2008, Holmes *et al.*, 2013). FilP also interacts with DivIVA, which indicates that these three proteins together form a large polar assembly that likely plays a role in the spatial and temporal control of apical growth (Fig. 2). Interestingly, during sporulation of *B. subtilis* DivIVA interacts with the chromosome segregation machinery, to aid in positioning the *oriC* region of the chromosome at the cell pole, in preparation for polar division (Thomaides *et al.*, 2001). Considering the polar interaction with ParA, this functionality of DivIVA is retained in streptomycetes.

3.2. Extracellular polymers and pellet morphology

Multicellular structures are typically held together by an extracellular matrix (Branda *et al.*, 2005, McCrate *et al.*, 2013, Vlamakis *et al.*, 2013). Although the composition of these matrices are diverse between different organisms, they typically contain, amongst others, proteins, polysaccharides, and extracellular DNA (White *et al.*, 2002, Zogaj *et al.*, 2003, Gebbink *et al.*, 2005, Claessen *et al.*, 2014). The matrix contributes to structural integrity of the multicellular community, while simultaneously providing protection against various stresses (Scher *et al.*, 2005, Romero *et al.*, 2010, DePas *et al.*, 2013). While matrices are usually mentioned in the context of biofilms, streptomycetes also make extracellular substances that contribute to morphology. Kim and Kim (2004) already demonstrated that pellets of *S. coelicolor* were susceptible to DNase treatment. In addition to extracellular DNA (eDNA), a role for hyaluronic acid in pellet integrity was proposed. Interfering with these matrix components made pellets fragile, leading to their (partial) disintegration (Kim & Kim, 2004). These data lead to a model in which an extracellular matrix, consisting of at least eDNA and hyaluronic acid, contributes to morphology of *Streptomyces* pellets by acting as



an adhesive. The eDNA component of this matrix is probably released in the environment during programmed cell death occurring in the central part of the pellet, and trapped within the pellet core.

Another component of such an extracellular matrix is the polymer produced by the cellulose synthase-like protein CslA (Xu *et al.*, 2008, de Jong *et al.*, 2009b). CslA was discovered as an interaction partner of DivIVA (Xu *et al.*, 2008). CslA is conserved in streptomycetes, and synthesizes a polymer consisting of β -(1-4) glycosidic bonds, consistent with a cellulose-like polymer, at hyphal tips and branch sites. The exact nature of the polysaccharide is still unclear. Deletion of the *cslA* gene has a pronounced effect on the morphology of liquid-grown mycelia, with a much more dispersed growth than wild-type cells (Fig. 1; (Xu *et al.*, 2008). This suggests that the polymer produced by CslA contributes to pellet architecture, perhaps by acting as an adhesive. Interestingly, deletion of the downstream-located gene *glxA*, which encodes a putative galactose-like oxidase, also results in an open mycelial morphology (our unpublished data), and GlxA may modify the CslA-synthesized polysaccharide. Indeed, both genes are transcriptionally coupled under most growth condition (Xu *et al.*, 2008, Liman *et al.*, 2013).

CslA is required for the hyphal attachment to surfaces (de Jong *et al.*, 2009b). This attachment coincides with the formation of an extracellular matrix, which is characterized by fimbrial structures that protrude from the cell surface of the adhering hyphae. Notably, while the absence of CslA had no visible effect on the number of fimbriae, their connection to the cell surface was considerably weakened. Further characterization of these fimbriae indicated that they were largely composed of bundled amyloid fibrils of so-called chaplin proteins (de Jong *et al.*, 2009b). Without chaplins, much thinner fibrils were observed that were susceptible to treatment with cellulase. This enzyme could also release wild-type fimbriae from the cell surface. This led to a model in which the CslA-produced polysaccharide provides a scaffold for fimbriae formation, while also contributing to their anchoring. It is tempting to speculate that the formation of pellets is also mediated via attachment and aggregation. Rather than connecting hyphae to surfaces, fimbriae would now mediate interactions between adjacent hypha, leading to a compact pellet structure. Consistent with this idea is the observation that the formation of pellets is not only disturbed without *cslA*, but also in the absence of chaplins (M.L.C. Petrus and D.C., unpublished data).

3.3. Proteins that control liquid-culture morphogenesis

Presently, there is relatively little known of the proteins that are specifically involved in the control of submerged sporulation. Indeed, scanning the literature shows that of the close to 500 publications on the topic of sporulation of *Streptomyces*, and fewer than 20 of those are primarily dedicated to the biology of submerged sporulation (PubMed search as of February 2014). The first studies into proteins that control submerged sporulation were done in the mid 90s of the previous century. Comparison of protein expression profiles between liquid-grown cultures prior to and at the onset of submerged sporulation identified

a 52 kDa sporulation-specific protein, designated EshA (for extension of sporogenic hyphae), as a cyclic nucleotide binding protein that is expressed during the first 12 hours of submerged sporulation and that is required for growth of sporogenic hyphae at an early stage of morphogenesis of *S. griseus* (Kwak & Kendrick, 1996). Interestingly, while *eshA* null mutants were inhibited in the elongation of sporogenic hyphae from new branch points in submerged culture, spore chains were instead formed ectopically in vegetative hyphae, apparently by accelerating septation and spore maturation at the pre-existing vegetative filaments (Kwak & Kendrick, 1996). This suggests that EshA is required for growth of sporogenic hyphae but not for sporulation *per se*. Saito, Ochi and colleagues demonstrated that EshA also plays a role in the control of antibiotic production, whereby deletion of *eshA* inhibits production of actinorhodin but not of prodigiosins in *S. coelicolor* (Kawamoto *et al.*, 2001) and streptomycin production in *S. griseus* (Saito *et al.*, 2003b). Furthermore, *eshA* is conditionally required for sporulation on surface-grown cultures of *S. griseus*, but not for *S. coelicolor* (Saito *et al.*, 2003b). Interestingly, EshA forms larger protein complexes, potentially forming icosahedron-like structures. While the protein and its orthologue MMPI of *Mycobacterium leprae* were reported to be membrane-associated (Winter *et al.*, 1995, Kwak *et al.*, 2001), consistent with the presence of putative transmembrane helices, at least the multimeric complexes were primarily identified in the cytoplasm of *S. griseus* (Saito *et al.*, 2003b). While the exact role of EshA is still unclear, large amounts of dNTPs accumulate in *eshA* null mutants, coinciding - and consistent - with strongly reduced rates of DNA synthesis, in particular at a time coinciding with the onset of development (Saito *et al.*, 2003b). It therefore seems likely that EshA plays a role in the activation of DNA synthesis during the onset of sporulation-specific cell division. It should be noted that *eshA* lies immediately upstream of the genes for synthesis of the volatile organic compound (VOC) 2-methylisoborneol (Wang & Cane, 2008), and analysis in String (www.string-emb.l.de) reveals strong phylogenetic linkage to the gene encoding the germacradienol/geosmin synthase *GeoA*, which synthesizes the VOC geosmin (Gust *et al.*, 2003a). It is yet unclear what the functional relevance is of this surprising linkage between EshA and VOC biosynthetic genes in streptomycetes.

Another protein with major impact on liquid-culture morphology is HyaS, which affects pellet morphology and integrity (Koebsch *et al.*, 2009). This protein is conserved in streptomycetes, and produced in liquid-grown cultures. HyaS associates with substrate hyphae and induces tight fusion-like contacts between hyphae (Koebsch *et al.*, 2009). Deletion of *hyaS* in *S. lividans* resulted in irregularly shaped pellets, which were less dense than those of the parental strain. Interestingly, the C-terminal part of the HyaS protein possesses amine oxidase activity, which is required for normal pellet morphology. Koebsch and colleagues speculate that this enzyme activity might induce cross-linking with other hyphae-associated protein(s) or compounds, in a similar manner as the eukaryotic cell surface-located lysyl oxidases are involved in matrix remodeling (Lucero & Kagan, 2006).

On searching for proteins that were able to suppress hypersporulation of a spontaneous



S. griseus mutant at high copy number, Kawamoto and Ensign identified SsgA as an important submerged sporulation-related protein (Kawamoto & Ensign, 1995). It was soon discovered that SsgA functions by stimulating fragmentation of hyphae by activating septum formation (Kawamoto *et al.*, 1997), and SsgA is required for both solid- and liquid-culture sporulation of streptomycetes (Jiang & Kendrick, 2000, van Wezel *et al.*, 2000a, Yamazaki *et al.*, 2003). On solid media, *SsgA* null mutants display a conditional “white” (non-sporulating) phenotype, as they are able to produce spores on mannitol-containing medium, but not in the presence of glucose (Jiang & Kendrick, 2000, van Wezel *et al.*, 2000a). Although many early developmental (*bld*) mutants are carbon source-dependent (Merrick, 1976, Pope *et al.*, 1996), such dependence is very rare among *whi* mutants and this may reflect the fact that SsgA also controls submerged sporulation by sporogenic vegetative hyphae. The function of SsgA is discussed in detail in the next section.

It is likely that more genes are involved in the control of morphogenesis. For example, non-pelleting mutants were obtained after selection for such a phenotype in continuous cultures (Roth *et al.*, 1985), and previous work identified several spontaneous mutants of *S. griseus* that were affected specifically in submerged sporulation (Kawamoto & Ensign, 1995, Kwak & Kendrick, 1996). Apparently, such mutants are readily obtained, and many have not yet been characterized, strongly suggesting that much is yet to be learned about proteins that control submerged morphogenesis.

3.4. Surface modification of *Streptomyces* spores

Streptomyces spores formed in submerged cultures are decorated by a pattern of pairwise aligned rods, called the rodlet layer (Claessen *et al.*, 2004). This layer, which apparently forms the same mosaic as that found on aerial spores, renders the surface of spores hydrophobic. Assembly of the rodlet layer involves two classes of proteins, rodlins (Claessen *et al.*, 2002) and chaplins (Claessen *et al.*, 2003, Elliot *et al.*, 2003). The chaplin proteins form the main building blocks of the rodlet layer, by assembling into thin fibrils that are aligned by the rodlin proteins into wild-type rodlets (Petrus & Claessen, 2014). Indeed, without rodlins the chaplin fibrils are randomly deposited on the spore surface. Recent evidence indicates that chaplins self-assemble into an asymmetric fibrillar membrane when confronted with a hydrophobic-hydrophilic interface (Bokhove *et al.*, 2013, Ekkers *et al.*, 2014). The hydrophilic side of this membrane is relatively smooth, while the hydrophobic side has a fibrillar appearance. While such an interface is present when hyphae grow out of the aqueous environment into the hydrophobic air, it is absent in sporogenic hyphae formed in liquid, such as those of *S. griseus* or *S. venezuelae*. This strongly implies that other factors contribute to the assembly process, at least in liquid environments. This is not uncommon for other fibril-forming proteins, including the fungal equivalents of the chaplins, called hydrophobins (Wösten, 2001). Here, the assembly of the SC3 hydrophobin from the filamentous fungus *Schizophyllum commune* is stimulated by schizophyllan, one of the glycans present in the cell wall (Scholtmeijer *et al.*, 2009). Also, SC3 assembly could

be induced when the concentration of the monomers was increased. In fact, this makes it tempting to speculate that the schizophyllan binds to hydrophobin monomers, which locally increases the concentration thereby initiating self-assembly. Notably, the polymer produced by CslA at the hyphal tip could have a similar role, which in particular in liquid environments could be critical (Xu *et al.*, 2008, de Jong *et al.*, 2009b, Chater *et al.*, 2010). However, this awaits further experimental evidence.

4. THE SSGA-LIKE PROTEINS

4.1. SsgA-like proteins and morpho-taxonomy of actinomycetes

SsgA is a small 15 kDa protein that has so far only been found in the streptomycetaceae *Streptomyces* and *Kitasatospora*. Homologues of SsgA - the SsgA-like proteins or SALPs - are found in all of what may be considered as morphologically complex actinomycetes, with a suggestive correlation between the number of SALPs and the number of spores produced per spore chain: species producing single spores (*e.g.* *Micromonospora*, *Salinispora*) typically have a single SALP, those producing short spore chains (*e.g.* *Saccharopolyspora*) typically have two SALPs and those forming spore chains (*Streptomyces*) or sporangia (*Frankia*) have multiple SALPs (Girard *et al.*, 2013, Traag & Wezel, 2008). Members of the SALP family of proteins are typically between 130-145 aa long, with 30-50% aa identity between the different family members. *S. coelicolor* contains seven SALPs (SsgA-G; (Noens *et al.*, 2005), of which SsgA, SsgB and SsgG play a role in septum-site localization. SsgB is the archetypal SALP and functions by recruiting FtsZ to septum sites during the onset of sporulation-specific cell division (see below). The crystal structure of SsgB from *Thermobifida fusca* (Xu *et al.*, 2009) revealed a bell-shaped trimer with - surprisingly - strong similarity to the structure of mitochondrial RNA binding proteins MRP1 and MRP2 (Schumacher *et al.*, 2006) and ssDNA binding protein PBF-2 (Desveaux *et al.*, 2002). Recently, a novel structural homologue of SsgB was identified in the spirochete *Borrelia burgdorferi*, a pathogen that causes lyme borreliosis (Bhattacharjee *et al.*, 2013). The *B. burgdorferi* OspE protein recruits the complement regulator FH onto the bacterial cell wall, which then results in immune evasion (Bhattacharjee *et al.*, 2013). Suggestively, as discussed below SsgB also functions by recruiting a protein, in this case FtsZ to the site of cell division (Willemse *et al.*, 2011).

SsgB is extremely well conserved in streptomycetes, with typically a maximum of one amino acid change between the orthologues, while at the same time the homology between orthologues in different genera is low (around 40% amino acid identity). This unique feature was used as a novel taxonomic analysis of actinomycetes to complement 16S rRNA-based taxonomy (Girard *et al.*, 2013). Phylogenetic analysis of the SsgA and SsgB proteins in streptomycetes showed that on the basis of the conservation of these proteins, streptomycetes fall apart into two subclasses, which are also distinct in terms of liquid-culture morphogenesis. The first class consists of species that produce mycelial clumps but fail to produce submerged spores, which cluster in the NLSp (No Liquid-culture



Sporulation) branch, and the second form the LSp (Liquid-culture Sporulation) branch of the streptomycetes. Strikingly, *Streptomyces* species of the LSp type have an SsgB orthologue with a Thr128, while those of the NLSp type have an SsgB with Gln128. The exception to the rule is *S. avermitilis*, which (as far as we know) does not sporulate in submerged cultures, but contains SsgB variant T128. This apparently correlates with the absence in *S. avermitilis* of SsgG, which is functionally related to SsgB (GPvW, unpublished).

4.2. How does SsgA control hyphal morphogenesis?

SsgA localizes to sites where cell wall remodeling is required and in both vegetative and aerial hyphae, namely at sites for germination, branching and septum formation (Noens *et al.*, 2007). SsgA activates all of these processes, although the precise mechanism is not always clear. In terms of germination, SsgA-overexpressing strains have been shown to form on average around 2.5 germ tubes per spore (against 2.0 germ tubes per spores for the wild-type strain and 1.7 for *ssgA* null mutants), whereby even five or more germ tubes emerge from a single spore (Noens *et al.*, 2007). Secondly, enhanced expression of the protein stimulates branching, whereby many short branches are formed that fail to grow out to normal length (van Wezel *et al.*, 2000a). The best-studied activity of SsgA relates to its ability to activate cell division, and over-expression of SsgA results in a large number of very thick septa produced in vegetative hyphae (van Wezel *et al.*, 2000a). Thus, SsgA activates cell-wall remodeling processes, perhaps via physical modification of the peptidoglycan. The latter is among others suggested by the strongly increased sensitivity of SsgA-overexpressing cells to lysis (GPvW, unpublished).

The effect of SsgA on hyphal morphology is highly pleiotropic, as underlined by two further observations. Firstly, enhanced expression of SsgA does not only stimulate cell division, but enforces pleiotropic changes of the morphology of the hyphae. Hyphae become

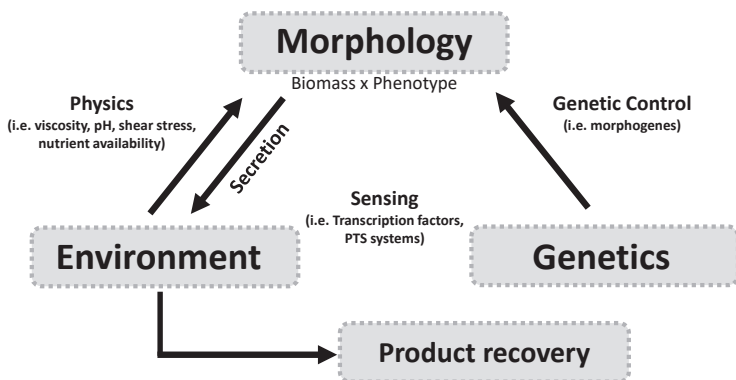


Figure 3. *Streptomyces* morphology is determined by environmental and genetic determinants. An important factor for the behavior and productivity of streptomycetes in bioreactors is morphology, which is influenced by physical and genetic parameters. In turn, morphology and growth affect the environmental conditions, such as rheology and nutrient composition, and reactor conditions and morphology affect the global gene expression profile.

twice as wide as normal vegetative hyphae (around 1 μm instead of 0.5 μm), giving the appearance of aerial hyphae, and submerged sporulation is observed in *S. coelicolor*, which normally only sporulates in surface-grown cultures (van Wezel *et al.*, 2000a). Secondly, microarray studies revealed that some 1000 genes were more than two-fold deregulated in an *ssgA* null mutant of *S. coelicolor*, and most notably almost all developmental genes (*bld*, *whi*), as well as *divIVA*, *ftsI*, *chp* and *rdl* for the chaplin and rodlin spore coat proteins, genes for the components of the Sec and Tat secretion systems and many genes involved in DNA segregation and topology (Noens *et al.*, 2007). The remarkable upregulation of these genes indicates a major disturbance in the control of development and secretion.

Finally, SsgA also has a major impact on antibiotic production, although it is likely that this is due to its influence on morphology. Colonies that over-express the SsgA protein fail to produce actinorhodin, while production of prodigionines (Red) is strongly enhanced (van Wezel *et al.*, 2000b). In fact, in batch fermentations, Red production is some 20-50 times enhanced as compared to the wild-type strain (van Wezel *et al.*, 2006). The most logical explanation is that SsgA induces fragmentation and fast growth, which is detrimental for the production of antibiotics that are produced later during growth, such as Act (Gramajo *et al.*, 1993). Red production occurs during vegetative growth (Takano *et al.*, 1992), and (perhaps as a consequence) benefits from fast and fragmented growth (van Wezel *et al.*, 2006).

4.3. SsgA and SsgB control the localization of FtsZ

Like SsgA, SsgB is also required for sporulation (Keijser *et al.*, 2003) and it is part of the cell division complex (divisome) during sporulation-specific cell division. These studies were done in surface-grown cultures, but most likely translate to submerged sporulation. However, this needs to be experimentally validated. During sporulation, SsgB functions by actively recruiting FtsZ, which forms the contractile cell division ring (Bi & Lutkenhaus, 1991), to division sites. SsgB localizes to future division sites prior to FtsZ, and live imaging showed that soon after the appearance of SsgB foci, also FtsZ arrives at these sites, after which they fully colocalize during the entire division process (Willemse *et al.*, 2011). SsgB interacts with FtsZ and activates polymerization of FtsZ protofilaments *in vitro*, resulting in 450 nm long FtsZ filaments (Willemse *et al.*, 2011). Different modes of action have been described for proteins involved in FtsZ filament formation, such as ZipA, which stimulates the formation of filament networks (Raychaudhuri, 1999), or ZapA, which promotes bundling of the filaments (Gueiros-Filho & Losick, 2002, Low *et al.*, 2004). The activity of SsgB is mechanistically most similar to that of ZipA.

The next step in understanding the role of the SALPs in the control of cell division in *Streptomyces* is to find out how SsgB itself is localized. SsgA plays a role in this process during sporulation in solid-grown cultures, and the two proteins transiently interact prior to the start of division. Little is known of how cell division is controlled during vegetative growth. SsgA in fact acts by triggering an aerial-type cell division in vegetative hyphae, leading to cell fission (fragmentation, submerged sporulation); this likely requires an intact divisome, while



vegetative cell division takes place in the absence of canonical cell division proteins like FtsI and FtsW (Mistry *et al.*, 2008, McCormick, 2009)2008, McCormick, 2009. We anticipate that the (size of the nucleoid) may play an important role in spatially determining the sites for division, as control systems should be in place that prevent septum formation over nonsegregated chromosomes, as is the case in all bacterial systems (Wu & Errington, 2012). This idea waits further experimental testing.

5. ENVIRONMENTAL AND REACTOR CONDITIONS

So far, we have mainly focused on the genetic factors influencing morphology of streptomycetes in liquid-grown environments. However, mycelial morphology and development is also strongly influenced by environmental factors and by the reactor set-up (Fig. 3). Such factors include nutrients (Naeimpoor & Mavituna, 2000, Jonsbu *et al.*, 2002), pH (Glazebrook *et al.*, 1992), viscosity (O’Cleirigh *et al.*, 2005), agitation (Belmar-Beiny & Thomas, 1991, Ayazi Shamlou *et al.*, 1994, Cui *et al.*, 1997, Heydarian *et al.*, 1999), dissolved oxygen (DO) levels (Vecht-Lifshitz *et al.*, 1990) and surface tension (Vecht-Lifshitz *et al.*, 1989). Here, we will discuss the environmental factors that affect pellet morphology.

5.1. Culture heterogeneity

Heterogeneity is a common trait in microbial communities, which probably contributes to increased fitness (Smits *et al.*, 2006). However, in industrial settings heterogeneity is an unwanted feature, because it contributes to an unpredictable outcome of the fermentation process. Mycelia growing in flasks or bioreactors are highly heterogeneous in terms of morphology. One cause of heterogeneity is asynchronous initiation of germination and subsequent outgrowth of spores (Hardisson *et al.*, 1978). Analysis of *Streptomyces antibioticus* indicated that approximately 20% of the spores showed no visible signs of germination 5 hr after inducing this process (Hardisson *et al.*, 1978). The asynchrony might result from substances that are released during spore germination, which would inhibit germination of neighboring spores (Grund & Ensign, 1985, Aoki *et al.*, 2011).

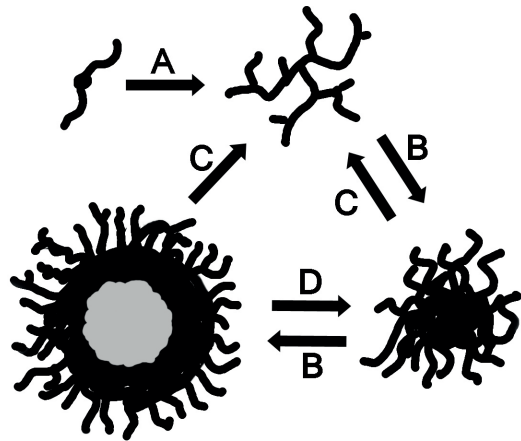


Figure 4. Proposed life cycle of a *Streptomyces* pellet. Germination (A) leads to the formation of a mycelial network that grows (B) into a clump. Continued growth leads to the formation of dense pellets. Clumps and pellets can also fragment (C) or disintegrate (D; in particular for pellets) to give rise to new mycelia or clumps. The grey area represents the ‘dead’ core of a large pellet.

Notably, heterogeneity also develops during growth. This heterogeneity is heritable and characterized by the presence of two populations of pellets that differ in size (van Veluw *et al.*, 2012, Petrus & Claessen, 2014). This heterogeneity was also observed when spore germination was synchronized, or when cultures were inoculated with precultured mycelia. Analysis of a range of different streptomycetes indicated similar behavior with two different populations, regardless of strain, culturing conditions or culture age. Interestingly, the average pellet size of the population of small pellets was rather constant throughout growth, and similar between strains (van Veluw *et al.*, 2012). In contrast, the average size of the larger pellets was variable. This indicates that environmental parameters known to influence morphology, such as flask geometry, stirring speed and medium composition in particular affect the population of large pellets (Tough & Prosser, 1996, Celler *et al.*, 2012).

5.2. Nutrients and morphology

The availability and diversity of nutrients strongly affects *Streptomyces* morphogenesis and antibiotic production (Ueda *et al.*, 2000, Bibb, 2005, Sanchez *et al.*, 2010, van Wezel & McDowall, 2011, Gubbens *et al.*, 2012). The frequency of branching of the vegetative hyphae is strongly dependent on the growth conditions, whereby nutrient-rich conditions favor branching, so as to allow acquisition of nutrients in the soil, while under nutrient-depleted conditions branching is reduced, and growth is dictated by tip extension, which favors the formation of so-called “searching hyphae” (Bushell, 1988). Both branching and cross-wall formation reduce hyphal strength (McCormick *et al.*, 1994, Wardell *et al.*, 2002). As discussed above, over-expression of SsgA leads to strongly enhanced cell division in vegetative hyphae, coinciding with fragmentation, which is often seen occurring at the septa.

The critical role of sugar metabolism on morphogenesis is underlined by the fact that mutation of any of a range of different sugar transport systems results in vegetative arrest on surface-grown cultures: in essence, they are *bld* genes (Seo *et al.*, 2012, Rigali *et al.*, 2006, Colson *et al.*, 2008, Chater *et al.*, 2010). In an attempt to create a more reproducible morphology, *Streptomyces akiyoshiensis* was grown on various carbon sources (Glazebrook *et al.*, 1992). The largest pellets were obtained by growth on lactose (over 600 μm), while growth on glucose resulted in the smallest pellets (less than 200 μm). Growth on either of these carbon sources resulted in some five-fold lower biomass as compared to growth on starch, which highlights the complex link between growth and morphology. The optimal carbon source for production varies between species. Mannitol was the best carbon source for the geosmin production by *Streptomyces halstedii* (Schrader & Blevins, 2001), a combination of fructose and mannose was best for rapamycin production by *Streptomyces hygroscopicus* (Kojima *et al.*, 1995) and glycerol was needed for good production of clavulanic acid by *Streptomyces clavuligerus* (Romero *et al.*, 1984). Media composition also had a major impact on the hyphal stability of *S. clavuligerus*, with cells cultured in media containing glutamate, glycerol and ammonia being more shear resistant as compared to



cells grown in different media (Roubos *et al.*, 2001).

5.3. Fragmentation

The mechanical forces encountered in the submerged environment leads to fragmentation of the pellets, which occurs on a stochastic basis and counter-balances the size increase of a growing pellet (Fig. 4). The mechanical forces in a reactor originate from the combination of agitation, gas hold-up and the rheology of the culture fluid (van't Riet & Tramper, 1991, Olmos *et al.*, 2013). Especially the water swirls, or eddies, which arise under turbulent flow velocities, stretch hyphae in opposite direction with fragmentation as a logical result (Ayazi Shamlou *et al.*, 1994, Heydarian *et al.*, 2000). For filamentous microorganisms the importance of understanding the relationship between the mechanical forces and growth is non-trivial because the mycelia themselves influence the rheology of the culture broth. Entanglement of the mycelia can dramatically increase the viscosity, which affects the shear stress and can reduce the transfer of heat and nutrients (Metz & Kossen, 1977). This process occurs when the biomass grows as a mat, but it has also been observed when pellets are the predominant morphology (Mehmood *et al.*, 2010).

Fragmentation can occur as small hyphal fragments detach from the periphery of the pellet, or via disintegration of pellets into multiple parts (Cui *et al.*, 1997, Kelly *et al.*, 2006). For an exposed hypha to break, the force applied must be greater than its tensile strength. Studies using a blender showed that the fungus *Penicillium notatum* is about four times more likely to break in the middle of a hypha than at the septum (Savage & Vander Brook, 1946). A correlation exists between the likelihood of hyphal breakage and the presence of vacuoles, which are hypothesized to cause localized weak spots (Paul *et al.*, 1994, Papagianni *et al.*, 1999). However, in *Streptomyces* vacuoles are rarely seen in vegetative mycelia (Wildermuth, 1970). Notably, stimulating septation via overproduction of SsgA increases fragmentation of streptomycetes, although these septa more resemble sporulation-type septa (see above). Conversely, less branching in *Saccharopolyspora erythraea* decreased fragmentation (Wardell *et al.*, 2002). Because crosswalls are often found near branch points these results suggest that they in fact represent local weak spots along the hyphae.

Disintegration of pre-existing pellets is the second mechanism by which new pellets can be established. The combined strength of the forces that keeps a pellet together is much larger than the tensile strength of individual hyphae. It seems therefore that this process can only occur when the interactions between hyphae are diminished. This can be caused by a changing environment, for example a change in pH (Glazebrook *et al.*, 1992), but also due to a lack of nutrients, oxygen or the buildup of toxins that induce lysis in the center of a pellet (Papagianni, 2004, Hille *et al.*, 2005). Notably, the susceptibility to fragmentation changes over the course of growth. Generally the pellet size seems to increase during exponential growth, but decreases when entering end-log or stationary phase (Reichl *et al.*, 1992, van Veluw *et al.*, 2012). Susceptibility of *Sacch. erythraea* to fragmentation is almost twice as

high in the stationary phase compared to exponential growing cells (Stocks & Thomas, 2001). This probably relates to programmed cell death in the center of a pellet (Manteca *et al.*, 2010, Rioseras *et al.*, 2014), consistent with the observation that in filamentous fungi pellets become hollow in the center, severely reducing stability (El-Enshasy *et al.*, 1999). This hollowing was observed in cross-sections of a pellet of *Streptomyces tendae* with a diameter of 120 μm (Braun & Vecht-Lifshitz, 1991), but it is unclear in how far this occurs in pellets of other streptomycetes.

5.4. Relationship between agitation, oxygenation, morphology and productivity

As a rule of thumb, and expectedly, more vigorous stirring leads to smaller pellet size (Ohta *et al.*, 1995, Tough & Prosser, 1996, Bellgardt, 1998). However, the morphology of *Streptomyces fradiae* showed an inverse correlation, with low or medium shear stress favoring pelleted growth, while high shear stress caused mycelia of *S. fradiae* to fragment. Interestingly, the pellets grown under low shear stress continued to increase in size, while under medium shear a decrease in size was observed after the exponential growth phase (Tamura *et al.*, 1997, Heydarian *et al.*, 1999). Because faster mixing also increases mass transfer, it typically increases growth rate and biomass accumulation (Heydarian *et al.*, 1999) and can therefore also have a major impact on the production of secondary metabolites (Heydarian *et al.*, 1999, Rosa *et al.*, 2005, Cerri & Badino, 2012). Most studies show an optimum stirring speed for production of the metabolite of interest, where initially the production increases with stirrer speed and then decreases again at very high speeds (Large *et al.*, 1998, Heydarian *et al.*, 1999, Roubos *et al.*, 2002, Mehmood *et al.*, 2010). This decrease in yield is most likely the result of cell damage caused by high shear conditions, as illustrated by the comparison of growth and lipase production of *Streptomyces fradiae* in an airlift with a stirred vessel. Leakage of lipase into culture fluid, indicative of cell damage, was exclusively observed in stirred vessels (Ohta *et al.*, 1995).

Because oxygen transfer is closely linked with agitation, the effects of the one from the other need to be distinguished (Bartholomew *et al.*, 1950, Shioya *et al.*, 1999, Rocha-Valadez *et al.*, 2007, Mehmood *et al.*, 2010). Due to its low solubility and the high energetic cost of antibiotic production, dissolved oxygen (DO) levels are often rate-limiting and oxygen depleted in the center of a pellet (Hille *et al.*, 2005, Wucherpfennig *et al.*, 2010, Olmos *et al.*, 2013). Fermentations in the presence of a saturated DO levels increased the production of cephamycin by *S. clavuligerus* more than two-fold (Yegneswaran *et al.*, 1991), increasing the DO levels using perfluorocarbon increased the production of actinorhodin by *S. coelicolor* about five-fold (Elibol & Mavituna, 1999), and extra oxygen supplied by producing haemoglobin in *Sacch. erythraea* increased the production of erythromycin (Brünker *et al.*, 1998). These results clearly demonstrate the critical role that oxygen has on productivity.

DO levels also affect pellet morphology. Vecht-Lifshitz observed a proportional decrease of pellet size when DO levels were lower (Vecht-Lifshitz *et al.*, 1990). From a biological perspective, regulation of the morphology by oxygen is may be needed to balance



the physical protection offered by the mycelium with the ability to produce secondary metabolites, which offer chemical protection. Biofilms of filamentous fungi are known to contain channels through which liquid and nutrients can flow towards the internal parts of these structures (Wimpenny *et al.*, 2000). They have recently also been identified in bacterial biofilms (Wilking *et al.*, 2013). It will therefore be interesting to see if *Streptomyces* pellets also possess these 'artery-like' structures.

6. MORPHOLOGY AND ANTIBIOTIC PRODUCTION

6.1. Impact of morphology on antibiotic production

The formation of pellets is a major drawback for industrial applications, as pellets represent a slow-growing morphology (Liu *et al.*, 2013b). Therefore, many efforts have focused on obtaining a more open or dispersed morphology. Addition of charged polymers like junlon or carbopol has been applied as a means to obtain a dispersed morphology (Hobbs *et al.*, 1989, Harriott & Bourret, 2003). These compounds probably interfere with the electrostatic properties of the cell wall, which prevents initial aggregation (Wargenau *et al.*, 2013). Lowering the pH also influences the surface charge of the cell wall, thereby yielding a similar effect (Braun & Vecht-Lifshitz, 1991, Wargenau *et al.*, 2011). Increasing the viscosity of the broth also induces more fragmented growth because it increases shear stress, while reducing pellet-pellet collisions, which could also lead to their aggregation (O'Cleirigh *et al.*, 2005). However, higher viscosity demands more energy input to obtain sufficient stirring, which increases production costs. For some products, mostly enzymes but also some antibiotics, dispersed growth can increase yields (van Wezel *et al.*, 2006), while for the production of the majority of the antibiotics pelleted growth is preferred (Pickup & Bushell, 1995, Martin & Bushell, 1996). The latter often leads to a situation whereby morphology is suboptimal as a compromise to maintain relatively high antibiotic yields (Braun & Vecht-Lifshitz, 1991, Martin & Bushell, 1996).

In surface-grown cultures of *Streptomyces* there is a clear link between the production of antibiotics and the developmental cycle (Bibb, 2005, van Wezel & McDowall, 2011). Well-established is the growth-phase dependence of production, where the onset of synthesis usually occurs when growth stalls (Bibb, 2005, van Wezel & McDowall, 2011). However, once activated, there apparently is no additional control; placing *redD*, the pathway-specific activator gene for production of prodigionines in *S. coelicolor*, under the control of the promoter of the gene for the global nitrogen regulator (*glnR*) or a sporulation-specific sigma factor (*sigF*), ensures that production of the antibiotic is controlled by nitrogen or produced in aerial hyphae, respectively (van Wezel *et al.*, 2000b). This implies that at least for some antibiotics, there are no metabolic limitations as to when or where they are produced, and therefore that restrictions on production imposed by growth and morphology-related control mechanisms can be overcome.

In submerged cultures, the linkage between mycelial morphology and production is

exemplified by avermectin production by *S. avermitilis*, which is highest when small dense pellets were formed (Yin *et al.*, 2008), and by the fact that a high-producing variant of *Streptomyces noursei* formed dense pellets, while the wild-type strain formed loose clumps (Jonsbu *et al.*, 2002). Pellets were a prerequisite for the production of a hybrid antibiotic by *S. lividans* (Sarrà *et al.*, 1999), and filtering of a culture of *Sacch. erythraea* revealed that small pellets with a diameter below 88 μm were unable to produce erythromycin (Martin & Bushell, 1996). As discussed in section 4, fragmentation of mycelia by enhanced expression of SsgA has a major effect on antibiotic production by *S. coelicolor*, with a block of Act production, while Red is massively upregulated, again underlining the major influence of morphology on production.

6.2. Programmed cell death and antibiotic production

Mycelial development in liquid-grown cultures may be more similar to that in surface-grown cultures than initially thought. Life/dead staining showed that the early mycelium is compartmentalized in *S. coelicolor*, similar to the initial mycelium in surface-grown cultures. A fraction of this early mycelium undergoes a process that strongly resembles programmed cell death (PCD), with two rounds of PCD occurring during the *Streptomyces* life cycle (Manteca *et al.*, 2011). After spore germination, a compartmentalized mycelium grows and then undergoes a first round of PCD, formed during early vegetative growth (Manteca *et al.*, 2011). The second round of PCD starts during the onset of development, which corresponds to the transition phase between exponential growth and stationary phase in liquid-grown cultures (Granozzi *et al.*, 1990, Manteca *et al.*, 2005). During PCD, specific nucleases are activated that are involved in degradation of chromosomal DNA (Granozzi *et al.*, 1990, Fernández & Sánchez, 2002, Manteca *et al.*, 2006a, Rioseras *et al.*, 2014). Following this PCD event, secondary mycelium emerges from the center of a pellet (Park *et al.*, 1997, Manteca *et al.*, 2008). The secondary mycelium was found to be distinct from the initial mycelia by being multinucleated, which is again similar to solid cultures (Yagüe *et al.*, 2014).

The idea that *Streptomyces* mycelia also undergo a developmental cycle in submerged cultures was suggested by the first microarray experiments done on *S. coelicolor*, which showed that the transcription of many developmental genes is switched on during the transition phase, which is the phase when growth slows down in submerged cultures (Huang *et al.*, 2001). More recently, this was also shown by proteomic comparison of young and older mycelia, with early mycelium enriched in primary metabolic enzymes while proteins involved in secondary metabolism and those associated with development and sporulation were enriched in the multinucleated secondary mycelium (Manteca *et al.*, 2010, Yagüe *et al.*, 2014). Interestingly, many developmental genes are actively transcribed in the secondary mycelium, including several *bld* genes (*i.e.* *bldB*, *bldC*, *bldM*, *bldN*), but also those involved in formation of the rodlet layer (*chpC*, *chpD*, *chpE*, and *chpH*; (Claessen *et al.*, 2004, Manteca *et al.*, 2007). The antibiotics undecylprodigiosin and actinorhodin were exclusively produced by the secondary mycelium in both solid- and liquid-grown cultures (Manteca *et*



al., 2008). Various sporulation-specific genes are upregulated in older cultures (Huang *et al.*, 2001, Yagüe *et al.*, 2014). These data strongly suggest that liquid-grown mycelia also undergo differentiation. In fact, a small fraction of the mycelium appeared to be initiating a sporulation-like process, which is rarely seen for *S. coelicolor* (Rioseras *et al.*, 2014)2014. Indeed, overexpression of *whiG* or *ssgA* induced a certain degree of submerged sporulation in submerged cultures of *S. coelicolor* (Chater *et al.*, 1989, van Wezel *et al.*, 2000a).

A direct link between PCD and antibiotic production was revealed when it was established that cell wall-derived N-acetylglucosamine (GlcNAc) acts as an important signaling molecule for the onset of development and antibiotic production in *Streptomyces* (Rigali *et al.*, 2006, Rigali *et al.*, 2008). In the competitive soil habitat, postponing sporulation is important if sufficient nutrients are available, while during starvation sporulation and ensuing dispersal are essential for survival. In nature, GlcNAc is obtained from hydrolysis of the abundant natural polymer chitin by the chitinolytic system. For bacteria GlcNAc is a favorable C- and N-source, and a major constituent of cell wall peptidoglycan. Some 13 chitinases and chitosanases have been identified in *S. coelicolor* (Delic *et al.*, 1992, Saito *et al.*, 2003a, Colson *et al.*, 2007), and GlcNAc and glutamate are preferred over glucose in fermentations of *S. coelicolor* (van Wezel *et al.*, 2009).

Under poor nutritional conditions such as on minimal media, supplementing

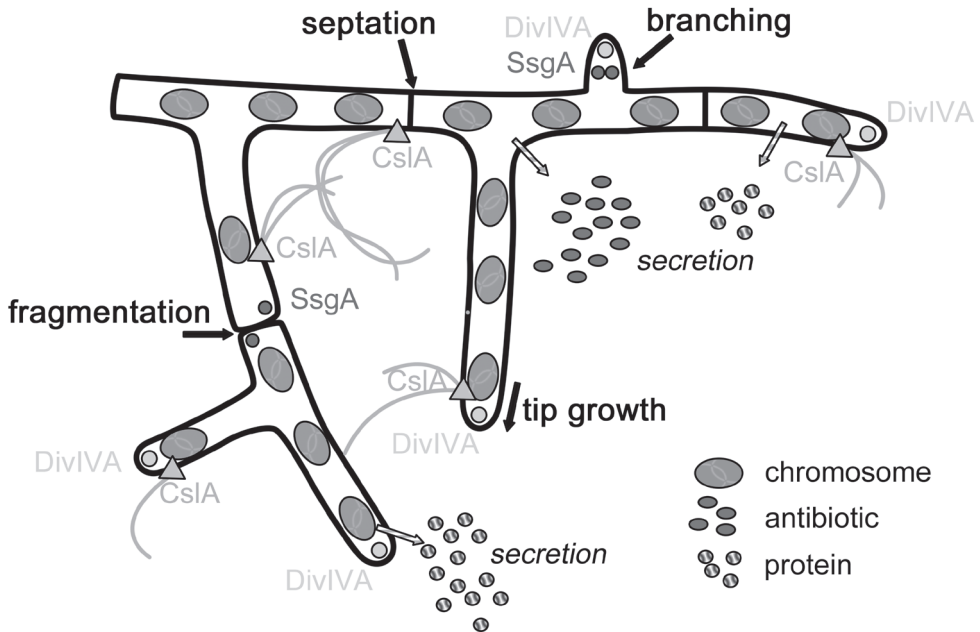


Figure 5. Control of growth of *Streptomyces* hyphae during fermentation. Branching frequency, tip growth rate and fragmentation and aggregation are determined by the activity of morphoproteins and by growth conditions (pH, feedstock, stress). Morphology has a major impact on production and secretion. Some enzymes are secreted near the tips of the hyphae, as was shown recently for Tat substrates (Willemsse *et al.*, 2012), but it is unclear if this is also true for Sec substrates. Where antibiotics and other natural products are secreted is unknown. The drawn secretion sites are hypothetical.

GlcNAc accelerates both the onset of development and antibiotic production, suggesting that under these conditions GlcNAc signals nutrient stress, resulting in accelerated development. Conversely, in rich media, higher concentrations of GlcNAc block development and antibiotic production, thus resembling conditions that promote vegetative growth (Rigali *et al.*, 2008). These growth conditions may thus resemble conditions of *feast* or *famine* in the natural environment, whereby GlcNAc would be derived from chitin in nutrient-rich soil (*feast*), or from the *Streptomyces* cell wall during PCD (*famine*), respectively. The secret appears to lie in the nature of the sugar transporters. Monomeric GlcNAc enters the cell via the NagE2 permease (Nothaft *et al.*, 2010), which is part of the PEP-dependent phosphotransferase system (PTS; (Postma *et al.*, 1993, Titgemeyer *et al.*, 1995), while chitobiose (dimeric GlcNAc), which is the subunit of chitin, enters via the ABC transporters DasABC or NgcEFG (Schlösser *et al.*, 1999, Nothaft *et al.*, 2010, Saito *et al.*, 2007, Colson *et al.*, 2008). Subsequently, internalized GlcNAc is converted by the enzymes NagA and NagB to glucosamine-6-phosphate (GlcN-6-P; Świątek *et al.*, 2012a), a central metabolite that can then enter glycolysis (as fructose-6P) or the pathway towards peptidoglycan synthesis.

GlcNAc-derived GlcN-6-P acts as an allosteric effector of the GntR-family regulator DasR (Rigali *et al.*, 2006), a highly global regulator that controls the GlcNAc regulon (Rigali *et al.*, 2006, Świątek *et al.*, 2012a, Nazari *et al.*, 2013), but also the production of antibiotics (Rigali *et al.*, 2008) and siderophores (Craig *et al.*, 2012). GlcNAc-dependent nutritional signalling is most likely mediated through changes in the intracellular level of GlcN-6-P, which binds as a ligand to the GntR-family regulator DasR, leading to derepression of DasR-mediated control of antibiotic production (Rigali *et al.*, 2008). Recent work showed that addition of phosphorylated sugars to growth media under phosphate limitation delays the occurrence of the second round of PCD and results in vegetative arrest, also preventing antibiotic production (Tenconi *et al.*, 2012).

The pleiotropic DasR control network is well conserved in actinomycetes, and can be manipulated to activate antibiotic production. Addition of GlcNAc to cultures of streptomycetes grown on nutrient-depleted media accelerates development and enhanced antibiotic production by many streptomycetes (Rigali *et al.*, 2008). This concept can be applied to activate cryptic antibiotic gene clusters, which are not or poorly expressed under normal growth conditions (Baltz, 2008). Indeed, GlcNAc induces expression of the *cpk* gene cluster for the cryptic polyketide Cpk (Rigali *et al.*, 2008, Gottelt *et al.*, 2010). Thus, understanding of the correlation between morphogenesis and antibiotic production may be employed for drug discovery approaches.

7. OUTLOOK: THE CORRELATION BETWEEN MORPHOLOGY AND PRODUCTION

As the producers of a wide range of medically important natural products, streptomycetes are very important microorganisms for the pharmaceutical industry (Hopwood, 2007, Baltz, 2008, Olano *et al.*, 2009). Moreover, the streptomycetes also produce a plethora of



extracellular enzymes that allow them to degrade almost any naturally occurring polymer, such as cellulose, mannan, chitin, xylan, starch, glycan and agar (Vrancken & Anne, 2009, Anné *et al.*, 2014). However, as discussed in this review, streptomycetes grow as complex mycelia, which forms a major bottleneck for industrial fermentations, as mycelial growth is associated with slow growth, culture heterogeneity and high viscosity of the fermentation broth. These factors typically have an adverse effect on the yield. Heterologous expression in a host with better growth properties, such as *Bacillus* or yeast, is not an option for natural products with their very complex biosynthetic machinery and dependence on metabolic pathways, and also many actinomycete-derived enzymes require actinomycete-specific machinery for proper folding, modification and/or secretion, and can therefore not be produced in a bioactive form in other hosts.

In terms of process engineering, the focus typically lies on changes in reactor or media conditions, by for instance changing stirring speed, pH, or nutrients, which have a pronounced effect on mycelial morphology. The advantage of this approach is that production yields for a particular compound can be improved fairly quickly. The disadvantage of this approach, however, is that results are difficult to translate to other streptomycetes, which often respond differently to changed conditions. These different responses might relate to for instance changes in cell wall composition, thereby influencing processes such as fragmentation and aggregation. In this respect, better understanding of the genetic factors involved in mycelial growth and architecture are a prerequisite to find general leads to improve streptomycetes in industry. However, while detailed insights into the molecular determinants of mycelial growth are critical for *Streptomyces* strain improvement, it is good to realize that the eventual productivity is determined by many different process technological and genetic parameters, whereby the effect of those parameters on productivity also largely depends on the product to be produced.

To predict the effect of culturing conditions as well as genetic factors on morphology, many different *in silico* models have been designed in the past (Nielsen & Villadsen, 1992, Yang *et al.*, 1992, Meyerhoff *et al.*, 1995, Tough & Prosser, 1996, Liu *et al.*, 2005). The older models largely focused on the influence of environmental factors on morphology, while genetics-based modeling had not been attempted (Kossen, 2000). Two new models of *Streptomyces* growth have been developed recently, which should lead to new impetus for modeling of *Streptomyces* growth and production (Celler *et al.*, 2012, Nieminen *et al.*, 2013). Taking advantage of the incredible increase in computing power since the design of previous models, a three-dimensional *in silico* model was developed that allows visualization of growth of mycelial pellets with distinct morphologies (Celler *et al.*, 2012). As parameters, this model includes among others oxygen diffusion, hyphal growth, branching, fragmentation, cross-wall formation as well as a novel collision detection algorithm. The model was designed with industrial application in mind, allowing the user to change both physical and genetic parameters and see what the predicted effect is on pellet growth and yield. However, for such an approach to function as say an *in silico* test system for the fermentation industry,

better insight in the genetic parameters that control morphogenesis is required, as well as an iterative process of modeling and experimentation.

In recent years, progress has been made in our understanding of the factors that govern mycelial growth, such as DivIVA, Scy and CslA that coordinate tip growth, and the SsgA-like proteins that control hyphal morphology and cell division (Fig. 5). Better understanding of the genetic parameters that control growth should allow us to better control the morphology of the mycelia in the fermentation broth. For example, fragmented growth of streptomycetes can be achieved by overexpression of SsgA, a property that is applied successfully in the industrial domain (van Wezel *et al.*, 2006). For rational design of streptomycetes as production hosts we will also need to understand how morphology affects yield. Live imaging showed that the twin arginine translocation (Tat) secretion system localizes highly dynamically and directly behind the tip complex (Celler *et al.*, 2012, Willemse *et al.*, 2012), which suggested that fragmented growth and therefore increased number of apical sites, should favor secretion of Tat-dependent proteins. Indeed, secretion of the Tat substrate tyrosinase is strongly enhanced in fragmenting strains of *S. coelicolor* and *S. lividans* (van Wezel *et al.*, 2006). The majority of the genetic studies have focused on the micromorphology, while little is known of how these proteins eventually influence macromorphology, such as the formation of clumps or pellets. Conversely, industrial strain engineering has led to mutant strains with often very good reactor properties, but with the many mutations that have occurred during the strain improvement programs, it is hard to identify the changes that may be exploited for rational strain engineering. One important approach that has become feasible in this era of genomics and next-generation sequencing is comparing the genome sequences and the global expression profiles of several generations of one production strain. This should allow identification of genes that may form novel targets for morphological engineering. Analysis of the mutations will provide valuable biological information that might be widely applicable to actinomycete production strains. In this way the historically used black-box approach can be replaced by rational design of future production strains.

ACKNOWLEDGMENTS

We are grateful to Maureen Bibb, Mark Buttner, Martin Roth and Erik Vijgenboom for discussions. The work is supported by VIDI and VICI grants from the Netherlands Technology Foundation STW to DC and GPvW, respectively.



3

A novel locus for mycelial aggregation forms a gateway to improved *Streptomyces* cell factories

This chapter was published as:

van Dissel, D., Claessen, D., Roth, M., & van Wezel, G. P. (2015). *Microbial cell factories*, 14(1), 1.

ABSTRACT

Background

Streptomycetes produce a plethora of natural products including antibiotics and anticancer drugs, as well as many industrial enzymes. Their mycelial life style is a major bottleneck for industrial exploitation and over decades strain improvement programs have selected production strains with better growth properties. Uncovering the nature of the underlying mutations should allow the ready transfer of desirable traits to other production hosts.

Results

Here we report that the *mat* gene cluster, which was identified through reverse engineering of a non-pelleting mutant selected in a chemostat, is key to pellet formation of *Streptomyces lividans*. Deletion of *matA* or *matB*, which encode putative polysaccharide synthases, effects mycelial metamorphosis, with very small and open mycelia. Growth rate and productivity of the *matAB* null mutant were increased by over 60% as compared to the wild-type strain.

Conclusion

Here, we present a way to counteract pellet formation by streptomycetes, which is one of the major bottlenecks in their industrial application. The *mat* locus is an ideal target for rational strain design approaches aimed at improving streptomycetes as industrial production hosts.



INTRODUCTION

Members of the genus *Streptomyces* are of great importance for biotechnology due to their ability to produce a large array of natural products, including antibiotics, anticancer agents and immunosuppressants (Hopwood, 2007), as well as a plethora of industrially relevant enzymes, such as cellulases, amylases and proteases (Vrancken & Anne, 2009). As surface-grown cultures, streptomycetes exhibit a complex multicellular life cycle (Claessen *et al.*, 2014). This starts with a single spore that germinates to form vegetative hyphae, which then grow out following a process of hyphal growth and branching to produce a branched vegetative mycelium (Chater & Losick, 1997). Nutrient scarcity or other stresses induce the developmental program, whereby aerial hyphae differentiate into long chains of spores following a complex cell division event whereby ladders of septa are produced within a short time span (Jakimowicz & van Wezel, 2012, McCormick, 2009). In a submerged environment streptomycetes grow as mycelial networks, typically forming large pellets or clumps. From the industrial perspective, growth as pellets is unattractive, in particular because of mass-transfer problems, slow growth and culture heterogeneity (reviewed in (van Dissel *et al.*, 2014)). Pellets restrict the efficient transfer of nutrients and gasses to the center, which lowers the maximal obtainable product yield (Celler *et al.*, 2012). The growth rate is also limited by the rate at which new pellets can be formed, which requires fragments of viable mycelia to be released from the pellet. Fragmentation is highly depended on the shear forces present in the environment (Cerri & Badino, 2012, Tough & Prosser, 1996). Because high shear can cause cell damage it needs to be balanced for efficient growth and mass transfer and therefore production (Roubos *et al.*, 2001).

Industrial strain optimization programs often make use of black-box approaches to select for desirable traits, typically using mutagens or protoplast fusion (Crook & Alper, 2012). As an example, penicillin yield has been improved at least three orders of magnitude since the isolation of the original *Penicillium chrysogenum* strain. In the improvement program the growth characteristics were also improved upon, which contributed both to the production titers and the fermentability of the strain (van den Berg *et al.*, 2008). Production of clavulanic acid by *Streptomyces clavuligerus* underwent a similar improvement program (Koekman & Hans, 2012). Classical strain improvement, however, is also slow and labor-intensive, and typically associated with a large number of mutations that may later slow down further improvement. Rational strain design requires understanding of the system, but changes can be made fast. Also, directed mutagenesis should result in fewer additional mutations and the changes can be transferred from one strain to another (Oud *et al.*, 2012). The latter is of particular importance for *Streptomyces*, where secondary metabolites cannot easily be moved to generally preferred production host such as *E. coli* or *B. subtilis*.

Relatively little is known of the genetic factors that control pellet morphology in submerged cultures of *Streptomyces*. Growth rate and enzyme production by *S. lividans* are improved significantly by inducing mycelial fragmentation via the increased expression of the cell division activator protein SsgA (van Wezel *et al.*, 2006). SsgA belongs to the family of

SsgA-like proteins that occur exclusively in actinomycetes (Traag & Wezel, 2008), and SsgA not only effects a significant increase in the number of septa, but also has a major impact on the overall hyphal morphology (Colson *et al.*, 2008, van Wezel *et al.*, 2000a). Several other proteins have been identified that affect morphology in submerged culture. These include HyaS, which is involved in cell-wall fusion (Koebsch *et al.*, 2009) and CslA, a cellulose synthase-like protein that is required for pellet formation (van Veluw *et al.*, 2012).

To search for novel genes that may be applied for growth improvement, reverse engineering of randomly obtained mutants is a logical approach that has become feasible in the genomics era (Bailey *et al.*, 1996, Oud *et al.*, 2012). This allows identification of the mutations that have been sustained during the development of industrial production strains. Together with metabolic engineering and synthetic biology approaches, this accelerates the development of microbial factories, exemplified by industrial isobutanol production by *Escherichia coli* (Smith & Liao, 2011), ethanol production by yeast (Swinnen *et al.*, 2012) and lysine or glutamate production by the industrial actinomycete *Corynebacterium glutamicum* (Ikeda *et al.*, 2006, Ravasi *et al.*, 2012).

A regime to improve growth of *Streptomyces lividans* 66 by selection in a chemostat for over 100 generations resulted in a stable derivative with a non-pelleting phenotype (PM02), and an intermediate mutant forming loose pellets (PM01) (Roth *et al.*, 1985). PM02 was used to study the segregational stability of plasmids in continuous culture with different growth limiting substrates (Roth *et al.*, 1994, Roth *et al.*, 1985). In this work, we identified the mutations accumulated during the generation of *S. lividans* 66-PM01 and 66-PM02. The mutation responsible for the non-pelleting phenotype was subsequently identified in a gene for a membrane protein that is co-transcribed with a gene for a bifunctional polysaccharide deacetylase/synthase. Both of these genes, designated *matA* and *matB*, respectively, were shown to be required for pellet formation. Thus, reverse engineering elucidated a novel molecular determinant underlying pellet morphogenesis.

MATERIALS AND METHODS

Bacterial strains, culturing conditions and batch fermentations

Bacterial strains used in this work are listed in Table S1. *E. coli* JM109 (Sambrook *et al.*, 1989) was used as host for routine cloning, and *E. coli* ET12567 (Macneil *et al.* 1992) to produce non-methylated DNA for introduction into *Streptomyces*. *E. coli* ET12567 harboring pUZ8002 was used as host for conjugative transfer of knock-out cosmids to *Streptomyces* as described (Kieser *et al.*, 2000, Fernández-Martínez *et al.*, 2011). *Streptomyces lividans* 66 and *Streptomyces coelicolor* A(3)2 M145 were obtained from the John Innes Centre strain collection. Cells of *E. coli* were grown in Luria–Bertani broth (LB) at 37°C. All *Streptomyces* media and routine *Streptomyces* techniques are described in the *Streptomyces* manual (Kieser *et al.*, 2000). R2YE (regeneration media with yeast extract) agar plates were used for protoplast regeneration, while SFM (soy flour mannitol) agar plates were used to prepare



spore suspensions and SFM supplemented with 10 mM MgCl₂ for conjugation experiments. Phenotypic characterization was done on R2YE and SFM agar plates.

For screening purposes, strains were grown in baffled shake flasks in TSBS (tryptic soy broth with 10% sucrose) for 48h. Small-scale batch fermentations were performed in 1.3 L BioFlow 115 bioreactors (New Brunswick), at a temperature of 30°C and at constant pH (pH 7). The initial stirrer speed was set to an average 300 rpm to promote growth and fragmentation and was automatically increased to maintain a dissolved oxygen (DO) concentration above 50%. The latter was only needed during late exponential growth and therefore stirring issues did not influence the outcome of the morphological studies. Off gas was analyzed by an EX-2000 (New Brunswick) and dry weight was measured by freeze-drying filtered and washed biomass obtained from 10 mL culture broth. Cultures were inoculated with spores at a density of 10⁶ cfu/mL. Reactor experiments were performed in triplicate. For the production of tyrosinase the medium was supplemented with 25 μM CuCl₂ and 2.5 μg/mL thiostrepton (Keijser *et al.*, 2000).

Constructs and mutants

All constructs described in this work are listed in Table S3 and oligonucleotides in Table S4.

Constructs for the deletion of SCO2963 / SCO2962 and SLI_3306a / SLI3306

In-frame deletion mutants for SCO2963 / SCO2962 and SLI_3306 / SLI_3306a were created as described earlier (Świątek *et al.*, 2012b). In brief, the upstream region of SCO2963 ranging from -1326 to +43 and the downstream region of SCO2962 from +2190 to +3610 were amplified by PCR from the *S. coelicolor* as described in (Colson *et al.*, 2007) and cloned into the unstable shuttle vector pWHM3 (Vara *et al.*, 1989). An engineered *Xba*I site was used for insertion of the apramycin resistance cassette *aacC4* flanked by *loxP* sites between the flanking regions. The presence of the *loxP* recognition sites allows the efficient removal of the apramycin resistance cassette following the introduction of a plasmid pUWLcre expressing the Cre recombinase (Khodakaramian *et al.*, 2006, Fedoryshyn *et al.*, 2008).

A Redirect mutant for *matB* (SCO2962) in *S. coelicolor* was made using primers matB_FW_REDIRECT and matB_REV_REDIRECT (Table S3) as described previously (Gust *et al.*, 2003b).

A construct for the complementation of the mutants of SLI_3306a in *S. lividans* was designed. For this, the region of SLI_3306a from -500 to +1485 (relative to the start of *matA*) were amplified by PCR from *S. lividans* genomic DNA. This fragment was ligated into pSET152, an *E. coli-Streptomyces* shuttle vector which integrates in the genome at the ΦC31 attachment site (Bierman *et al.*, 1992).

Creating mutants using knock-out cosmids

Knock-out cosmids (Fernández-Martínez *et al.*, 2011) were obtained from the collection

of Paul Dyson (Swansea, UK). For details see Table S2. The cosmids were introduced into *S. coelicolor* and *S. lividans* by conjugative transfer and selected for apramycin resistance, while nalidixic acid was used to prevent growth of the *E. coli* donor strain. After several rounds of non-selective growth, colonies were selected for loss of kanamycin resistance, which is the marker for the cosmid sequences. Ex-conjugants with the expected phenotype (Apra^R/Kana^S) were checked by PCR for absence of the wild-type gene.

Microscopy

The mycelial morphology of *Streptomyces* in liquid-grown cultures was monitored using a Zeiss Standard 25 phase-contrast microscope and colony morphology of surface-grown cultures were imaged using a Zeiss Lumar V12 stereomicroscope as described (Colson *et al.*, 2008).

Tyrosinase activity assay

The specific activity of the tyrosinase enzyme produced by the *S. lividans* transformants with pIJ703 (Katz *et al.*, 1983) was determined as described earlier (Kieser *et al.*, 2000) by measuring over time the conversion of l-3,4-dihydroxyphenylalanine spectrophotometrically at a wavelength of 475 nm.

Whole genome sequencing and SNP analysis

Genomic DNA was isolated from liquid-grown cultures as described previously (Busarakam *et al.*, 2014). Paired-end sequencing using an ILLumina HiSEQ 2000 sequencer and mapping of the individual reads against the *Streptomyces lividans* 66 reference genome was performed at Baseclear BV (Leiden). Genome annotation was performed as described (Busarakam *et al.*, 2014). Variants were detected using the CLC Genomics Workbench version 6.5. The initial list of variants was filtered using the Phred score and the number of false positive was reduced by setting the minimum variant frequency to 70% and the minimum reads that should cover a position was set to 10. All variants were curated manually and verified by PCR analysis and routine DNA sequencing.

RESULTS

Derivatives of *S. lividans* 66 with improved growth characteristics

Many *Streptomyces* species produce large mycelial clumps when grown in liquid media, which is a disadvantage for industrial application as it is associated with slow growth and poor nutrient utilization. In an attempt to obtain faster growth with less dense pellets, a non-pelleting derivative of *S. lividans* 66 (also known as *S. lividans* 1326) was obtained previously through growth of some 100 generations in continuous culture at a medium



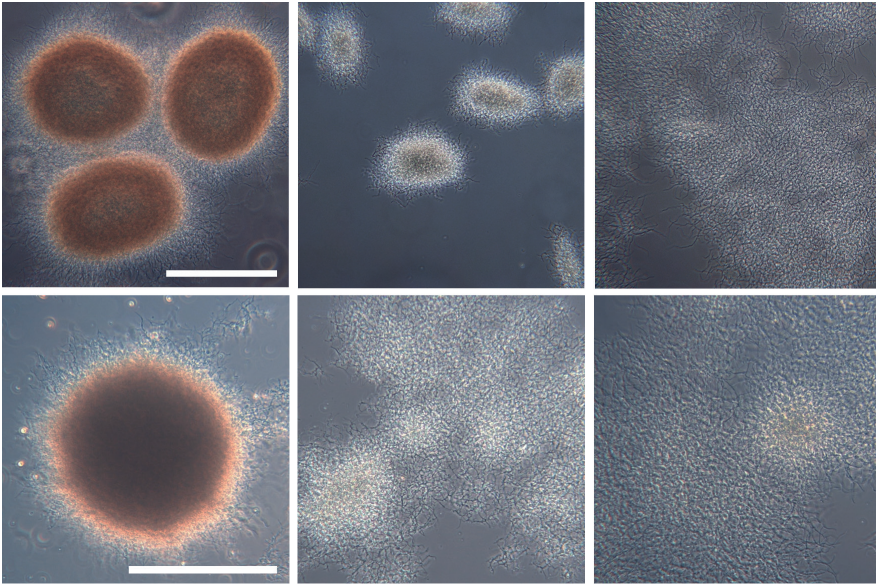


Figure 1. Morphology of *S. lividans* 66 and its derivatives PM01 and PM02 in submerged culture. PM01 was obtained after 70 generations in a nitrogen-limited chemostat at a dilution rate (D) of 0.1 h^{-1} . PM02 was obtained after evolving PM01 for another 30 generations in a phosphate-limited chemostat at 36°C and $D = 0.1 \text{ h}^{-1}$. Row (A) growth of strains in a baffled shake flask for 30 h on TSBS. Row (B) cultivation of strains in a 900 ml bioreactor in TSBS media after 24 h of growth. Scale bar, 200 μm .

dilution rate, called PM02, while a strain with an intermediate phenotype was obtained after 70 generations, called PM01, which grows as small loosely packed mycelial pellets (Figure 1). While the parent grew as large pellets with an average diameter of around 250 μm , the pellets of PM01 were much smaller, averaging around 150 μm . PM02 did not form any mycelial pellets, except that on increasing biomass densities patches of dispersed mycelia entangled into open pellet-like structures. To quantitatively describe the growth characteristics, the strains were compared in a bioreactor with TSBS as the growth medium. On TSBS medium PM02 had a maximal growth rate of around $0.41 \pm 0.09 \text{ h}^{-1}$ (doubling time of 1.7 h), which was significantly faster than the parental strain that had a maximal growth rate of around $0.25 \pm 0.02 \text{ h}^{-1}$ (doubling time of 2.7 h) under the chosen conditions. The benefits of a dispersed morphology, a higher average growth rate and shorter batch duration, are clearly present (Figure 2). In contrast to shake flask cultivation, under the conditions in the bioreactor PM01 also grew dispersed, resulting in a growth rate of $0.36 \pm 0.06 \text{ h}^{-1}$ (1.9 h doubling time). The difference between growth in shake flasks and in a bioreactor in terms of the morphology is likely explained by the differences in shear and aeration.

Genome analysis of *S. lividans* PM01 and PM02

To investigate the genetic basis for the changes in phenotypes in derivatives PM01 and PM02 relative to the parental strain, we analyzed the single nucleotide polymorphisms

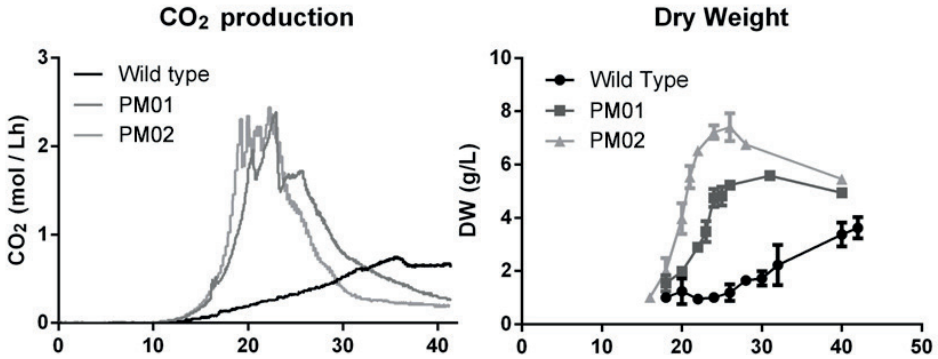


Figure 2. Growth of *S. lividans* 66 and its derivatives PM01 and PM02 in a bioreactor. 1.3 liter reactors were inoculated with 106 spores/mL in TSBS medium. CO₂ levels were measured by an off-gas analyser and biomass accumulation was measured as dry weight from 10 mL freeze-dried broth that was collected and washed on a glass fibre filter.

(SNPs). For this, whole genome sequencing was performed on the parental strain and on PM01 and PM02 using illumina paired-end sequencing and the sequences were then compared to the draft genome sequence of *S. lividans* 66 (Cruz-Morales *et al.*, 2013). The genome sequence of the parental strain was used to filter out all nt changes relative to the published draft genome. After this filtering step, we identified in total 19 SNPs, 17 between PM01 and the parent, and two more between PM02 and the parent. These mutations resulted in 10 aa substitutions and four frameshifts in putative proteins of PM01 relative to the parental strain *S. lividans* 66 and an additional two aa changes in PM02 relative to PM01 (Table 1). Additionally, the *bldA* gene for the tRNA-Leu that recognizes the rare codon UUA in the mRNA was also mutated in PM01 and PM02. This mutation probably explains the developmental block in both strains, as *bldA* mutants fail to erect an aerial mycelium (Lawlor *et al.*, 1987, Leskiw *et al.*, 1991).

Analysis of mutations that may relate to the PM02 phenotype

To identify the mutations that gave rise to the non-pelleting phenotype of PM01 and PM02, we used directed mutagenesis followed by morphological characterization of the mutant derivatives in comparison to PM01 and PM02. In total seven genes were initially prioritized for genomic disruption (highlighted in grey in Table 1). Of these, five were found in PM01: SLI_2849, SLI_5273 and SLI_6232 for putative DNA binding proteins, SLI_6089 for a serine protease, which is located next to the principal sigma factor gene *hrdB* and SLI_6469 for a dipeptidase. The two additional mutations found only in PM02 were in SLI_3391, which encodes a LytR-type transcriptional attenuator associated with cell-wall remodeling and biofilm formation (Chatfield *et al.*, 2005, Kawai *et al.*, 2011, Hübscher *et al.*, 2009) and in SLI_6143 for an osmosensitive potassium channel histidine kinase (KdpD). A gene-disruption library is available for the majority of the *S. coelicolor* genes, whereby genes have been



Table 1. SNPs identified in mutants PM01 and PM02 as compared to the wild-type reference strain *S. lividans* 66

| <i>Variants detected in PM01</i> | | | | | | |
|---|-----------|---------|-------------|------------|---------|---|
| position | reference | variant | codonChange | Sli GN | SCO GN | Description |
| 1188051 | C | T | Gly344Asp | SLI_1181 | SCO0948 | Alpha-mannosidase |
| 2924224 | G | A | Ala104Thr | SLI_2849* | SCO2513 | Putative DNA-binding protein |
| 3429004 | - | - | Leu165fs | SLI_3306a* | SCO2963 | putative membrane protein |
| 3586487 | C | T | C16T | SLI_10025 | bldA | tRNA-Leu |
| 3717404 | C | T | Val70Ile | SLI_3556 | SCO3202 | RNA polymerase sigma factor |
| 4336711 | - | C | Gly121fs | SLI_4122 | SCO3868 | Uncharacterized protein |
| 4499627 | C | G | Ala83Pro | SLI_4277 | SCO4043 | Uncharacterized protein |
| 4568325 | G | A | Pro119Leu | SLI_4341 | SCO4111 | tRNA (guanine-N(7)-methyltransferase |
| 4967084 | A | - | Leu130fs | SLI_4756 | SCO4477 | Transcriptional regulator, MerR family |
| 5479836 | - | CC | Ala67fs | SLI_5273* | SCO4998 | DNA-binding protein |
| 5700075 | T | A | Val30Asp | SLI_5487 | SCO5200 | Putative membrane protein |
| 5763756 | G | - | - | - | - | 119bp before start SLI_5553 |
| 6362450 | A | G | Thr271Ala | SLI_6089* | SCO5821 | Putative serine proteinase |
| 6513051 | C | T | Pro142Leu | SLI_6232* | SCO5952 | Uncharacterized protein |
| 6750912 | G | C | Ala27Pro | SLI_6469* | SCO6076 | Putative dipeptidase |
| 7227219 | C | - | - | - | - | 109bp before start SLI_6876 |
| 7560900 | A | G | Thr484Ala | SLI_7172 | SCO6968 | Long-chain-fatty-acid--CoA ligase |
| <i>Additional variants detected in PM02</i> | | | | | | |
| 3537971 | G | A | Val496Ile | SLI_3391* | SCO3043 | Cell envelope-associated transcriptional attenuator LytR-CpsA-Psr |
| 6420301 | G | C | Ala652Pro | SLI_6143* | SCO5871 | Osmosensitive K ⁺ channel histidine kinase KdpD |

The nt position refers to the published genome sequence of *S. lividans* (Cruz-Morales et al., 2013). Only non-silent mutations inside CDSs are shown. Genes followed by an asterisk were selected for targeted gene disruption. Database numbers for *S. lividans* (Sli GN) and *S. coelicolor* (Sco GN) are given, based on the nomenclature of the StrepDB database (<http://strepdb.streptomyces.org.uk>).

mutated on cosmids using transposon mutagenesis, which facilitates a rapid first assessment of gene function (Fernández-Martínez *et al.*, 2011). These gene-disruption cosmids were used to create mutants in the seven genes mentioned above in both *S. lividans* 66 and *S. coelicolor* M145. For exact genomic position of the transposon insertion we refer to Table S2. Disruption of SLI_3391 (SCO3043), , resulted in a white (non-sporulating) phenotype on solid media and pellets with a slightly more open perimeter in liquid-grown cultures (Figure S1). Likewise, mutants deleted for either SLI_6143 (SCO5871) or SLI_6089 (SCO5821), had a

phenotype with a slightly decreased pellet density, but this did not compare to the drastic morphological changes seen in the PM01 and PM02 lineages.

Since none of these mutations could explain the non-pelleting phenotype of PM01 and PM02, we scrutinized the list of SNPs further. This identified a conspicuous mutation 216 bp upstream of SLI_3306, which encodes a bi-functional transferase/deacetylase. The predicted protein has an N-terminal NodB-like polysaccharide deacetylase domain, and a C-terminal PgaC-like glycosyltransferase type 2 domain. Comparison of the genomic region to that of the close relative *S. coelicolor* revealed that the SNP upstream of SLI_3306 corresponds to a position *inside* the annotated gene SCO2963, which encodes a putative membrane protein that is well conserved in streptomycetes. This gene is translationally coupled with SCO2962. Resequencing of the region between SLI_3306 and the downstream SLI_3307

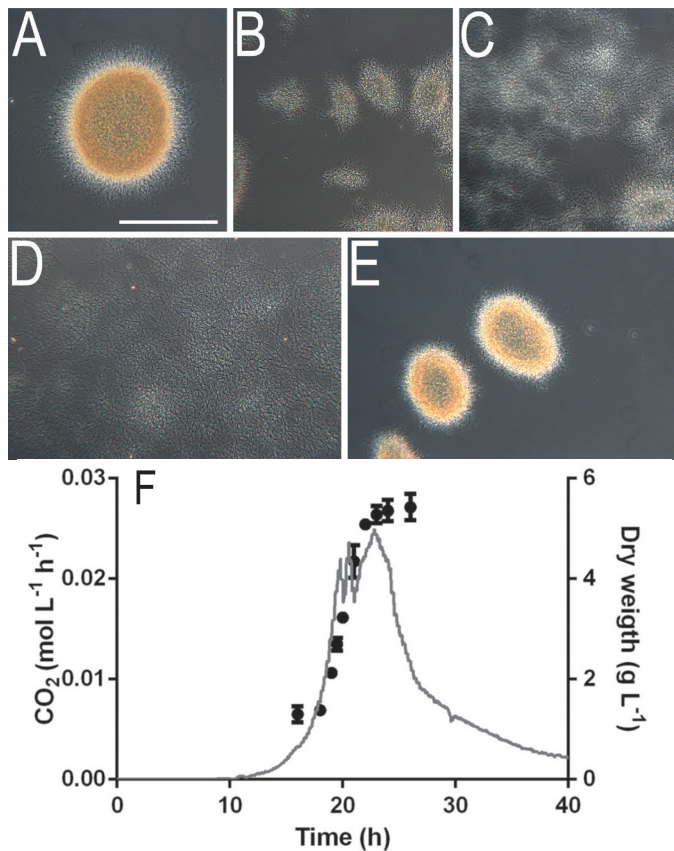


*Figure 3. Liquid-culture morphology of the mat mutants. A-E shows wide field images of strains grown in shakeflask on TSBS medium. Pictures were taken at 24 h of growth representing late log phase morphology. Scale bar equals 200 μ m. A) wild type *S. lividans* 66, B); GAD02 ($\Delta matA$); C) GAD03 ($\Delta matB$); D) GAD05 ($\Delta matAB$); E) PM02 harboring the *matA* containing plasmid pMAT03. F) shows the growth profile of GAD05, indicated by the CO_2 production (grey line) and the biomass concentration (black dots). The strain was grown in a 1.3 L benchtop bioreactor in TSBS medium. Inoculation density was 106 spores/mL. The strain had a growth rate of 0.39 h^{-1} .*



revealed a mistake in the *S. lividans* 66 genome sequence, and in fact the SNP lies inside an orthologue of SCO2963 with very high similarity between the predicted gene products (99 % aa identity). This gene was designated SLI_3306a. The deletion of nt position 3429004 in SLI_3306a found in strain PM01 results in a frame shift which introduces a premature stop codon at amino acid residue 176, most likely rendering the SLI_3306a protein non-functional. Since SLI_3306a and SLI_3306 have overlapping stop and start codons and are therefore most likely translationally coupled, the premature termination of SLI_3306a may have major consequences for the translational efficiency of SLI_3306 and other putative co-translated genes (Levin-Karp *et al.*, 2013).

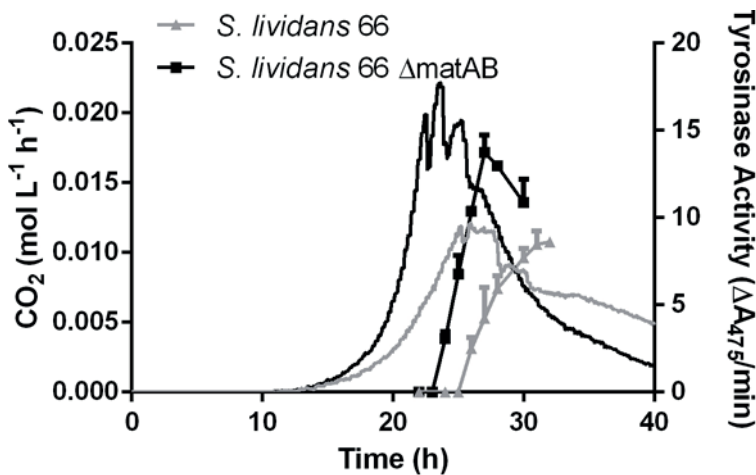


Figure 4. Effect of deletion of *matAB* on tyrosinase production by *S. lividans*. Transformants of the parental strain *S. lividans* 66 (grey curves) and its *matAB* null mutant (black curves) contained plasmid pIJ703, leading to the expression of tyrosinase from *S. antibioticus*. Strains were grown in 1.3L bench-top bioreactors with a 900ml working volume on TSBS medium with 25μM CuCl₂. CO₂ production (continues lines) was calculated by measuring the concentration in the off gas and tyrosinase activity (lines with blocks) was measured spectrophotometrically.

Deletion of SLI_3306/3306a or SCO2962 causes a non-pelleting phenotype

To investigate the role of SLI_3306 and SLI_3306a in mycelial morphogenesis, both genes were simultaneously replaced with the apramycin resistance cassette *aacC4* by homologous recombination. The *aacC4* gene was flanked by *loxP* sites, allowing the subsequent removal by expression of the Cre recombinase, resulting in a clean deletion of the genes and leaving only the start region of SLI_3306a and the stop region of SLI_3306 (see Materials and Methods section for details). The removal of the region yielded the strains GAD02 (ΔSLI_3306a) and GAD05 (ΔSLI_3306a + ΔSLI_3306) (Figure 3). GAD02 showed an altered morphology with small pellets, while the removal of both *mat* genes yielded a highly dispersed phenotype. Considering their apparent involvement in mycelial aggregation, SLI_3306a and SLI_3306 were renamed *matA* and *matB* (for mycelial aggregation).

Analysis of a number of streptomycetes showed that the *mat* genes and flanking regions are conserved in around two-thirds of all *Streptomyces* genomes (not shown). Besides *S. coelicolor* and *S. lividans*, these include for example *S. albus*, *S. griseus*, *S. hygroscopicus* and *S. avermitilis*. The *mat* cluster was not found in *S. venezuelae* (which hypersporulates in submerged culture) or in *S. clavuligerus* (which forms large mycelial mats). A more detailed phylogenetic analysis is required to establish the possible correlation, if any, between morphogenesis and the presence of the *mat* genes.

We also analyzed a mutant of *S. coelicolor* $\Delta matB$ (SCO2962, the orthologue of SLI_3306). This mutant was created using the Redirect strategy (Gust *et al.*, 2003b), and had a phenotype that was highly similar to that of the *S. lividans* *matAB* null mutant (Figure 3), providing further evidence that the non-pelleting phenotype indeed correlates to the *mat* locus and also that the phenomenon is more widely applicable than only in *S. lividans*. The mutants were then complemented with a wild-type copy of *matA* to establish if the mutation was indeed the sole cause of the non-pelleting phenotype. For this, the entire *matA* gene and 500 bp upstream (promoter) region were amplified by PCR from the *S. lividans* genome and cloned into the integrative vector pSET152, generating plasmid pMAT04. This plasmid integrates at the $\Phi C31$ attachment site on the genome. Introduction of pMAT04 completely restored pellet formation to mutant PM02, resulting in a wild-type morphology (Figure 3). This strongly suggests that the frameshift inside SLI_3306a is indeed the main cause for the observed metamorphosis.

The growth characteristics of the *matAB* double mutant GAD05 were tested in small-scale bioreactors to compare them with the original mutant PM01 and PM02. Growth of the mutant on TSBS showed striking similarity with the growth profile to PM02, with a completely dispersed morphology throughout the cultivation, reaching a maximal growth rate of $0.39 \pm 0.005 \text{ h}^{-1}$ (doubling time of 1.8 h; Figure 3), which is highly similar to that of PM02 (0.41 h^{-1} ; doubling time of 1.7 h).

Effect of the *mat* mutation on productivity

As an initial test to establish the effect of the non-pelleting phenotype for production in a bioreactor, we compared the ability of GAD05 with its parent *S. lividans* 66 to produce the secreted enzyme tyrosinase (Katz *et al.*, 1983), which is secreted via the Twin Arginine Transport (Tat) pathway. For this, plasmid pIJ703 harboring *melC2* for tyrosinase was introduced into both strains. Tyrosinase activity can easily be measured via an enzyme assay, and is therefore a very suitable reporter protein for heterologous protein production in *Streptomyces* (van Wezel *et al.*, 2006). Growth and productivity of *S. lividans* 66 and its *matAB* double mutant GAD05 was compared in a 1.3 L bioreactor in TSBS media (Figure 4).

The morphology of mutant GAD05 positively contributed to the production capacity of *S. lividans*, with more enzyme produced in a shorter time (Figure 4). Notably, also under production conditions the specific growth rate increased by nearly 60% from 0.25 h^{-1} to 0.39 h^{-1} . A tyrosinase enzyme assay based on the conversion of dihydroxy-L-phenylalanine



revealed that the maximal tyrosinase activity increased by around 65%, from 8.7 ± 1.0 AU to 13.7 ± 1.4 AU. Additionally, the fermentation time for GAD05 was around 5 h shorter than for its parent *S. lividans* 66. This indicates that the non-pelleting phenotype may have strong potential for biotechnological applications.

DISCUSSION

The applicability of chemostats in the (directed) evolution of strains has a long-standing history (Novick & Szilard, 1950). Because less fit variants wash out over time there is a strong selection for increased growth rates and high substrate uptake rates. The high dilution rate used for the evolution of the *S. lividans* derivatives PM01 and PM02 30 years ago (Roth *et al.*, 1985) resulted in dramatic morphological changes of this streptomycete that normally grows as dense clumps. Instead, the derivatives produced small and open pellets (PM01, selected after 70 cycles) or complete lack of any pellets (PM02, after 100 cycles). We reverse engineered the morphology of these mutants and identified a single point mutation that was the basis for the observed mycelial metamorphosis. The phenotype associated with this mutation was designated Mat (mycelial aggregation).

It is likely that other mutations also contributed to the adaptation to the high growth rate regime. The genetic complementation of the non-pelleting phenotype of PM02 by the introduction of plasmid pMAT04 - which contains wild-type *matA* - shows that the mutation in the *mat* locus is the main source for the morphogenesis, but the difference between PM01 and PM02 remains unclear. Most likely, the mutation in SLI_3306a causes the phenotype of PM01 and PM02 has sustained a secondary mutation that further progresses the dispersed phenotype. We tried to look into the effects of other SNPs found in PM02, by disrupting SLI_3391 (SCO3043) and SLI_6143 (SCO5871) in PM01. Of these, PM01 Δ SLI_3391 had an altered phenotype more similar to PM02 in submerged culture (Figure S2). Perhaps SLI_3391 attenuates another adhesion system that is subordinate to the Mat system, which would allow the restoration of the pelleting phenotype when *matA* was reintroduced into PM02.

What then is the function of the Mat proteins? We propose that they may fulfil a function that is similar to that of enzymes responsible for adherence and biofilm formation in other bacteria. The various systems that are responsible for enabling biofilm formation in nature utilize different ways of adherence between cells, such as extracellular DNA (eDNA) or direct contact by either cell-wall fusion or via pili (O'Toole *et al.*, 2000). Indeed, study of the literature combined with Blast analysis suggests that all these three systems may be present in *Streptomyces* spp. (Kim & Hancock, 2000, Koebsch *et al.*, 2009). Interestingly, the genetic configuration of the *mat* operon is similar to that of the *Ica* gene cluster for the intracellular adhesion system found in *Staphylococcus* spp. (Archer *et al.*, 2011, Mack *et al.*, 1996). The *Ica* operon produces a capsular extracellular polysaccharide (EPS) consisting of β -1,6-linked N-acetylglucosamine molecules, which mediates cell-cell adhesion and is required

for biofilm formation (McKenney *et al.*, 1998). This five gene system (*icaABCDR*) encodes a chitin synthase (*IcaA*), a polysaccharide deacetylase (*IcaB*), an acyltransferase (*IcaC*) and a membrane protein (*IcaD*), which is required for production of a mature EPS (Archer *et al.*, 2011, Götz, 2002). These genes are under the control of *IcaR* which controls the expression of the *icaABCD* operon. SCO2962, a predicted bifunctional polysaccharide deacetylase and glycosyltransferase, appears to be a fusion protein of *IcaA* and *IcaC*, while SCO2961 encodes an acetyl transferase, analogous to *IcaB*. The IclR-family regulator SCO2964 candidates as the regulator of the *mat* genes (similar to *IcaR*). A membrane protein homologous to *IcaD* is absent.

Similar to the *ica* gene cluster, the *pgaABCD* locus in *E. coli* and the *hmsHFRS* locus in *Yersinia pestis* also produce an EPS that is important for biofilm formation (Wang *et al.*, 2004, Khweek *et al.*, 2010). Interestingly, in the streptomycetes *S. lividans* and *S. coelicolor* the cellulose synthase-like protein *CsIA* produces a yet undetermined EPS that plays a major role in pellet morphology in submerged cultures, with a dispersed morphology of *csIA* null mutants (van Veluw *et al.*, 2012, Xu *et al.*, 2008). Whether either of the *mat* genes is also involved in the production of an EPS requires further investigation. Suggestively, the String database indicates functional linkage between *matB* and several cell division-related genes, namely *ftsI* for the enzyme FtsI that is involved in peptidoglycan synthesis during cell division (Pogliano *et al.*, 1997), and *mraY* which is required for synthesis of the peptidoglycan precursor Lipid I (Ikeda *et al.*, 1991, Boyle & Donachie, 1998). Also, the *matAB* locus is separated by only two genes from *ftsEX* (SCO2966-SCO2967 in *S. coelicolor*), which encode the FtsEX membrane permease and associated ATPase that are required for cell division (de Leeuw *et al.*, 1999). This suggests that *matAB* may relate to the synthesis of peptidoglycan rather than EPS, in particular during cell division. This may explain the absence of a membrane component similar to *IcaD* in the *mat* cluster. In terms of a linkage to cell division and cell-wall synthesis, it is important to note that over-expression of the cell-division activator protein SsgA has a major effect on mycelial morphology in submerged culture, with formation of mycelial mats at lower expression and small fragments and even submerged spores at high levels of expression (van Wezel *et al.*, 2000a). The possible functional relationship between MatAB, SsgA and cell-wall synthesis needs to be analyzed further.

Streptomyces lividans is a preferred host for the industrial production of enzymes from actinomycete origin (Ferrer-Miralles & Villaverde, 2013, Vrancken & Anne, 2009). However, its morphology with large pellets formed in submerged culture hampers productivity in the bioreactor. Availability of bioreactor capacity is of the essence, and slow growth of actinomycetes therefore imposes a major burden on reactor time. Similarly to what we report here for the effect of the *mat* mutation, the mycelial fragmentation of *S. lividans* effected by the enhanced expression of SsgA led to enhanced productivity in batch fermentation with tyrosinase as the reporter, as well as reduced fermentation times (van Wezel *et al.*, 2006). Faster growth is potentially an important step towards biotechnological application



of actinomycetes for enzyme production. The strong mycelial fragmentation effected by the enhanced expression of SsgA had major consequences for antibiotic production, with enhanced production of undecylprodigiosin but a complete block in actinorhodin production (van Wezel *et al.*, 2009). The latter most likely relates to the fact that many antibiotics are produced only when pellets of a certain size are produced (Martin & Bushell, 1996). Importantly, we did not observe major differences in antibiotic production between *S. coelicolor* M145 and its *mat* mutants.

Besides as sources of enzymes, streptomycetes are particularly well known for their ability to produce antibiotics, anti-cancer compounds and other important natural products. Genome sequencing has revealed that actinomycetes have the potential of producing far more natural products than originally anticipated, which has led to a revival of antibiotic discovery (Baltz, 2008). This also raises the question as to how we can best harness the plethora of novel gene clusters that are currently being uncovered (Pidcock, 2011, Zhu *et al.*, 2014). One logical way forward is combining synthetic biology approaches to efficiently synthesize biosynthetic gene clusters with the development of heterologous expression hosts for efficient production (Medema *et al.*, 2011). Examples of the latter include derivatives of *Streptomyces avermitilis* (Komatsu *et al.*, 2010) and *Streptomyces coelicolor* (Flinspach *et al.*, 2010) that have been stripped of many of their native antibiotic clusters. Morphological engineering should allow the development of these heterologous hosts into more efficient and cost-effective production platforms.

The obvious question to ask is, are all streptomycetes subject to growth improvement by modulating *mat* expression or deletion? Indeed, several streptomycetes lack the *mat* genes altogether. A drawback of the clavulanic acid producer *S. clavuligerus* is that rather than forming pellets, it makes very dense mycelial mats, causing very high viscosity. Preliminary evidence showed that introduction of the *S. coelicolor mat* gene cluster (SCO2961-SCO2964) into *Streptomyces clavuligerus* resulted in the formation of small pellets (our unpublished data). The biotechnological relevance and applicability of introduction or deletion of the *mat* genes in industrial streptomycetes, in particular with respect to enzyme and antibiotic production, is currently being investigated in more detail. Furthermore, we seek to unravel the molecular composition of the polysaccharide that most likely causes the mycelial aggregation.

CONCLUSIONS

Our study provides new means to obtain a more dispersed morphology during fermentation, which has a positive impact on productivity, both in terms of fermentation time and yield per volume. *S. lividans mat* null mutants, designed based on reverse engineering of a mutant arisen in a chemostat, produced significantly higher titers in a shorter time frame as compared to the parent. The fact that *S. coelicolor matB* mutants showed a similar improvement of growth suggests that this may be widely applicable strategy for the rational strain design of streptomycetes that form mycelial pellets, with the aim to accelerate

fermentation time and enhance productivity.

ABBREVIATIONS

aa: amino acid

bp: base pair

nt: nucleotide

PCR: polymerase chain reaction

SNP: Single nucleotide polymorphism

ACKNOWLEDGEMENTS

We like to thank Geneviève Gerard for help with bioinformatics, and Karin Perlet for performing continuous cultures of *S. lividans* 66. The research was supported by a VICI grant from the Netherlands Technology Foundation STW to GVW.

SUPPLEMENTAL INFORMATION

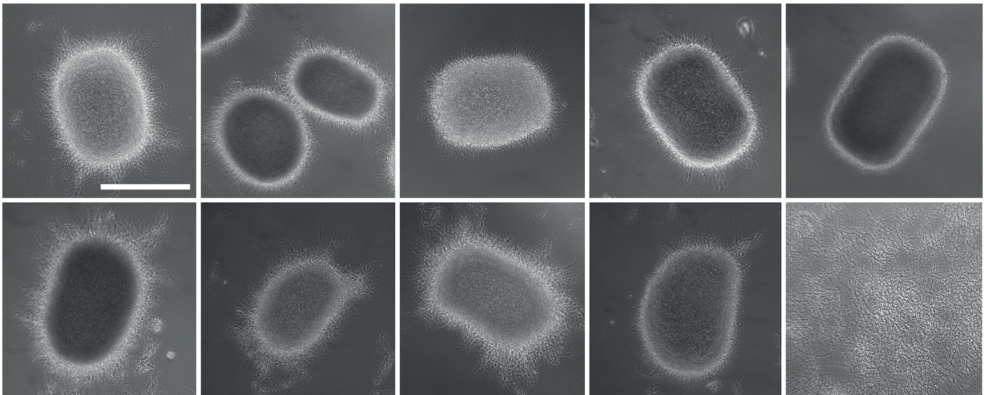


*Figure S1. Phenotypes of disruption mutants of S. coelicolor in submerged cultures. SCO2513, SCO2963, SCO3042, SCO5821, SCO5871, SCO5952 and SCO6076 were disrupted by a transposon insertion. The region of SCO2962-SCO2963 was removed by homologous recombination replacement. J1681 (*S. coelicolor* $\Delta bldA$) was published previously (Leskiw *et al.* 1993). Cultures were grown in baffled shake flasks in TSBS for 48 h. Scale bar, 200 μm .*



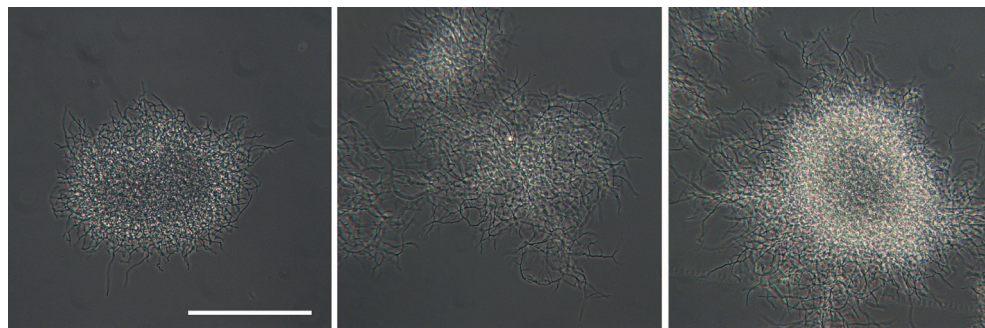


Figure S2: Identification of suppressor mutations in *S. lividans* PM01 and PM02. Engineering of PM01 to obtain the phenotype of PM02. SLI_3391 and SLI_6143 were identified by SNP analysis as the major changes during evolution of PM02 from PM01. Note that mutation of SLI_3391 enhanced dispersed growth of PM01, giving a phenotype similar to that observed for PM02.

Table S1: Bacterial strains.

| Strain | Description and genotype | Reference |
|--|---|-----------------------------|
| <i>Streptomyces lividans</i> 66 (1326) | SLP2+ SLP3+ | Kieser <i>et al.</i> , 2000 |
| PM01 | Evolved from <i>S. lividans</i> 66 | Roth <i>et al.</i> , 1985 |
| PM02 | Evolved from PM01 | Roth <i>et al.</i> , 1994 |
| J1681 | J1501 $\Delta bldA$ | Leskiw <i>et al.</i> , 1993 |
| GnD01 | <i>S. lividans</i> 66 Δ SLI_3306a::aacC4 Apr ^R | This study |
| GnD02 | <i>S. lividans</i> 66 Δ SLI_3306a ^{IFD} | This study |
| GnD03 | <i>S. coelicolor</i> M145 Δ SCO2962::aacC4 Apr ^R | This study |
| GnD04 | <i>S. lividans</i> 66 Δ SLI_3306a-Sli_3306::aacC4 Apr ^R | This study |
| GnD05 | <i>S. lividans</i> 66 Δ SLI_3306a-SLI3306 ^{IFD} | This study |

IFD, in-frame deletion mutant; Apr^R apramycin resistant.

Table S2: Transposon-mediated gene-replacement cosmids used in this study. Cosmid nomenclature refers to the *Streptomyces coelicolor* genome database (strepdb.streptomyces.org.uk). The genomic location of the insertion of the apramycin cassette is given for the *S. coelicolor* genome.

| Cosmid name | target gene | Cosmids location in genome | Start gene | position relative to start |
|--------------|-------------|----------------------------|------------|----------------------------|
| SCI7.2.C04 | SCO1907 | 2043368 | 2044163 | 795 |
| C121.1.E05 | SCO2513 | 2709849 | 2709485 | 364 |
| E34.2.E04 | SCO3043 | 3331409 | 3331178 | 231 |
| 2SCK36.1.F01 | SCO4998 | 5437068 | 5437222 | 154 |
| SC5B8.1.F05 | SCO5821 | 6369817 | 6369367 | 450 |
| SC2E9.1.F02 | SCO5871 | 6426513 | 6426319 | 194 |
| 7H1.2.H01 | SCO5952 | 6521053 | 6520547 | 506 |
| SC9B1.2.C03 | SCO6076 | 6670727 | 6670057 | 670 |

Table S3. Plasmids and constructs

| Plasmid or Construct | Description | Reference |
|----------------------|---|-------------------------|
| pWHM3 | Cloning vector, <i>colE1</i> replicon, <i>pSG5</i> replicon, Thio ^R , Amp ^R | Vara et al., 1989 |
| pSET152 | Complementation vector, <i>oriT RK2</i> , pUC18 replicon, Apra ^R | Bierman et al., 1992 |
| pUWLcre | pUWLoriT derivative with <i>creA</i> gene under <i>ermE*</i> promoter, Thio ^R | Fedoryshyn et al., 2008 |
| pMAT1 | pWHM3 containing flanking regions of <i>S. coelicolor</i> SCO2963 and SCO2962 with a <i>aac(3)IV-loxP</i> XbaI inserted between them in pWHM3 EcoRI-HindIII | this work |
| pMAT2 | pWHM3 containing flanking regions of <i>S. coelicolor</i> SCO2963 with a <i>aac(3)IV-loxP</i> XbaI inserted between them in pWHM3 EcoRI-HindIII | this work |
| pMAT3 | Cosmid StE59 derivative in which the <i>matB</i> coding sequence was replaced by the <i>aac(3)IV</i> resistance cassette | this work |
| pMAT4 | pSET152 containing SCO2963 with the 500bp upstream (promoter) region | this work |

**Table S4. Oligonucleotides.**

| Name | Primer Sequence |
|------------|-----------------------------------|
| matB_+2190 | AGTCTCTAGAAGCCGGTTCGGATGACCACC |
| matB_+3610 | AGTCAAGCTTCCCTGTTCACTCCCGCAACCG |
| matA_-1326 | AGTCGAATTCCAGCCGGGCGGTGAGATTCC |
| matA_+43 | ACTGTCTAGACGAGCACTCGTCGGCCGAAC |
| matA_2809 | AGTCAAGCTTAGACGGTGTCCGCTCCATC |
| matA_+1466 | ACTGTCTAGACCCGGAGAACCCTCTGATGG |
| matA_-54 | TTCTTTGCCTGAGCACGGTGTGATAC |
| matB_+1528 | TGGTACAGGACCACCCGAAGAG |
| pmatA_-537 | AGCTGAATTCGGCGGTTACGAGAGCGGACTGAC |
| matA_1485 | GATCTCTAGATCAGAGGGTGTCTCCGGGGACAG |

Restriction sites are underlined. TCTAGA, XbaI; AAGCTT, HindIII; GAATTC, EcoRI.

4

Hyphal aggregation and surface attachment of *Streptomyces* is governed by extracellular poly- β -1,6-*N*-acetylglucosamine

van Dissel, D., Willemse, J., Claessen, D., Pier, G.B., van Wezel, G.P.

ABSTRACT

Streptomycetes are multicellular filamentous microorganisms, which are major producers of antibiotics, anticancer drugs and industrial enzymes. When grown in submerged cultures, the preferred enzyme producer, *Streptomyces lividans*, forms dense mycelial aggregates or pellets, which requires the activity of the proteins encoded by the *matAB* and *csIA-glxA*. Here we show that *matAB* encodes the biosynthetic genes for the extracellular polymeric substance (EPS) poly- β -1,6-*N*-acetylglucosamine or PNAG. Heterologous expression of *matAB* in actinomycetes that naturally lack these genes was sufficient for PNAG production and induction of mycelial aggregation. Also, overexpression of *matAB* in a non-pelleting *csIA* mutant restored pellet formation, which could effectively be antagonized by the PNAG-specific hydrolase, dispersin B. Extracellular accumulation of PNAG allowed *Streptomyces* to attach to hydrophilic surfaces, unlike attachment to hydrophobic surfaces, which involves a cellulase-degradable EPS produced by *CsIA*. Altogether, our data support a model in which pellet formation depends on hydrophilic interactions mediated by PNAG and hydrophobic interactions involving the EPS produced by *CsIA*. These new insights may be harnessed to improve growth and industrial exploitation of these highly versatile natural product and enzyme producers.



INTRODUCTION

The ability of many microorganisms to organize themselves into biofilms has a huge impact on human society, impacting human health (Hall-Stoodley *et al.*, 2004), waste treatment (Liu and Tay, 2002) and crop production (Ramey *et al.*, 2004). Within a biofilm many different individual cells aggregate into a multicellular community where they coexist in a relatively complex and coordinated manner (Vlamakis *et al.*, 2013; Claessen *et al.*, 2014). The cells are held together by an extracellular matrix, often referred to as extracellular polymeric substance (EPS), that can comprise to 90% of the mass in a biofilm (Branda *et al.*, 2005; Wingender *et al.*, 2012).

The presence of extracellular polysaccharides in the matrix is in most cases essential for a persisting biofilm. Although many different kinds of exo-polysaccharides are employed by different bacterial species (Boyd and Chakrabarty, 1995; Ruas-Madiedo *et al.*, 2002), pathogenic bacteria often produce poly- β -1,6-*N*-acetylglucosamine (PNAG) to stick to the biotic surface of a host, which often is a requirement, but not by itself sufficient for biofilm formation (Wang *et al.*, 2004, Roux *et al.*, 2015, Mack *et al.*, 1996, Beenken *et al.*, 2004). Interestingly, the soil bacterium *Bacillus subtilis* also produces PNAG, suggesting that this EPS is abundantly present in natural matrices (Roux *et al.*, 2015). In *Staphylococcus epidermis*, the organism in which PNAG was first detected, the *icaADBC* gene cluster encodes proteins responsible for the production of PNAG. IcaAD form a glycosyltransferase that synthesizes the PNAG chain intracellularly, while IcaB partially deacetylates the polymer extracellularly, thereby changing the net charge, and allowing better association with the cell surface (Vuong *et al.*, 2004). IcaC likely plays a role in the export and possibly O-succinylation of the PNAG polymer (Atkin *et al.*, 2014).

Streptomycetes are multicellular filamentous bacteria that reproduce by sporulation and are the source of the majority of the antibiotics as well as many other compounds of medical, agricultural and biotechnological importance (Hopwood, 2007; Barka *et al.*, 2016). The production of such natural products is under extensive genetic and morphological control (van Wezel *et al.*, 2009; Liu *et al.*, 2013). In submerged cultures, many *Streptomyces* species form pellets, which may be regarded as self-immobilizing biofilms (van Dissel *et al.*, 2014). Because of their dense architecture, which among other issues, causes significant mass transfer limitations, pellets are often undesirable for industrial production; however, antibiotic production often benefits from mycelial clumps compared with mycelial fragments (Wardell *et al.*, 2002a; van Wezel *et al.*, 2006a). Pellet architecture depends on genetic and environmental factors, like the septum formation (Noens *et al.*, 2007; Traag and Wezel, 2008), cytoskeleton (Celler *et al.*, 2013), shear stress (Heydarian *et al.*, 1999), pH (Glazebrook *et al.*, 1992) and cell wall fusions (Koebisch *et al.*, 2009). Two extracellular polysaccharides are of particular important for cellular aggregation, namely a cellulose-based EPS that is produced by the concerted action of CslA, GlxA and DtpA (Xu *et al.*, 2008; de Jong *et al.*, 2009; Chaplin *et al.*, 2015; Petrus *et al.*, 2016), which mediates attachment in cooperation with the amyloid-forming chaplin proteins, and a putative second extracellular

polysaccharide that is synthesized by the MatAB proteins (van Dissel *et al.*, 2015). Loss of either system results in similar dispersed morphology, suggesting that both systems might work in unison in a so far unclear way (Zacchetti *et al.*, 2016).

The *matAB* gene cluster shows significant resemblance to the PNAG biosynthetic gene cluster *icaADBC* from *S. epidermidis*, with the bifunctional MatB likely corresponding functionally to both IcaA and IcaB, forming an intracellular glycosyltransferase domain and an extracellular oligo-deacetylase domain, respectively. SCO2961, which is located directly downstream of *matB*, is an orthologue of *icaC* that might also play a role in formation of the mature polymer. The function of MatA is unclear as it lacks known functional domains, but as deletion of the *mata* gene reduces hyphal aggregation it may assist in efficient polymerization of the EPS, similarly to IcaD (Gerke *et al.*, 1998).

In this study we show that MatAB is responsible for the production of PNAG. The MatAB-dependent EPS is required for adherence to hydrophilic surfaces, while a second EPS produced by the action of CslA and GlxA mediates attachment to hydrophobic surfaces. The combination of these two systems make up the architecture of a pellet, creating a strong, robust structure. Since natural product formation and enzyme production depend strongly on the morphology of the mycelia, this also has major implications for biotechnological exploitation.

MATERIALS AND METHODS

Bacterial strains and plasmids

Table 1: Strains and vectors used in the study

| Strain or plasmid | Description and genotype | Reference |
|--|--------------------------------------|-----------------------------------|
| <i>Streptomyces lividans</i> 66 (1326) | SLP2+ SLP3+ | (Kieser <i>et al.</i> , 2000) |
| <i>Saccharopolyspora erythraea</i> | | (Labeda, 1987) |
| $\Delta cslA$ | <i>S. lividans</i> 66 $\Delta cslA$ | (Chaplin <i>et al.</i> , 2015) |
| GAD05 | <i>S. lividans</i> 66 $\Delta matAB$ | (van Dissel <i>et al.</i> , 2015) |
| GAD06 | <i>S. lividans</i> 66 $\Delta matB$ | this work |
| GAD07 | $\Delta cslA$ + pMAT7 | this work |
| GAD08 | <i>Sacch. erythrea</i> + pMAT7 | this work |

| Vector | Description | Reference |
|---------|--|--------------------------------|
| pSET152 | <i>oriT</i> RK2, pUC18 replicon, Apra ^R | (Bierman <i>et al.</i> , 1992) |
| pMAT7 | pSET152-P ^{gapA} -matAB | this work |

The bacterial strains and plasmids used in this study are listed in Table 1. *E. coli* JM109 (Sambrook and Russell, 2001) was used as a routine host for plasmid construction. The native *matAB* locus and *gapA* promoter region were PCR-amplified from the *S. coelicolor* genome as described using primers SCO2963_F, SCO2962_R and PSCO1947_F, PSCO1947_R respectively (Table S1). The *matAB* locus was cloned as an EcoRI/BamHI fragment into the



integrative vector pSET152 (Bierman *et al.*, 1992) and the promoter region was placed in front of the *matAB* locus as an EcoRI/NdeI fragment, resulting in construct pMAT7. Conjugative plasmid transfer to *Streptomyces* was done using *E. coli* ET12567 (MacNeil *et al.*, 1992) harboring pUZ8002 as the host (Kieser *et al.*, 2000).

Culture conditions

Streptomycetes were grown in shake flasks with a coiled stainless steel spring in 30 ml tryptic soy broth (Difco) with 10% sucrose (TSBS). Cultures were inoculated with 10⁶ cfu/ml and grown at 30°C. To assess growth in the presence of hydrolytic enzymes, strains were grown in 96-well plates where the agitation was facilitated by a Microplate Genie Digital mixer (Scientific Industries, USA) set to 1400 rpm, which was found to reproduce native morphologies at a micro scale (DVD and GVW, unpublished data). Dispersin B (100 µg/ml), cellulase (SigmaAldrich, C1184) (2 U/ml) or chitinase (SigmaAldrich C8241) (0.5 U/ml) were added during growth to degrade EPS. The strains were observed after 24 h of growth by wide field microscopy.

Bioinformatics

The genomes of *Streptomyces coelicolor* A3(2) M145 (Bentley *et al.*, 2002) and *S. lividans* 66 (Cruz-Morales *et al.*, 2013) have been published. Protein domains were annotated using the conserved domain search v3.14 (Marchler-Bauer *et al.*, 2014), using default settings. Homology searches were performed using the local Blast+ software v2.2.30 (Camacho *et al.*, 2009). A BlastP database was built from the amino acid sequences of all characterized type 2 glycosyltransferases and type 4 carbohydrate esterases listed in the CAZy database (www.CAZy.org). The amino acid sequences were retrieved from the Uniprot database (www.uniprot.org). *In silico* structure prediction of MatB was performed with the Protein Homology/analogy Recognition Engine Version 2 (PHYRE2) (Kelley *et al.*, 2015). Structural analysis and alignment was performed in Pymol (v1.7.4). Sequence alignments were done in MEGA (v7.0.9) using the ClustalW algorithm (Thompson *et al.*, 2002). Maximum likelihood trees were constructed using default settings and a bootstrap with 500 iterations.

Production and isolation of dispersin B

Dispersin B from *Aggregatibacter actinomycetemcomitans* ATCC 29522 was produced and purified as described (Kaplan *et al.*, 2003). The specific activity, determined as the amount of enzyme needed to hydrolyze 1 µmol 4-nitrophenyl-β-D-N-acetylglucosaminide per minute in 50 mM sodium phosphate buffer (pH 5.5) 100 mM NaCl was 570 U /mg protein.

Calcofluor white staining

The presence of (1-3) or (1-4) glycans was assessed by calcofluor white staining (Wood, 1980b). Strains were grown over night in 8-well microscope chambers (LabTech II) in 300 µl

TSBS medium. 30 μ l calcofluor white (CFW) solution (Sigma Aldrich) was added and after 5 min incubation the samples were imaged on a Zeiss LSM5 Exciter/ Axio observer with a 405 nm laser, a 405/488 nm beam splitter and 420-480 nm bandpass filter (Colson *et al.*, 2008).

Immunofluorescence

Immunofluorescence microscopy was performed as described (Roux *et al.*, 2015), with small adaptations. In short, *S. lividans* 66 was grown in TSBS media for 6 hours at 30°C. A 50 μ l culture aliquot was spotted inside circles drawn with a PAP pen on adhesive microscope slides (Klinipath, The Netherlands). After 15 min the media was removed gently and the cell layer was air dried for 10 min and fixed with 4% paraformaldehyde in PBS for 15 min. After washing samples twice with PBS, monoclonal antibodies against PNAG (mAb F598) were added to a final concentration of 10 μ g/ml in PBS with 0.1% BSA-c (Aurion, the Netherlands) and samples incubated for 16 h at 4°C. The samples were then washed three times with PBS with 0.1% BSA-c and fluorescently-labeled goat-anti-human IgGs (Life Technologies) added to a final concentration of 4 μ g/ml and incubated in the dark for 2 h. After washing twice with PBS with 0.1% BSA-c, some PBS with propidium iodide at a concentration 1 μ g/ml was added and the samples were imaged on an axiovision Zeiss microscope equipped with a mercury lamp.

Cryo scanning electron microscopy

Mycelia from cultures grown for 6 h, fixed by 1,5% glutaraldehyde and immobilized on isopore membrane 0.8 μ m filter discs (Millipore) by pushing the liquid through using a syringe and placing the filter in a filter holder. The discs were cut to size and placed on the SEM target immobilized with Tissue Tek® and quickly frozen in liquid nitrogen slush and transferred directly to the cryo-transfer attachment of the scanning electron microscope. After 10 minutes sublimation at -90 °C specimens were sputter-coated with a layer of 2 nm Platinum and examined at -120 °C in the JEOL JSM6700F scanning electron microscope at 3 kV as described (Keijser *et al.*, 2003).

Negative stain TEM microscopy

For negative staining, 5 μ l of young mycelium was placed on a copper TEM grid and air dried for 15 min. The cellular material was stained with 3% PTA for 5 min, followed by 5 times washing with miliQ. The samples were placed in a JEOL 1010 transmission electron microscope and observed at 60 kV as described (Piette *et al.*, 2005).

Adhesion Assays

Attachment of strains to polystyrene surfaces was tested as described (van Keulen *et al.*, 2003). In short 106 CFUs/ml were inoculated into 4 ml NMMP (Kieser *et al.*, 2000) without



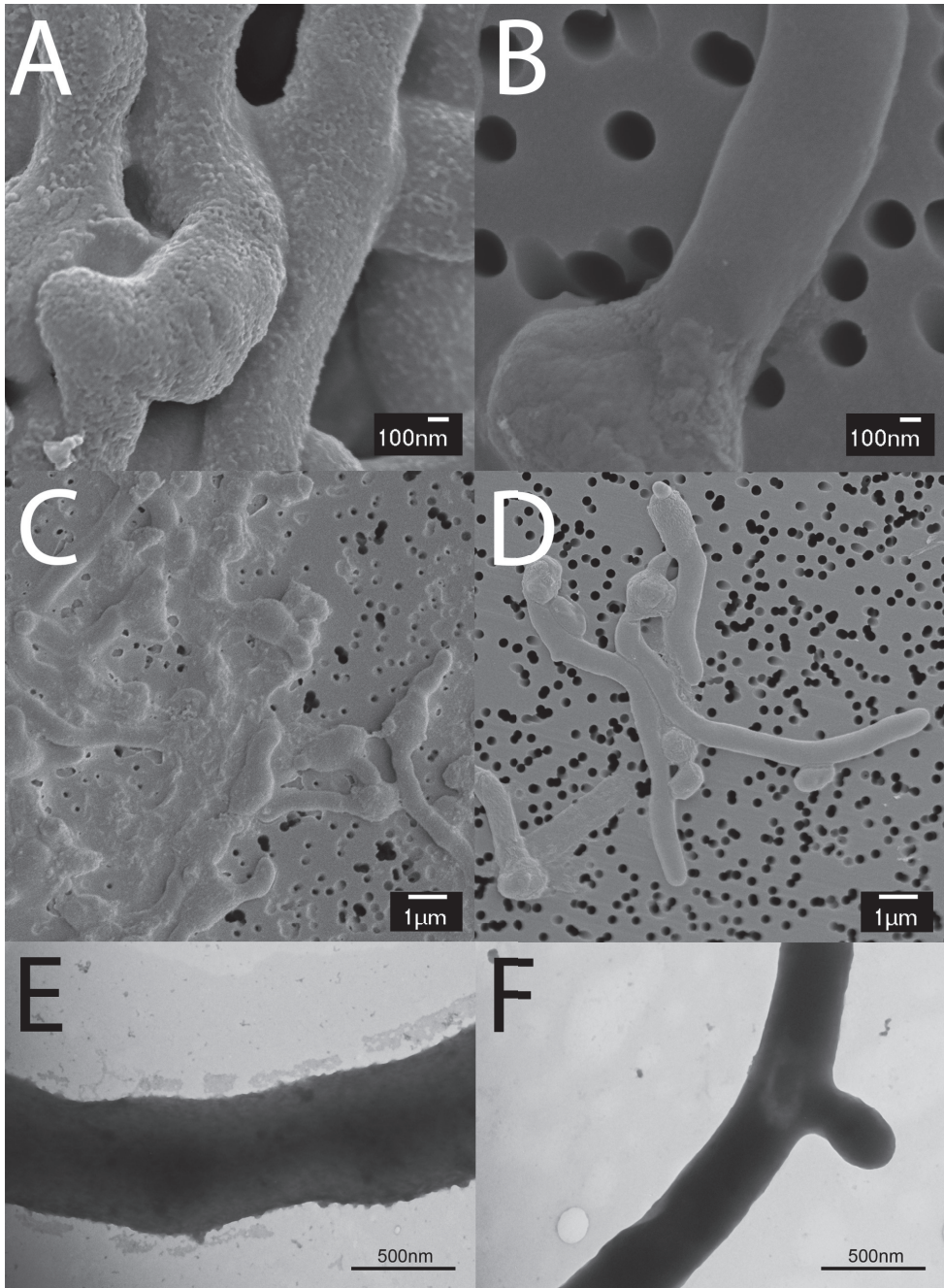


Figure 1. Demonstration of the extracellular layer produced by the *mat* genes. Cryo SEM of young vegetative mycelium (A-D) shows an abundance of extracellular material in wild type *S. lividans* covering the outside of hyphae (A) and between hyphae (C). This extracellular material is absent in the *mat* mutant (B and D). Negatively stained hyphae with tungsten acid, specific for polymeric substances, reveals a scabrous outside coating in wild-type hyphae (E) that is absent in the *mat* mutant (F). All strains were grown for 8 h in TSBS media in a shake flask.

polyethylene glycol and casamino acids, using 2% mannitol as the sole carbon source. After 5 days at 30°C the standing cultures were stained with crystal violet. After washing the attached cells were quantified by extracting the crystal violet with 10% SDS and measuring the absorption at 570 nm. Attachment to glass surfaces was tested in a similar fashion, using glass bottom 96 wells plates (Greiner Bio-One, Austria) and 200 µl NMMP medium without polyethylene glycol, but with 0.5% casamino acids and 2% glucose as the carbon source. These were cultivated overnight at 30°C and the attached biomass was quantified as for polystyrene.

RESULTS

Mat facilitates the formation of a granular layer on the outside of the hyphae

Previous studies showed that the *mat* genes encode a putative extracellular polysaccharide synthetase system in *Streptomyces* that is required for mycelial aggregation and pellet formation in submerged cultures, most likely by mediating cell-cell bonding (van

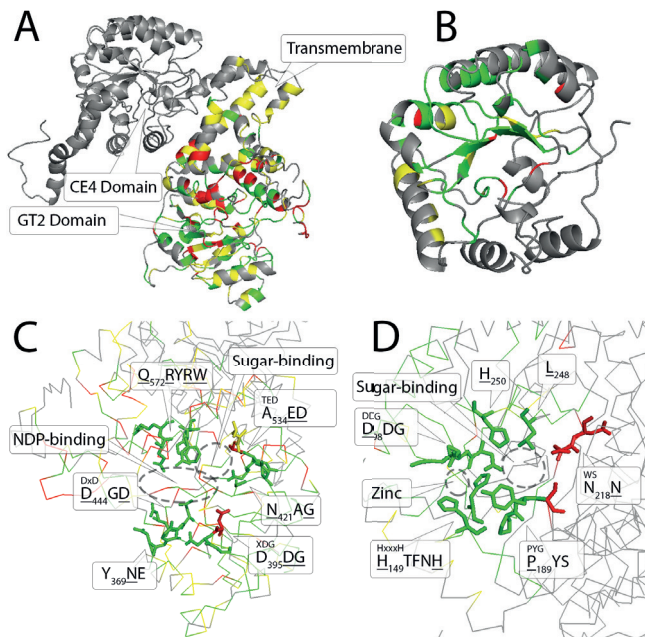


Figure 2. Structural model of the MatB protein. Model of predicted MatB using PHYRE² where the two predicted domains were submitted as a whole and separately. The intracellular GT2 domain (aa 354-734) (A and C) was based on the cellulose synthase BcsA (4HG6), while the extracellular CE4 domain (aa 1-342) was based on a combination of 6 templates (PDB 2c1l, 1ny1, 4nz3, 1w17, 4m1B, 4l1G) (B and D). The coloring represents the conservation from the top 5 blast scores where green is 80% conserved in homologues and MatB, yellow is a conserved aa type and red represents 80% conservation in homologues, but different in MatB. Gray represents non conserved residues. The putative active sites and important amino acids involved in the enzymatic reactions are indicated in C and D for the glucosyltransferase domain and the carbohydrate esterase domain respectively.



Dissel *et al.*, 2015). To elucidate the underlying mechanism, we here investigated the cell surface mechanism by which this is mediated, aiming to elucidate the nature of the EPS. Although the Mat proteins are expressed throughout growth (Zacchetti *et al.*, 2016), the Mat polymer was most apparent in young mycelia. High resolution imaging by cryo-scanning electron microscopy (SEM) revealed a surface layer that decorated the entire outer surface of the hyphae (Figure 1A). Transmission electron microscopy (TEM) of Tungsten acid-negative stained cells, which images electron dense polymeric surface structures, highlighted an extracellular surface layer (Figure 1E). Between the hyphae a deposit of extracellular matrix could also be observed by SEM (Figure 1C). Conversely, the hyphae of the *matB* mutant have instead a smooth surface, observed both with SEM (Figure 1B) or negative staining in the TEM (Figure 1F). We also failed to detect any extracellular material between the hyphae of *matB* mutants (Figure 1D).

MatB correlates to the production of poly-N-acetylglucosamine

Bioinformatics analysis of MatA failed to identify known protein domains. MatB contains two functional domains, namely an intracellular glycosyltransferase type 2 (GT2) domain and a type 4 carbohydrate esterase (CE4) domain, connected by a predicted transmembrane helix. Sequences of glycosyltransferases and carbohydrate esterases were extracted from CAZy, which catalogs enzymes with characterized function, and assembled in a local database for Blast analysis. The glycosyltransferase domain of MatB returned PgaC from *E. coli* as the top hit (Table S2). *E. coli pgaC* encodes a glycosyltransferase that synthesizes Poly- β -1,6-*N*-acetylglucosamine (PNAG) (Itoh *et al.*, 2008). The next nearest homologs were enzymes with the same function in *Acinetobacter baumannii*, *Staphylococcus epidermis*, *Aggregatibacter actinomycetemcomitans* and *Actinobacillus pleuropneumoniae*, all with similar scores.

A similar blast comparison with the MatB carbohydrate esterase domain returned PgdA (BC_3618), a peptidoglycan N-acetylglucosamine deacetylase from *Bacillus cereus* as

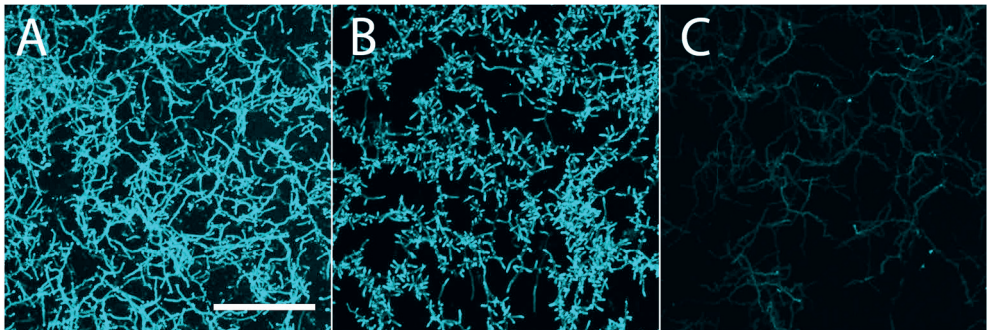


Figure 3. Calcofluor white staining. S. lividans (A), the *matAB* mutant (B) and Δ *cslA* (C) were stained with CFW to assess the presence of extracellular (1,3)- or (1,4)-glycans. The staining patterns indicate the presence of (1,3)- or (1,4)-glycans in both the parental strain and its *matAB* mutant, while it is absent in the *cslA* mutant. Scale bar equals 50 μ m.

nearest characterized homologue (Table S2). Other top hits include a chitin deacetylase from *Caldanaerobacter subterraneus* and NodB proteins from *Rhizobium* species, all with similar scores. Interestingly, these enzymes all act on 1,4-linked oligo-chitin like substrates, in contrast to poly- β -1,6-N-acetylglucosamine glycosyltransferases. Submission of the MatB protein sequence to the PHYRE2 webserver, which models 3D protein structures using known crystal structures as inputs (Kelley *et al.*, 2015) returned a putative protein model where 86% of the residues could be modeled with more than 90% confidence (Figure 2A). The GT2 domain could be modeled with 100% confidence, using BcsA of *Rhodobacter sphaeroides* (PDB 4hg6) as template and the CE4 domain was modeled with 100% confidence, using a combination of six oligo-chitin/GlcNAc peptidoglycan deacetylases (PDB 2c1l, 1ny1, 4nz3, 1w17, 4m1b, 4l1g) (Figure 2B). The structure of the N- and C-termini and the transmembrane helix that connects the two domains could only be modeled with low confidence. Nearly all amino acid residues involved in binding of the UDP-sugar moiety in various PNAG biosynthetic glycosyltransferases are conserved in MatB (Figure 2C; Figure S1; Figure S2), while residues in the active site of the MatB CE4 domain had very high

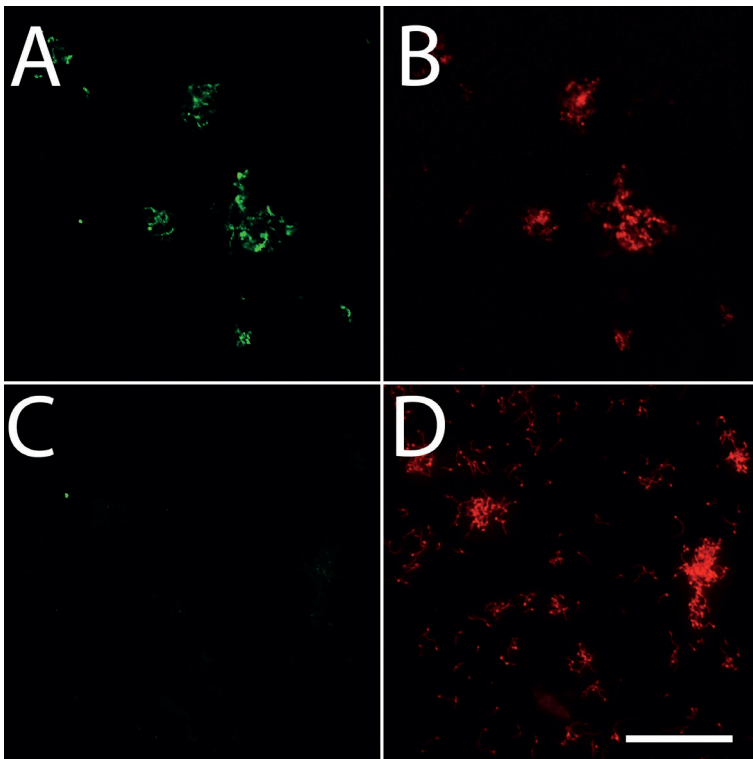


Figure 4. Immunofluorescence micrographs of *S. lividans* and its *matB* null mutant to identify extracellular PNAG. Young mycelia from 6 h old cultures of *S. lividans* 66 and its *matB* mutant were analyzed for the presence of PNAG with the specific monoclonal antibody mAb F598 and secondary anti-human IgG Alexa 488 conjugate. The presence of cells is indicated by the DNA binding dye SYTO 85. These experiment demonstrate that PNAG was produced by wild-type cells but not by *matB* mutants. Bar, 100 μ m.



homology to those of oligo-chitin deacetylases (Figure 2D). Interestingly, neither PNAG deacetylases nor chitin synthases share a high homology with the respective MatB domains, and phylogenetic analysis using a maximum-likelihood tree build places MatB in the middle for both CE4 or GT2 domains (Figure S3). Taken together, bioinformatics analysis predicted that MatB synthesizes poly-*N*-acetylglucosamine, which could be either in the (1,4)- or in the (1,6)-configuration.

MatB produces a PNAG-like EPS

To analyze if the Mat proteins may be involved in the biosynthesis of (1,3-) or (1,4-) glycans, hyphae of *S. lividans* 66 and its *matB* null mutant were stained with calcofluor white (CFW) (Wood, 1980a). Apical sites of both wild-type and *matB* mutant cells were stained with equal efficiency (Figure 3). This is contrary to the absence of staining in *csIA* null mutants, where the synthesis of (1,3)- or (1,4)-glycans is impaired (Xu *et al.*, 2008; Chaplin *et*

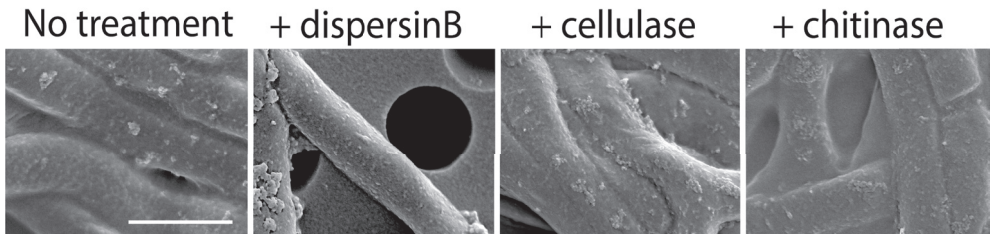


Figure 5. Effect of hydrolytic enzymes on the accumulation of EPS on hyphae of *S. lividans* 66. Mycelia of wild-type *S. lividans* 66 were treated with either 50 µg/ml dispersin B, 0.5 U/ml chitinase or 2 U/ml cellulase for 4 h. The biomass was imaged with cryoSEM to visualize the extracellular matrix. Note that treatment with dispersin B, which degrades PNAG, resulted in smooth hyphae. Bar, 1 µm.

al., 2015). *CsIA* and its partner *GlxA* synthesize a cellulose-like polymeric substance, which is also involved in the aggregation of *Streptomyces* in liquid-grown cultures (Petrus and Claessen, 2014). This strongly suggests that MatAB do not synthesize (1,3)- or (1,4)-glycans.

To further characterize the product of the MatAB enzymes, we used monoclonal antibodies (mAb F598) that specifically recognize both intact and deacetylated PNAG (Kelly-Quintos *et al.*, 2006). Mycelia obtained from 6 h liquid-grown cultures of *S. lividans* 66 or its *matB* mutant were fixed in 4% PVA and incubated overnight with mAb F598. After washing and incubation with a fluorescently labeled secondary antibody conjugate, mounting fluid containing SYTO85 was added to stain the DNA and samples were then imaged with a fluorescence microscope (Figure 4). Wild-type cells were strongly stained with mAb F598, indicating the production of a PNAG-like polymer. Co-localization with the DNA stain SYTO85 suggests that most PNAG-like molecules are located on the cell surface. Conversely, immunofluorescence microscopy of *matB* null mutants with mAb F598 only resulted in background fluorescence, strongly suggesting that the Mat proteins indeed synthesize PNAG or a highly related PNAG-like polymer.

To further ascertain the presence of PNAG, the mycelia were treated for 2 h with a

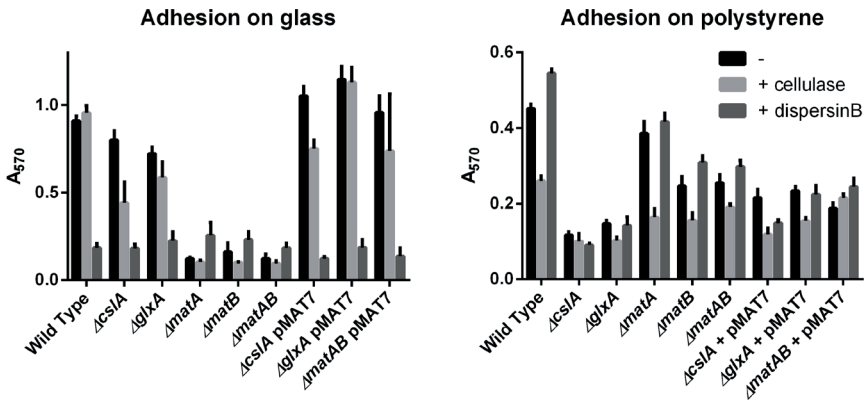


Figure 6. Quantification of attachment to solid surfaces. Surface attachment was quantified for *S. lividans* 66 and its respective *csIA*, *matA* or *matB* mutants with and without added Dispersin B or cellulase. Quantification was performed by staining attached cells with crystal violet and measuring dissolved crystal violet spectrophotometrically at 570 nm. The average and standard deviation of five independent wells are given. A) Surface attachment on glass from overnight growth B) Surface attachment to polystyrene after 7 days of growth.

suspension containing either chitinases, cellulases or dispersin B. Only dispersin B, which specifically degrades PNAG (Kaplan *et al.*, 2003), significantly affected EPS accumulation as visualized by SEM microscopy, further indicating that the extracellular *mat*-dependent EPS is indeed PNAG (Figure 5).

Mechanistic insight into *matA* and *matB* in relation to *csIA* and *glxA*

As mentioned above, the inhibition of mycelial pellet formation by *S. lividans* in liquid-grown cultures is not uniquely associated with *matA* or *matB*, but has also been observed when *csIA* and/or *glxA* are disrupted. When grown in liquid cultures the phenotypes of *csIA*, *glxA* or *matB* null mutants are phenotypically highly similar, with highly dispersed growth, highlighting the importance of both the *matAB* and *csIA-glxA* gene clusters for pellet formation. In an attempt to increase our understanding of how the two different EPSs might coordinate aggregation, we investigated the attachment behavior

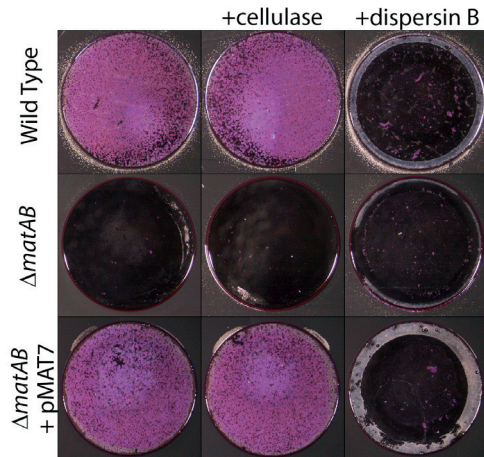


Figure 7. Visualization of adhesion to glass. *S. lividans* 66, its *matAB* null mutant and the *matAB* mutant complemented with pMAT7 grown for 20 h. Cellulase at a concentration of 0.2 U/ml had no effect on glass surface attachment, in contrast to 50 $\mu\text{g}/\text{ml}$ dispersin B, which efficiently inhibited attachment. Complementation of the *matAB* mutant with pMAT7 restored attachment, which could in turn be antagonized again by the addition of dispersin B.



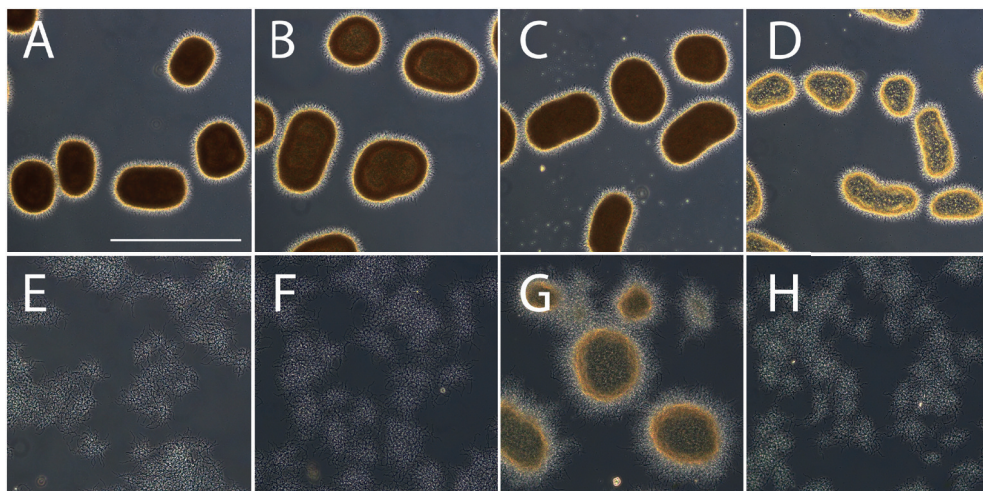


Figure 8. Effect of cellulase and dispersin B on mycelial morphology. Light micrographs show *S. lividans* 66 (A), *S. lividans* 66 treated with 2 U/ml cellulase (B), 100 µg/ml dispersin B (C) or both cellulase and dispersin B (D), the *matB* (E) and *csIA* mutants (F) and the *csIA* mutant harboring pMAT7 without (G) or with (H) added dispersin B. All strains were grown in TSBS medium for 24 h at 30°C. The effects on morphology were visualized by widefield microscopy. Bar, 500 µm.

on hydrophobic and hydrophilic surfaces, via adherence assays on glass and polystyrene, respectively. Attachment of the *matA* and *matB* mutants to polystyrene attachment was similar to that of the parental strain, while attachment of *csIA* or *glxA* mutants was strongly reduced (Figure 6A). Conversely, attachment to glass is mostly depended on *matA* and *matB*, and was less affected in the *csIA* or *glxA* mutants (Figure 6B and Figure 7). This indicates that the EPS produced by CslA and GlxA plays a dominant role in adherence to hydrophobic surfaces, while the PNAG produced by MatAB is particularly relevant for adherence to hydrophilic surfaces.

MatAB expression is responsible for pellet formation

Pellet formation in shaken liquid cultures appears to depend on both hydrophilic and hydrophobic adhesive forces, as deletion of either *csIA* or *matB* prevented pellet formation (Figure 8 E and F). However, it might be more complicated than the sum of the two factors, as the addition of high concentrations of either cellulase (2 U/ml) or Dispersin B (100 µg/ml) was unable to alter the phenotypic characteristics of pellets (Figure 8 A-C). A mix of both enzymes did induce a morphological change, but did not prevent pellet formation, indicating that more factors determine the integrity of pellets than the *csIA*- and *matAB*-dependent EPSs (Figure 8 D). However, pellet formation could be restored to *csIA* mutants by the introduction of the pMAT7 construct, which over-expresses *matAB* from the strong constitutive *gapA* (SCO1947) promoter (Figure 8 G and H). Importantly, this MatAB-driven complementation of pellet formation by *csIA* mutants could be readily antagonized by the

addition of dispersin B, which underlines that PNAG formation was responsible for the complementation. These data indicate that the enzymatic resistance of native pellets is the result of the complex composition of the extracellular matrix. Finally, we tested if addition of *matAB* to an actinomycete that does not have the genes on its chromosome would be sufficient to alter the mycelial morphology. As a test system we used the non-pelleting *Saccharopolyspora erythraea*. Introduction of plasmid pMAT7 into the strain indeed induced pellet formation, and again this phenotype was reversible by the addition of the PNAG-antagonizing enzyme dispersin B (Figure 9). The heterologous production of PNAG by MatAB shows that the presence of this polymer by itself suffices to induce pellet formation in filamentous actinomycetes, which opens new perspectives for morphological engineering approaches.

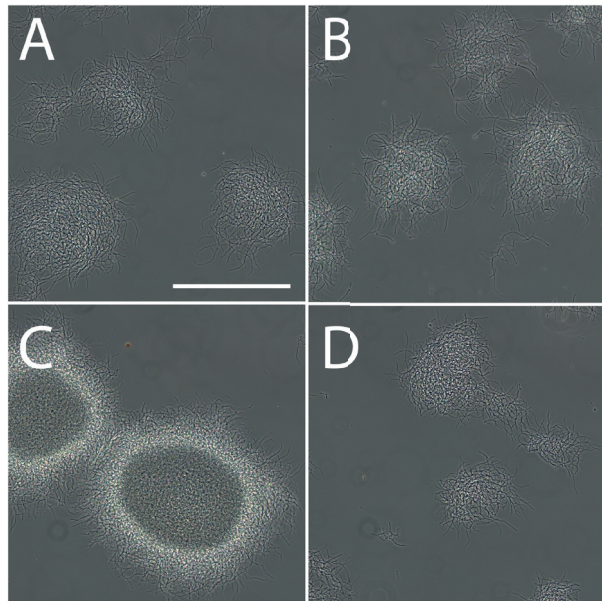


Figure 9. Effect of dispersin B on the mycelial morphology of *Saccharopolyspora erythraea*. *S. erythraea* transformants harboring the empty vector pSET152 (A and B; control) or pMAT7 (C and D) were grown for 24 h in TSBS media with (B and D) or without (A and C) 50 µg/ml dispersin B. The effects on mycelial morphology were visualized by widefield microscopy. Note the increased aggregation of *matAB* transformants, which could be reversed by adding dispersin B. Bar, 200 µm.

DISCUSSION

Members of the multicellular filamentous genus *Streptomyces* have an innate ability to self-aggregate in liquid-grown cultures, with the mycelia of several species forming dense pellets. This mode of aggregation contrasts with other surface-attached biofilms, which typically consist of aggregating single cells, held together by an extracellular matrix (Vlamakis *et al.*, 2013; Claessen *et al.*, 2014). The matrix contributes to structural integrity of the multicellular community, while simultaneously providing protection against various stresses (Scher *et al.*, 2005; Romero *et al.*, 2010; DePas *et al.*, 2013). Multiple matrix layers may be formed, with an outer layer containing a soluble EPS and a core with insoluble EPS and hydrophobic proteins (Sheng *et al.*, 2006). While matrices are usually mentioned in the context of biofilms, streptomycetes also make extracellular substances that contribute to morphology. Pellets of *S. coelicolor* were proposed to contain extracellular DNA (eDNA) and hyaluronic acid, and interference with these matrix components resulted in (partial)



disintegration of mycelial pellets (Kim & Kim, 2004). In this work, we report the discovery of a similarly multi-layered and multi- component system in *Streptomyces*. Besides the previously identified cellulose-like EPS that is produced by the action of CslA and GlxA, we here show that the MatAB enzymes produce PNAG, which is also a well-known EPS that plays a role in biofilm formation by many planktonic bacteria (Wang *et al.*, 2004, Roux *et al.*, 2015, Mack *et al.*, 1996, Beenken *et al.*, 2004). These data strongly suggest that the formation of pellets by liquid-grown mycelia of streptomycetes may be based on the same principles as the formation of biofilms by planktonic bacteria. This apparently supports the hypothesis that hyphal growth of mycelial microorganisms may have evolved from the less permanent aggregation of single cells (Claessen *et al.*, 2014). Adhesion assays with glass (hydrophilic) and polystyrene (hydrophobic) revealed that PNAG is primarily responsible for adhesion to hydrophilic surfaces (*i.e.* to glass), while the cellulose-like EPS promotes hydrophobic adhesion (to polystyrene). Both types of EPS play a crucial role in the maintenance of mycelial pellets in submerged cultures, and deletion of either *csIA* (Xu *et al.*, 2008) or *matAB* (van Dissel *et al.*, 2015) results in highly dispersed growth, although overexpression of *matAB* is sufficient for the formation of pellets by *csIA* null mutants. With both systems present, the obtained rigidity of the pellet architecture is more than the sum of its parts, as indicated by the resistance against the combination of dispersin B and cellulases. In *S. epidermis*, PNAG has been linked to adherence to both hydrophilic and hydrophobic surfaces (Cerca *et al.*, 2005). Why PNAG alone is not enough for hydrophobic adherence in *Streptomyces* requires further investigation, but might be related to the larger multicellular size of the organism, requiring a greater force for adherence. Although not understood in detail, hydrophobic adherence of *Streptomyces* is likely the result of a more complicated system, which besides the product of CslA also involves the hydrophobic chaplin proteins (de Jong *et al.*, 2009). As the chaplins are expressed late in the life cycle, involvement of these proteins might also explain why strong attachment to polystyrene is a multi-day process (de Jong *et al.*, 2009). Chaplins are also involved in pellet formation, although the absence of the chaplin layer has less severe morphological consequences than lack of the cellulose-like or PNAG-based EPSs (unpublished data). The chaplin based hydrophobic forces, likely located in the core of a pellet, might contribute to strengthening the pellet, but cannot fully explain the role of CslA/GlxA in cellular aggregation. Earlier work indicated that the polymer produced by CslA/GlxA plays a role in stabilization of the tip complex (Xu *et al.*, 2008), which might explain its pleiotropic involvement in multiple systems throughout the life cycle. We can speculate that aggregation by PNAG is to some extent dependent on the proper organization of the tip complex supported the polymer produced by CslA/GlxA. It is our hope that high resolution spatial co-localization studies of CslA/GlxA, the chaplins and MatAB in native pellets, currently in progress in our laboratory, shed light on the involvement of these systems and their interactions in controlling the mycelial architecture.

Understanding how hyphal aggregation and pellet formation is controlled brings us one step closer to controlling the morphology of streptomycetes in liquid-grown cultures, which

is highly relevant for tuning the morphology to product formation (Celler *et al.*, 2012; van Dissel *et al.*, 2014) After all, several antibiotics such as erythromycin (produced by *Saccharopolyspora erythraea*) and actinorhodin (by *S. coelicolor*) are solely produced when a minimum pellet size is achieved, while enzyme production is typically favored by fast growing and fragmenting hyphae (Wardell *et al.*, 2002b; van Wezel *et al.*, 2006b). Previously, primarily genetic approaches were followed to tune mycelial morphology. Over-expression of *srgA*, which controls hyphal morphogenesis and activates cell division (Noens *et al.*, 2007; Traag and Wezel, 2008), effects fragmentation of the hyphae by enhancing cell division, resulting in increased growth and enzyme production rates (van Wezel *et al.*, 2006b). However, a drawback to this approach is the major effect of *SrgA* on the cell cycle, with enhanced sensitivity to shear stress as a result. In this respect morphological engineering targeting extracellular glue-like substances such as PNAG- and cellulose-like EPSs, offers an attractive alternative, as the effects on the internal physiology are likely minimal. Thus, besides their high relevance for our ecological understanding of how streptomycetes grow and attach to surfaces in their natural environment, the insights gained by this work may also help to develop novel technologies that improve growth and productivity of streptomycetes.

ACKNOWLEDGEMENTS

We like to thank Marleen Janus for the supply of *A. actinomycetemcomitans* gDNA and Ellen de Waal for the production of dispersin B. The research was supported by VIDI grant 12957 and VICI grant 10379 from the Netherlands Technology Foundation STW to DC and GVW, respectively.



SUPPLEMENTAL INFORMATION

Table S1: Oligonucleotides

| Name | Sequence |
|-----------|---|
| MatB_Rev | ATCGGATCCTCATCCGACCGGCTCCCGTCCATGGC |
| MatA_Fw | CAGTGAATTCATATGGGGCCGGTTCGGCCGACGAGTGCTC |
| PgapA_Fw | AGTCGAATTCATCGGTACGTCACCGACCC |
| PgapA_Rev | ACTGTCTAGAGGATCCCATATGCCGATCTCCTGTTGGTACGCC |

Table S2: Similarities between matB and characterized glycosyltransferases type2 and carbohydrate esterase type 4 as found on the cazy database by blastp. Based on the annotation of the GT2 and CE4 domain found in matA its translated protein sequence was compared with similar typed proteins for which there is experimental evidence as tracked by the CAZY database. Two blast databases were made of the 266 GT2 proteins and the 58 CE4 proteins. The top 10 hits and the scores for both databases are given in the table.

blastP versus characterized glycosyltransferase type 2

| Uniprot | Gene | Organism | Discription | Score | E-value |
|---------|----------------|--|---|-------|---------|
| P75905 | <i>pgaC</i> | <i>Escherichia coli (K12)</i> | Poly-beta-1,6-N-acetyl-D-glucosamine synthase | 157 | 3E-43 |
| C8YH7 | <i>pgaC</i> | <i>Acinetobacter baumannii</i> | Poly-beta-1,6-N-acetyl-D-glucosamine synthase | 151 | 2E-41 |
| Q5HKQ0 | <i>icaA</i> | <i>Staphylococcus epidermidis</i> | Poly-beta-1,6-N-acetyl-D-glucosamine synthase | 150 | 6E-41 |
| Q5VJB2 | <i>aagC</i> | <i>Aggregatibacter actinomycetemcomitans</i> | Poly-beta-1,6-N-acetyl-D-glucosamine synthase | 140 | 2E-37 |
| Q5QFG3 | <i>aagC</i> | <i>Actinobacillus pleuropneumoniae</i> | Poly-beta-1,6-N-acetyl-D-glucosamine synthase | 137 | 2E-36 |
| Q84GC8 | <i>hasA</i> | <i>Streptococcus equi subsp. zooepidemicus</i> | Hyaluronan synthase | 89 | 2E-20 |
| O50201 | <i>hasA</i> | <i>Streptococcus dysgalactiae subsp. equisimilis</i> | Hyaluronan synthase | 89 | 2E-20 |
| Q9LJP4 | CLSC4 | <i>Arabidopsis thaliana</i> | Xyloglucan glycosyltransferase 4 | 87 | 1E-19 |
| P74165 | <i>sll1377</i> | <i>Synechocystis sp. (PCC 6803)</i> | Beta-monoglucosyldiacylglycerol synthase | 86 | 3E-19 |
| Q8YMK0 | <i>all4933</i> | <i>Nostoc sp. (PCC 7120)</i> | Beta-monoglucosyldiacylglycerol synthase | 85 | 4E-19 |

blastP versus characterized carbohydrate esterase type4

| Uniprot | Gene | Organism | Discription | Score | E-value |
|---------|-------------|---|---|-------|---------|
| Q81AF4 | BC_3618 | <i>Bacillus cereus (ATCC 14579)</i> | Peptidoglycan N-acetylglucosamine deacetylase | 140 | 3E-40 |
| Q8RBF4 | <i>cda1</i> | <i>Caldanaerobacter subterraneus</i> | chitin deacetylase | 133 | 2E-36 |
| Q81EK9 | BC_1960 | <i>Bacillus cereus (ATCC 14579)</i> | Peptidoglycan N-acetylglucosamine deacetylase | 123 | 2E-33 |
| Q8Y9V5 | lmo0415 | <i>Listeria monocytogenes serovar</i> | Peptidoglycan N-acetylglucosamine deacetylase | 125 | 5E-33 |
| P72333 | <i>nodB</i> | <i>Rhizobium sp. (N33)</i> | Chitooligosaccharide deacetylase | 120 | 7E-33 |
| P02963 | <i>nodB</i> | <i>Rhizobium meliloti</i> | Chitooligosaccharide deacetylase | 119 | 1E-32 |
| Q1M7W8 | <i>nodB</i> | <i>Rhizobium leguminosarum</i> | Chitooligosaccharide deacetylase | 118 | 3E-32 |
| P04339 | <i>nodB</i> | <i>Rhizobium leguminosarum bv. viciae</i> | Chitooligosaccharide deacetylase | 118 | 3E-32 |
| P50355 | <i>nodB</i> | <i>Rhizobium sp. (NGR234)</i> | Chitooligosaccharide deacetylase | 118 | 3E-32 |
| P50354 | <i>nodB</i> | <i>Rhizobium galegae</i> | Chitooligosaccharide deacetylase | 118 | 3E-32 |

| Protein | Organism | |
|---------|---------------------------------------|--|
| NodB | <i>Rhizobium sp. N33</i> | ----- |
| BC1960 | <i>Bacillus cereus</i> | ----- |
| LM00415 | <i>Listeria monocytogenes serovar</i> | MKIRWIRLSLVAILIIIVAVFIGVIGFQKYQFSKSRNKVIMQMDRLMKDQDGGNFRRLDKK |
| MatB | <i>Streptomyces coelicolor</i> | ----- |
| BC3618 | <i>Bacillus cereus</i> | ----- |
| Cda1 | <i>Caldanaerobacter subterraneus</i> | ----- |
| | | |
| NodB | <i>Rhizobium sp. N33</i> | ----- |
| BC1960 | <i>Bacillus cereus</i> | ----- |
| LM00415 | <i>Listeria monocytogenes serovar</i> | ENGVEIISYI PKTTEKKDNEIIQKEIGKATDAEVKLLNRDKETQGIIFVTVQKHRMAEQA |
| MatB | <i>Streptomyces coelicolor</i> | -----MASST |
| BC3618 | <i>Bacillus cereus</i> | ----- |
| Cda1 | <i>Caldanaerobacter subterraneus</i> | ----- |
| | | |
| NodB | <i>Rhizobium sp. N33</i> | ----- |
| BC1960 | <i>Bacillus cereus</i> | ----- |
| LM00415 | <i>Listeria monocytogenes serovar</i> | ISYKAVQSEYVKEGRTEFVLDKDKDICKNIIVTAETGALLTLGEVLIKSNQTKLNLKTAV |
| MatB | <i>Streptomyces coelicolor</i> | RRHGA--ARSAREGSRRLP-----LRLLPLLVLVAL--VAM---LM |
| BC3618 | <i>Bacillus cereus</i> | ----- |
| Cda1 | <i>Caldanaerobacter subterraneus</i> | -----MRFKS-----FAITLLVLSILVGS--VAFAYKYIT |
| | | |
| NodB | <i>Rhizobium sp. N33</i> | ----- |
| BC1960 | <i>Bacillus cereus</i> | -----MYFFYSPEMFAPYQW |
| LM00415 | <i>Listeria monocytogenes serovar</i> | EEELIKTGDFSLKDVGN--LGKIKSL-----VKWNQTFEITNSEIILPVKIPGAAPEP- |
| MatB | <i>Streptomyces coelicolor</i> | L-----RGYVHS----- |
| BC3618 | <i>Bacillus cereus</i> | ----- |
| Cda1 | <i>Caldanaerobacter subterraneus</i> | EDKYLQTNFYSANQKENVNLNTLSDKSNNSKITISEERPLSETEQNVVSSSTPEPSTPEKV |
| | | |
| NodB | <i>Rhizobium sp. N33</i> | -----MKNVDYMCVPE-----SDCA |
| BC1960 | <i>Bacillus cereus</i> | GLERDVSAYMPYNSFYGDYINSLPYAIPQNYEVQMKADDRGWSWTFPSWVEKYAYAFS |
| LM00415 | <i>Listeria monocytogenes serovar</i> | -----KKVKVKLADIASSVKNRYLPSS-----VKVPEVP |
| MatB | <i>Streptomyces coelicolor</i> | LADHRVQ---PPAA-----TDKVPQKILEGGFVLDV-----RGGRTES |
| BC3618 | <i>Bacillus cereus</i> | -----MLLRK-ELEP-----TGVTWE |
| Cda1 | <i>Caldanaerobacter subterraneus</i> | LEKHNKDLNDPNISQFLLNFVNRPERDKLFGS-PVAF-----SKKVLGS |
| | | |
| BC1960 | <i>Bacillus cereus</i> | GPYNKAEVALTFDDGDFLETPKILDKLQHNVKATFFLLGENAEKFFNIVKRIANECHV |
| LM00415 | <i>Listeria monocytogenes serovar</i> | KAKTNKRIALTFDDGSSSVTPGVLDLTKRHNVKATFFVLGSSVIQNPGLVKRELEEGHQ |
| MatB | <i>Streptomyces coelicolor</i> | LSVPDHRVLVTFDDGDPDPTWTPRVLVDLKKHDAHA FVVTGTMASRYPDVLRMVDGEGE |
| BC3618 | <i>Bacillus cereus</i> | VPNNEKI IAITFDDGDPDPTYTQVLDLRLQYKAEATFFMIGFRVQRNPNVQVQLKEGHE |
| Cda1 | <i>Caldanaerobacter subterraneus</i> | NPSSGKEVALTFDDGDFPIYTEKIVDILKSMVDKATFFVIGRHAEKHPELILKYIVENGENE : :***** * : * * . * * : * . * : . : * |
| | | |
| NodB | <i>Rhizobium sp. N33</i> | VANHTMTHPDLSRCEPGEVEIREIVEASNAIRMACPQATVRRMRAPYGVVWTEVDLVT--- |
| BC1960 | <i>Bacillus cereus</i> | IGNHTYSHPNLAKVNEDEYRNQIIKTEELNRLA-GYAPKFI RPPYGEILENQLKW--- |
| LM00415 | <i>Listeria monocytogenes serovar</i> | VGSHSWDHPQLTKQSTQEVYNYLTKTQKAVFDQT-GYFPTTMRPPYGA VNKQVAEE--- |
| MatB | <i>Streptomyces coelicolor</i> | VGLHTFNHPDLSFQSEKRI DWELSQNLAI FGAA-GVPTLSFRPPYSFADAMDNKSWPV |
| BC3618 | <i>Bacillus cereus</i> | IGNHTMNHLYASNSDEKLENDLIDGKG-FFEKW-VKEPLFRPPGGYINDAVFKT--- |
| Cda1 | <i>Caldanaerobacter subterraneus</i> | IGLHSYSHFNMKCLKPEKMVEELYKTQIIVEAT-GIKPTLFRPPFGAYNSTLIEI--- : . * : * : * * . |
| | | |
| NodB | <i>Rhizobium sp. N33</i> | ---SARAGLACVH--WSVDPDRWARPGVDAIVDEVLTVGPEGATVLLHDGWPEELKSATY |
| BC1960 | <i>Bacillus cereus</i> | ---ATEQNFMIVQ--WSVDVVDWKGVSADTITNNVLGNSFPGSVILQHSVTPGGH--- |
| LM00415 | <i>Listeria monocytogenes serovar</i> | -----IGLPIIQ--WSVDTEWKYRNAGIVTKKVLGATDGAIVLMDIHK----- |
| MatB | <i>Streptomyces coelicolor</i> | TEYIGGRGYLVVW--NNDTSEDWKKPGVDEIIRRA TPKGKGAIVLMDHSGG-D--- |
| BC3618 | <i>Bacillus cereus</i> | ---AKEAGYQTVLMSWHODPRDMPGVESIVNVVVKNAKSGDVI LLDHGGN-D--- |
| Cda1 | <i>Caldanaerobacter subterraneus</i> | ---SNAIGLKVVL--NNDVDPDRNPNPVSVVNRVLSHTRDGSIIIMHEGKP----- : : * * * : * * : * * * * |
| | | |
| NodB | <i>Rhizobium sp. N33</i> | ASLRDQVTVLALSRILPALHHRGCFVIRPLPQH-- |
| BC1960 | <i>Bacillus cereus</i> | ---LQGSVDALDKIIPQLKTKGAREVTLPSMFTQSKERK |
| LM00415 | <i>Listeria monocytogenes serovar</i> | ---TAAASLDTTLTKLKSQGYEFVITIDELYGEKLQIGKQ----YFDKTD-----S |
| MatB | <i>Streptomyces coelicolor</i> | ---RHQTVQALDRFLPDLKKKGYEFDNLTEALDAPGAMS PVTGAELWKGRAWVFLVQASE |
| BC3618 | <i>Bacillus cereus</i> | ---RSQTVAAALAKILPELKKQGYRFTVTSSELLRYKH |
| Cda1 | <i>Caldanaerobacter subterraneus</i> | ---SLLAALPQIKLKEEGYKFTVTSLELLEKRD----- : : * : * : * : * : * |
| | | |
| NodB | <i>Rhizobium sp. N33</i> | ----- |
| BC1960 | <i>Bacillus cereus</i> | ----- |
| LM00415 | <i>Listeria monocytogenes serovar</i> | RMVK- |
| MatB | <i>Streptomyces coelicolor</i> | KLTDGLVVGLAVIGTLVIGRFVMLLLLSGVHARRVRRRRFRWGPVAVTEPVT |
| BC3618 | <i>Bacillus cereus</i> | ----- |
| Cda1 | <i>Caldanaerobacter subterraneus</i> | ----- |

Figure S1: Alignment of translated amino acid sequences of selected CE4 genes with the CE4 domain of MatB (aa1-aa363) using ClustalQ. CE4 homologs represent the top blastp results of MatB versus characterized carbohydrate esterase type4 genes in the CAZY database. Marked in gray are the conserved amino acids. Marked in red are the conserved amino acids not conserved in MatB.



| Protein | Organism | |
|---------|--|---|
| MatB | <i>Streptomyces coelicolor</i> | ----- |
| IcaA | <i>Staphylococcus epidermidis</i> | -----MHVFNFLFFYPFMSIYIYVGSYYFFIKEKFF |
| PgaC | <i>Acinetobacter baumannii</i> | -----MSVFEILSIFVYVYPAGMAIYWFAGACYLFEKGL |
| AagC | <i>Actinobacillus pleuropneumoniae</i> | -----MLIEIFSLFVFAYPAMFAYWAFAGLTYFLFEKGL |
| PgaCD | <i>Escherichia coli</i> | MINRIVSFFILCLVLCPLCLVAYFHSGLMMEFVFFWFFSFMIMWIVGGVYFVYRERHW |
| AagC | <i>Aggregatibacter actinomycetemcomitans</i> | -----VMVGLWFFFKREYHE |
| MatB | <i>Streptomyces coelicolor</i> | ---WGP-----AVTEPVTVLVPAYNEAKICIENTVRSLVASDHP-VEVIIDGGSSDCT |
| IcaA | <i>Staphylococcus epidermidis</i> | NRSLL--VKSEHQQVEGISPLLACYNESETVQDTLSSVLSLEYPEKEIIINDGSSDNT |
| PgaC | <i>Acinetobacter baumannii</i> | NEPISRYLPG---EQVPMISLMVFCYNEGNLDESIPHLQLRYPNYELIFINDGSKDNT |
| AagC | <i>Actinobacillus pleuropneumoniae</i> | VPPNFQDMKH---EEVPLVSLMVFQYNSDNLEDAIPLHLNKYPNYELIFINDGSKDNT |
| PgaCD | <i>Escherichia coli</i> | --PWGENAPAPQLKDNPSISIIIFCNEKEVVEETHAALAQRYENIVETAVNDGSDTKT |
| AagC | <i>Aggregatibacter actinomycetemcomitans</i> | --Q---QLPEP--SSEGCSSIIIFCNEAEQVRQTIYVALQTKYPNFEIVAVNDGSSDST ::: :. : * * : : : : : : : : * * : * * : * * * |
| MatB | <i>Streptomyces coelicolor</i> | ARIVEGLGL--PGVRVIRQ-LNAGKPAALNRRGLANARYDIVVMDGCTVFPFESVRELVQ |
| IcaA | <i>Staphylococcus epidermidis</i> | AEIYDFKKN-HDFKFDVLEVNRRKANALNEGIKQASYEYVMCLDADTVIIDDAPFYMI |
| PgaC | <i>Acinetobacter baumannii</i> | AEVIDRWAKEPRITALHQ-ENQKASALNHGLTVAKGKYVACIDGDAVLDDYALDYMVQ |
| AagC | <i>Actinobacillus pleuropneumoniae</i> | GEIIDKWKAKRKRIVALHQ-ANSKASALNGLRIARGKYVCGIDGDAVLDDYALDYMVQ |
| PgaCD | <i>Escherichia coli</i> | RAILDRMAAQIPLHRLVHLAQNCKGKIALTKGAAAKSEYLVCGDGDALLDRDAAYIVE |
| AagC | <i>Aggregatibacter actinomycetemcomitans</i> | AEILDELAQDARLRVHVAENCKGKAVLRSGLVLSKYEYLVCGDGDALLHPHVAFLWLMQ : : : : : * * * * * : : : : * * : * * : : : : : |
| MatB | <i>Streptomyces coelicolor</i> | PF-GDPRVGVACNAKVGKNDKSLIGAWHIEYVWGNLDRRMYDVLQCMPTIFGAVGAER |
| IcaA | <i>Staphylococcus epidermidis</i> | DFKKNPKLGAVTGNPRIRNKSSILGKIQTIEYASITGCIKRSQSLAGAINITISGVVTFLE |
| PgaC | <i>Acinetobacter baumannii</i> | ALEQDPKYAATTGNPRVNRNSTILGRLQVSEFSSIIIGLINRAQGLMGTIFTVSGVCCLE |
| AagC | <i>Actinobacillus pleuropneumoniae</i> | ALESNPRYGAVTGNPRVNRNSTILGRLQVSEFSSIIIGLKRACGLMGTIFTVSGVCCLE |
| PgaCD | <i>Escherichia coli</i> | PMLYNPRYGAVTGNPRIRNRSTLVGKIQVGEYSIIIGLKRQRIRYGNVFTVSGVIAAF |
| AagC | <i>Aggregatibacter actinomycetemcomitans</i> | PFLNFRIRYGAVTGNPRILNRSTILGRLQVSEFSSIIIGLKRQRIRYGNVFTVSGVIAAF : * : * : * : * : * : * : * : * : * : * : * : * : * : * : * : * : * : * : * |
| MatB | <i>Streptomyces coelicolor</i> | RSALEPIGGSSDDTLAEDTDVIMALHRAGRVVYAENARAWTAEEESVCGQLWSQRYSY |
| IcaA | <i>Staphylococcus epidermidis</i> | KSALKDVGWDTDMITEDIASWKLHLDFDEKYEPRALCWMVLPEITIGGLWQRVRWAO |
| PgaC | <i>Acinetobacter baumannii</i> | KDVMEETGGWSTNMITEDIISWKIQTSGYDIFYEPRALCWMVLPEITINGLWQRVRWAO |
| AagC | <i>Actinobacillus pleuropneumoniae</i> | KDIMFEITGGWSTNMITEDIISWKIQTSGYDIFYEPRALCWMVLPEITINGLWQRVRWAO |
| PgaCD | <i>Escherichia coli</i> | RSALAEVYGSDDMITEDIISWKLQNLQMTFFYEPRALCWMVLPEITLGLWQRVRWAO |
| AagC | <i>Aggregatibacter actinomycetemcomitans</i> | KTALVRVGFWSDDKITEDIISWKLQMDHWDQIIPALCYIYMBETLGLWQRVRWAO : : * : : : * * : : : : : * : * : * : * : * : * : * : * : * : * |
| MatB | <i>Streptomyces coelicolor</i> | GTMQAIWKHRAVIEKPGSGRFGRVGLPFVS---LFMVLAFLAPLIDVFLLYLGVFGPT |
| IcaA | <i>Staphylococcus epidermidis</i> | GGHEVLRDFWPTIKTKKLSLVIMFEGIASITVWYIVLCLYSPLVITANI-LDITYLKY |
| PgaC | <i>Acinetobacter baumannii</i> | GGAEITIMKYFSKIWHNRRLWPMYIEYFATVIAFLVLLVALIALQRYI-FDISI--E |
| AagC | <i>Actinobacillus pleuropneumoniae</i> | GGAEITMMKYFQIWLKNRRLWPMYIEYIVTAVASLLVLSILG-SIYNLI-FDNQIGLL |
| PgaCD | <i>Escherichia coli</i> | GGAEVFLKNMTRLWRKNFRMWFYEFYICLTTIWAFTCLVGFIIYAVQLA-GVPLNIET |
| AagC | <i>Aggregatibacter actinomycetemcomitans</i> | GGVEVLLEYIPKMKLRLRRLMVMLEALISISINYSVMIFILFVFLGVLDLPQQFQIN * : |
| MatB | <i>Streptomyces coelicolor</i> | EKTIVAWLVLA----IQAVCAA-YAFRLDREKLTPLISLPLQOILYRQIMYVY---L |
| IcaA | <i>Staphylococcus epidermidis</i> | SFSIFFSSFTMTFINIIQTVALFIDSRYEKKNIV---GLIFLSWYBTLYWVINAUVV |
| PgaC | <i>Acinetobacter baumannii</i> | NMGLFETNISIMFFAPFLCCLLGLYIDSQYERN-LL--RYGLSICIWYEVYVWLLNTVTL |
| AagC | <i>Actinobacillus pleuropneumoniae</i> | DWAEKPSIAILFIAFFTQLSISYIDNRVEKGVV---KYAFSCIWYEWLYWLSNLTITL |
| PgaCD | <i>Escherichia coli</i> | HIAATHAGIILLCTLCLLQFIVSIMTENRYEHN-LP---SSLFMIWFVIFWMLSLATT |
| AagC | <i>Aggregatibacter actinomycetemcomitans</i> | S-LMPQYGVILGGTCLVQFLVLSLWIDHRVDRGRLE---RNYIYMWYVLEFLFWLLTLFTS * : |
| MatB | <i>Streptomyces coelicolor</i> | L---QSWITALTGGRLRWOKLRRSGGVSAPPAGDGVPPQRSGAMDGRPVG |
| IcaA | <i>Staphylococcus epidermidis</i> | IMAFPALKRKKGGYATWSSPDRGNIQR----- |
| PgaC | <i>Acinetobacter baumannii</i> | LIGIPKAIFRNKSKPAVWTSVDRGV----- |
| AagC | <i>Actinobacillus pleuropneumoniae</i> | LCGIPKAIFRNKTKLAVWTSVDRGV----- |
| PgaCD | <i>Escherichia coli</i> | LVSFTRVLMPPKQRARWVSDRGI LR----- |
| AagC | <i>Aggregatibacter actinomycetemcomitans</i> | VVAVPKTI-FNTKKRARWVSDRGRFGDHS----- : : : : * : * : * |

Figure S2: Alignment of translated amino acid sequences of selected GT2 genes with the GT2 region of MatB (aa354-aa734) using ClustalQ. GT2 homologs represent the top blastp results of MatB versus characterized glycosyltransferase type 2 genes in the CAZY database. Marked in gray are the conserved amino acids. Marked in red are the conserved amino acids not conserved in MatB.

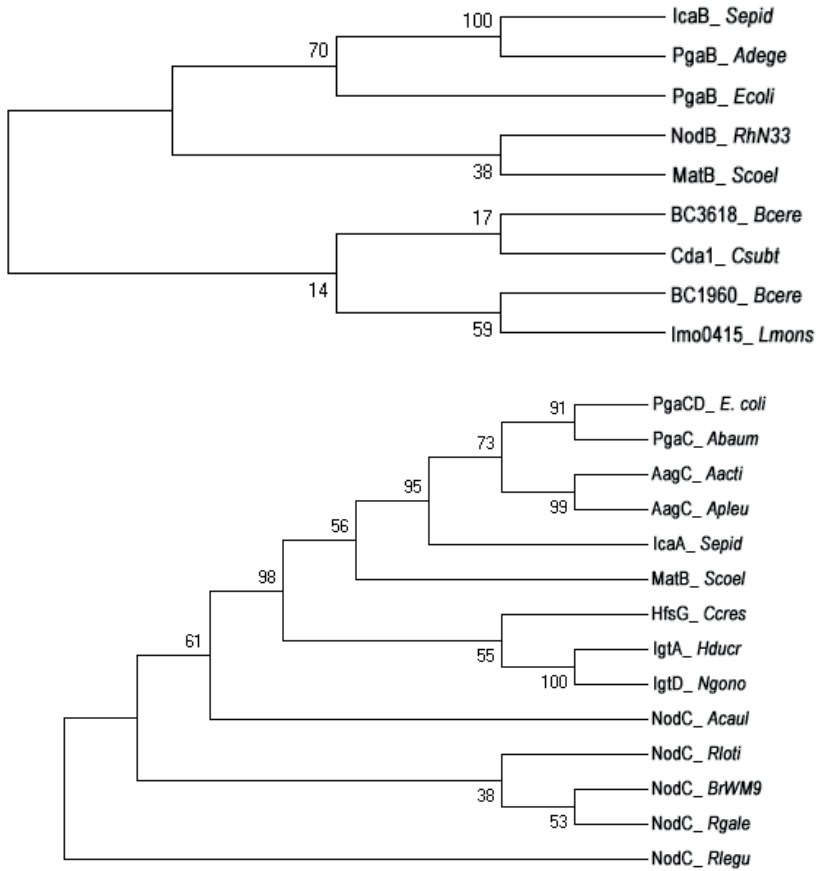


Figure S3: Probably evolutionary origin of the *matB* domains. Bootstrapped consensus tree calculated from the maximum likelihood JTT matrix based model to indicated the evolutionary history of the deacetylase domain of *matB* with selected PNAG deacetylases and the top 5 blast hits (A) and the glycosyl transferase domain was compared to the top 5 blast hits, consisting of PNAG glycosyltransferases and selection of 1,4-GlcNAc containing synthases (B). The consensus tree was calculated with the translated amino acid sequences using MEGA 7. The sequences were aligned using the clustalW algorithm using default settings and the maximum likelihood tree was calculated with a bootstrap of 500 replicates and default settings. Strains and their shortened names used for this comparison are: *Staphylococcus epidemidis*; *Sepid*, *Rhizobium sp. N33*; *RhN33*, *Ammoniflex degensii*; *Adege*, *Escherichia coli*; *Ecoli*, *Streptomyces coelicolor*; *Scoel*, *Bacillus cereus*; *Bcere*, *Caldanaerobacter subterraneus*; *Csubt*, *Listeria monocytogenes serovar*; *Lmons*, *Acinetobacter baumannii*; *Abaum*, *Aggregatibacter actinomycetemcomitans*; *Acti*, *Actinobacillus pleuropneumoniae*; *Apleu*, *Caulobacter crescentus*; *Ccres*, *Haemophilus ducreyi*; *Hducr*, *Neisseria gonorrhoeae*; *Ngono*, *Azorhizobium caulinodans*; *Acaul*, *Rhizobium loti*; *Rloti*, *Bradyrhizobium WM9*; *BrWM9*, *Rhizobium galegae*; *Rgale*, *Rhizobium leguminosarum*; *Rlegu*.



5

Control of pellet morphology by altering the timing of *matAB* transcription

van Dissel, D., & van Wezel, G.P.

ABSTRACT

The filamentous lifestyle of *Streptomyces* species limits the efficiency of submerged fermentations. Depending on the strain and culturing conditions, streptomycetes grow either as dispersed mycelia or as aggregated pellets during fermentation. Dispersed mycelia are characterized by faster growth, but also by higher viscosity, which negatively affects culture rheology. Pellets hardly affect the viscosity, but in turn are associated with slow growth and prolonged fermentation time. Here, we applied the Ostwald–de Waele power law model to compare rheology and growth of the pellet-forming *Streptomyces lividans* and its *matAB* mutant, which fails to produce the pellet-inducing poly-*N*-acetylglucosamine (PNAG). To create a strain with fast growth and better rheology, we placed *matAB* under the control of two different promoters that are transcribed later during growth, so as to activate aggregation at the end of the exponential growth phase. The recombinant strains showed more aggregation and resulted in up to eight times lower biomass-specific viscosity than the *matAB* mutant, whilst maintaining the 60% faster growth rate compared to wild type *S. lividans*. This is a step towards the best of both worlds, namely a production host that has a high maximum growth rate, whilst limiting the increase in viscosity typical of dispersed mycelia.



INTRODUCTION

Streptomyces are industrial bacteria that produce the majority of naturally occurring antibiotics, numerous anti-cancer compounds and a wide range of industrially relevant enzymes (Barka *et al.*, 2016, Bérdy, 2005, Hopwood, 2007). In contrast to most prokaryotes this phylum grows as multicellular filaments (Claessen *et al.*, 2014). Their filamentous life style negatively influences the rheology during industrial fermentation (van Dissel *et al.*, 2014). Especially high biomass concentrations lead to an enormous increase of the apparent viscosity, and hence a decrease in mixing efficiency, while lowering the oxygen transfer rates and increasing shear forces and thus cell lysis (Wucherpfennig *et al.*, 2010). This potentially results in a decrease in productivity, especially during large scale fermentation, which generally has lower agitation intensities (van't Riet & Tramper, 1991). The extent to which the rheology is altered is highly dependent on the morphology. In particular mycelia growing as loose or dispersed filaments, also referred to as mycelial mats, may lead to tremendous increase in the viscosity as a result of hyphal entanglement, resulting in a culture composition with non-Newtonian characteristics (Metz *et al.*, 1979).

Besides dispersed growth, many *Streptomyces* species aggregate into self-immobilized biofilms, typically referred to as pellets. Pellets do not significantly influence the viscosity, and measurements with filamentous fungi showed that pellets only induce pseudoplastically at very high biomass concentrations (Kim *et al.*, 1983). Although pellets have better rheological properties, a pellet's structure is tightly compacted, thereby restricting mass transfer towards the center. This decreases the overall substrate uptake rate and maximum achievable growth rate, often affecting product yield (van Dissel *et al.*, 2015, Olmos *et al.*, 2013).

Streptomyces lividans, which is considered the preferred *Streptomyces* strain for heterologous enzyme production (Anné *et al.*, 2012), natively grows as dense pellets, but certain morphogenes are known through which it is possible to drastically change this native liquid morphology (van Wezel *et al.*, 2006, Chaplin *et al.*, 2015, van Dissel *et al.*, 2015, Koebsch *et al.*, 2009, Petrus *et al.*, 2016). We recently reported on the discovery of the *matAB* locus, which is required for pellet formation (van Dissel *et al.*, 2015). Removal of the *mat* genes created a strain with a dispersed morphology, increasing the maximal growth rate and the enzyme production rate by over 60%.

To better control *Streptomyces* morphology, with the goal to increase its industrial exploitation, we aimed at optimizing the expression level and timing of the *mat* locus. To this end, the *matAB* genes were expressed from different promoters which activate transcription during late growth. Selecting a promoter which is not active during early exponential growth, but highly expressed in a later growth phase, resulted in a strain with a high initial growth rate, but with reduced viscosity increase seen with a dispersed phenotype. This represents a significant advance in the control of *Streptomyces* morphology and with that potentially also in the applicability of members of this genus in industry.

MATERIALS AND METHODS

Strains, Plasmids and strain construction

Streptomyces lividans 66 was obtained from the John Innes Centre strain collection. its genome was sequenced previously (Cruz-Morales *et al.*, 2013). *E. coli* JM109 was used as host for general cloning (Sambrook *et al.*, 1989). Non-methylating *E. coli* strain ET12567 (MacNeil *et al.*, 1992) harboring plasmid pUZ8002 was used for conjugation of different vectors from *E. coli* to *S. lividans*. *Streptomyces* techniques were performed as described (Kieser *et al.*, 2000). The native *matAB* locus was PCR-amplified from the *S. coelicolor* genome using primers SCO2963_F and SCO2962_R (Table S1). The 3712 bp DNA fragment was cloned as an EcoRI/BamHI fragment into the integrative vector pSET152 (Bierman *et al.*, 1992). The region was >99% homologous to the locus in *S. lividans*. The promoter regions of SCO1800 (P^{chpE}), SCO1947 (P^{gppA}) and of SCO1968 (P^{glpQ2}) were amplified from the *S. coelicolor* genome and ligated into EcoRV-digested pJET1.2. The different promoters were cloned EcoRI/ NdeI in front of *matAB*, creating pMAT6 (pSET152- P^{glpQ2} *matAB*), pMAT7 (pSET152- P^{gppA} *matAB*) and pMAT8 (pSET152- P^{chpE} *matAB*) (Table S2). These vectors were transformed to *E. coli* ET12567 + pUZ8002, which allowed conjugation of these vectors to *S. lividans* Δ *matAB* (GAD5), creating recombinant strains PXM1 (GAD5 + pMAT8), PXM2 (GAD5 + pMAT6) or PXM3 (GAD5 + pMAT7) (Table S2).

Culturing conditions

All *Streptomyces* strains were cultivated in tryptic soy broth medium (TSB). Fermentations were performed in 1.3 L benchtop bioreactors (Bioflow 115, New Brunswick) in duplicate. 900 mL TSB medium was supplemented with 0.1% antifoam. The medium was aerated at 0.5 vvm and the temperature was kept constant at 30°C. Dissolved oxygen concentrations were kept above 50% by controlling the agitation rate between 300-800 rpm. Concentrations of CO₂ and O₂ were measured in the off gas with an EX2000 gas analyzer (New Brunswick). The dry weight was determined by measuring the differential weight increase of a pre-weighted glass fibre filter disc on which a known culture volume was deposited, washed with at least two volumes demineralized water and followed by freeze drying. Dry weight values were used to calculate growth rates.

Determining the rheology

Viscosity measurements were performed with a DV-E viscometer (Brookfield, USA). A helical impeller, more suited for the measurement of pellet particles in a solution (Kim *et al.*, 1983), was used for measurements. The impeller had a diameter of 23 mm, 36 mm height and 24 mm pitch and was calibrated similarly as described by (Kim *et al.*, 1983) using a series of sucrose concentrations ranging from 70% to 60% and comparing the torque and viscosity values found with a traditional cylindrical spindle. Similar to (Kim *et al.*, 1983) the deviation between the different impeller types was constant in terms of changes in viscosity or torque



and shear rate.

The non-Newtonian behavior of mycelia was described according to the Ostwald–de Waele power law (Metz *et al.*, 1979). The consistency index (K) and the power law index (n) were calculated from the viscosity (η) and shear rate (γ) measurements according to:

$$\eta = K\gamma^{n-1}$$

Biomass specific viscosity index was determined as described by (Riley *et al.*, 2000):

$$\frac{K}{C_x^n}$$

with C_x being the dry weight biomass concentration and K and n being the values of the power law. Each sample was measured at several shear rates. Because of limitations inherent to the viscometer it was not possible to measure samples with a viscosity below 10 cp, *i.e.* the combination of low biomass and dense pelleting phenotype, and the power law was only fitted when the viscosity of at least four shear rate measurements could be accurately measured. To obtain higher biomass concentrations, in order to establish the relation between pellets and dispersed mycelia, 24h cultures were concentrated by centrifugation at 3000g for 20min and resuspended in fresh media.

Image analysis

Image analysis of *Streptomyces* mycelia was performed as described (Willemsse *et al.*, unpublished). In short, a 50 μ L culture was whole slide imaged with a Axio Observer (Zeiss, Germany) equipped with an automated XY stage, generating a mosaic of phase contrast images. The mosaic was analyzed with an ImageJ plugin designed for automated analysis of *Streptomyces* pellets. Morphological details were analyzed using the Feret length of the particles and the morphology number which was calculated according to:

$$\frac{2 \cdot \sqrt{A} \cdot S}{\sqrt{\pi} \cdot D \cdot E}$$

with A being the area of the particle, S the solidity, D the Feret length and E the aspect ratio (Wucherpennig *et al.*, 2011). Further data analysis, construction of histograms and fitting of Gaussian curves were performed with Python (v3.3.2) and the sklearn library.

RESULTS

Growth and rheological characteristics of S. lividans 66 and its matAB mutant

For the duration of a batch cultivation, the majority of *S. lividans* 66 biomass occurs as pellets. In previous work we showed the benefits for growth when the main phenotype is shifted towards an open or dispersed phenotype (van Dissel *et al.*, 2015). In this study the effects of the morphology on the rheology were assessed, to determine whether it is feasible to further improve the fermentability of *S. lividans*. For filamentous fungi it is known that there is a gap between the effects of pelleting and a dispersed phenotype on the apparent viscosity of a culture (Kim *et al.*, 1983). Although the same morphology dependence was assumed for streptomycetes, there is only little experimental data available to support this hypothesis. Therefore, the difference between *S. lividans* and its *matAB* mutant was assessed in terms of morphology and rheology, in a biomass-dependent manner. Overnight cultures of these strains grown in TSBS media were concentrated by centrifugation and resuspension in fresh media and the viscosity was determined over a range of shear rates and biomass concentrations. With a good fit for the Ostwald-de Waele power law model, the broth of the *matAB* mutant showed strong

non-Newtonian characteristics, even at low biomass concentrations (Figure 1). Up to a concentration of 8 g/L pellets did not yet have a major impact on the apparent viscosity. Once the biomass increased further it attained non-Newtonian characteristics, as observed by the dropping flow behavior index (Figure 1). These results revealed a big gap between the morphological phenotypes and their effect on the viscosity, which leaves room to further improve *S. lividans* fermentability.

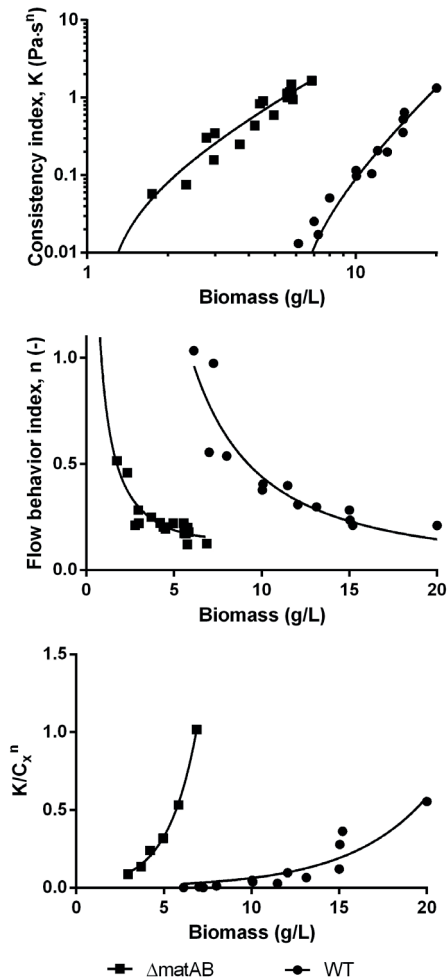


Figure 1. Rheology of *S. lividans* 66 and its *matAB* null mutant. Cultures of *S. lividans* 66 (wild type; closed circles) and its *matAB* null mutant (closed squares) grown for 24 h were concentrated and the viscosity was determined for a serial dilution of the broth. The viscosity was used to calculate the parameters of the power law, revealing large rheological differences between two strains.



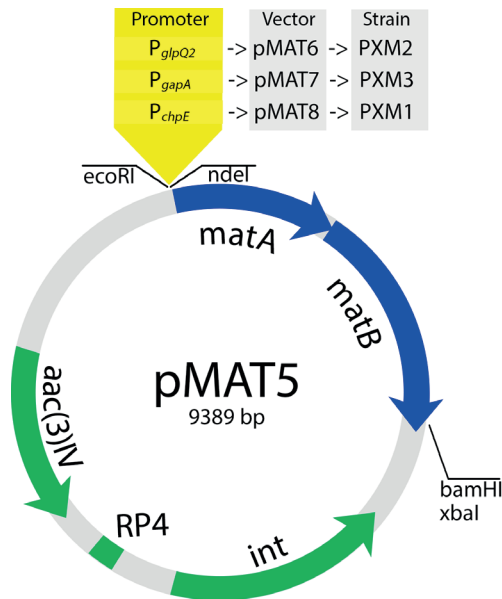


Figure 2. Map for the vectors with the *matAB* locus under the control of selected promoters.

Selection of promoters with favorable growth characteristics

Efficient mixing of nutrient and transfer of heat and gasses are highly dependent on the viscosity. In view of the trade-off between growth rate and rheology as a function of dispersed or aggregated growth, strain optimization approaches should consider a morphological profile that optimally profits from the advantages of dispersed mycelia (faster growth) and pellets (lower viscosity). To allow later expression of *matAB*, and hence delay production of the pellet-promoting PNAG, vectors were designed that allowed transcription of the *mat* locus from late promoters, and these constructs were then introduced into the *matAB* null mutant. The promoter regions of *chpE* and *glpQ2* were selected based on previously published timecourse transcriptomic data (Nieselt *et al.*, 2010). The *chpE* gene is developmentally controlled (Claessen *et al.*, 2003), resulting in low

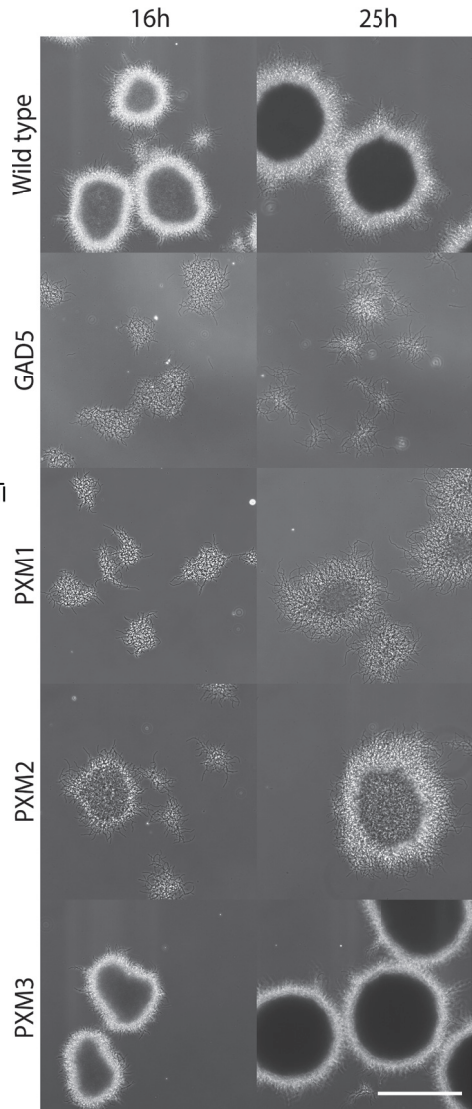


Figure 3. Mycelial morphology during early and late exponential growth. *S. lividans* 66 (Wild type), GAD5 ($\Delta matAB$), PXM1 (GAD5 + pMAT6), PXM2 (GAD5 + pMAT8) and PXM3 (GAD5 + pMAT7) were grown in a small benchtop bioreactor on TSB medium and sampled during the exponential growth curve. Overview microscope pictures were taken at 18 h and 25 h representing morphology during and late in the exponential growth phase respectively. The scale bar equals 500 μ m.

transcription at the start of cultivation, but its transcription increases significantly towards the end of an exponential growth curve, with a peak at the onset of the stationary phase (Figure S1, data from GEO GSE18489 and (Thomas *et al.*, 2012)). The *glpQ2* gene is regulated through the *phoP* regulon, making it dependent on the phosphate concentration (Nieselt *et al.*, 2010). This gene is poorly expressed until the metabolic switch, at which point it is upregulated several folds (Nieselt *et al.*, 2010). As control the *gapA* promoter region was, which is expressed strongly throughout growth ((Zacchetti *et al.*, 2016) and Figure S1). Each of the promoters was cloned upstream of *matAB* in pSET152, which integrates in the *Streptomyces* chromosome (Bierman *et al.*, 1992). For a map of the plasmids see Figure 2. The plasmids were introduced into *S. lividans matAB* null mutant GAD5, creating PXM1 (GAD5 + pSET152-P^{chpE} *matAB*), PXM2 (GAD5 + pSET152-P^{glpQ2} *matAB*) and PXM3 (GAD5 + pSET152-P^{gapA} *matAB*).

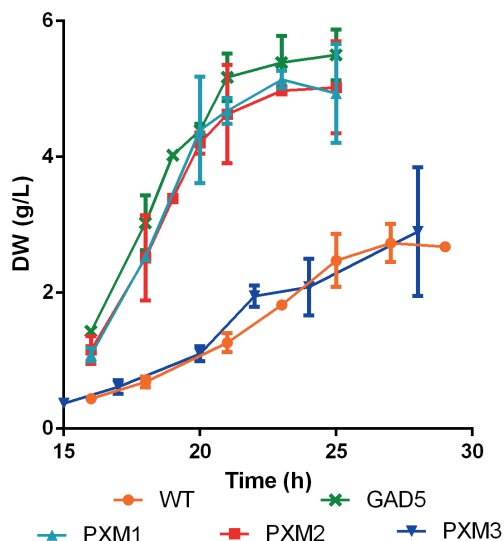


Figure 4. Growth curves of batch fermentations. Dry weight measurements taken during batch growth on TSB medium of all strains in small benchtop bioreactors. For strains see legend to Figure 3. Values represent the average of two experiments, with the error bars representing the deviation of the mean.

Variable *matAB* expression maintains fast growth with partial pellet formation

To assess their morphological behavior in relation to the parental strain and its *matAB* mutant, the transformants were batch-cultivated in a small benchtop bioreactors and the morphology and rheology determined over time. During cultivation the majority of the wild-

Table 1. Comparison of fermentation characteristics.

| | Max Growth rate | Mean particle size # | | | Morphology Number # | | |
|-----------|-----------------------------|----------------------|--------|--------|---------------------|------|------|
| | | 16h | 20h | 25h | 16h | 20h | 25h |
| Wild type | 0.19 ± 0.01 h ⁻¹ | 320 μm | 439 μm | 518 μm | 0.61 | 0.58 | 0.62 |
| GAD5 | 0.34 ± 0.01 h ⁻¹ | 103 μm | 127 μm | 91 μm | 0.13 | 0.18 | 0.13 |
| PXM1 | 0.35 ± 0.01 h ⁻¹ | 169 μm | 253 μm | 264 μm | 0.21 | 0.33 | 0.36 |
| PXM2 | 0.35 ± 0.01 h ⁻¹ | 196 μm | 258 μm | 243 μm | 0.38 | 0.33 | 0.34 |
| PXM3 | 0.19 ± 0.01 h ⁻¹ | 325 μm | 419 μm | 521 μm | 0.62 | 0.71 | 0.67 |

The averages correspond to the right fitted Gaussian curve for the particle size and the Morphology Number as found in Figure 5 and 6 respectively.



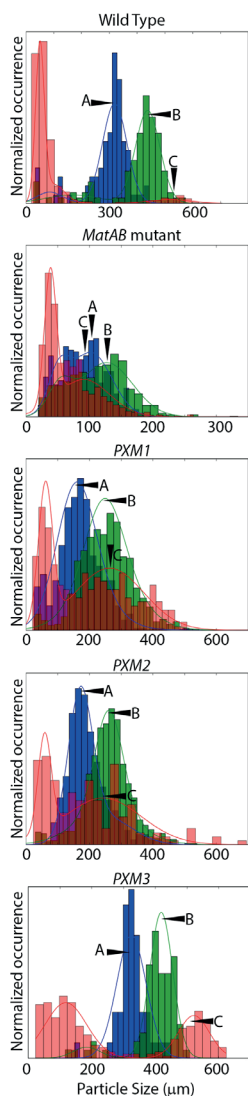


Figure 5. Particle size distribution of the fermentation at 16h, 20h and 25h. The maximum Feret length of particles were measured by image analysis for wild type *S. lividans* 66 the *matAB* null mutant *GAD5*, and transformants *PXM1*, *PXM2*, and *PXM3* expressing *matAB* from the *chpE*, *glpQ2* and *gapA* promoters, respectively. Times were 16h (blue), 20h (green) and 25h (red). Arrows indicate the primary peak of the pellet population, with A for 16h, B for 20h and C for 25h time points (values listed in Table 2). All strains had a large subpopulation of very small mycelial fragments at 25h. Two-component Gaussian curves were fit onto the raw data to estimate the average particle morphology number of multiple possible sub-populations of pellets and fragments.

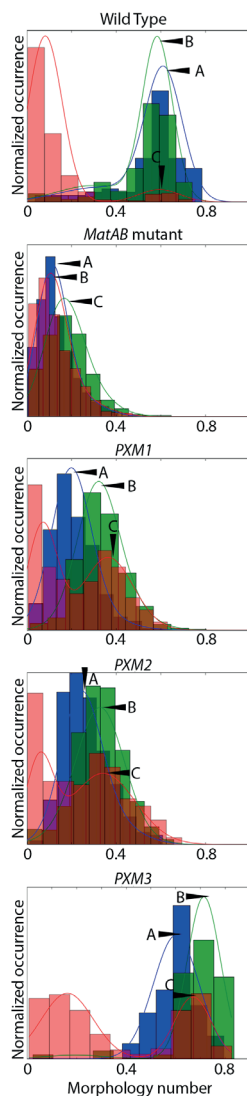


Figure 6. Morphology number distributions. Morphology numbers for *S. lividans* 66, *GAD5*, *PXM1*, *PXM2* and *PXM3* were determined after at 16 h (blue), 20 h (green) and 25 h (red). Calculations were done as described (Wucherpfennig et al., 2011). Two-component Gaussian curves were fit on the raw data to estimate the mean of particle morphology number of multiple possible sub-populations of pellets and fragments (triangles with A for 16 h, B for 20 h and C for 25 h). Values are summarized in Table 2.

type population consisted of pellets, while the *matAB* mutant had a characteristic dispersed morphology (Figure 3). The maximum growth rates were $0.19 \pm 0.01 \text{ h}^{-1}$ for the parent and $0.34 \pm 0.01 \text{ h}^{-1}$ for its *matAB* mutant (Figure 4 and Table 1), in line with earlier observations (van Dissel *et al.*, 2015).

16 h after inoculation, strains expressing *matAB* under the control of the developmentally controlled P_{chpE} or P_{glpQ2} promoters formed open clumps, which is intermediate between the morphologies of *S. lividans* 66 and its *matAB* mutant. After 25 h of growth the clumps had increased in size and density, forming what is best described as fluffy pellets, although more open clumps were also still part of the population (Figure 3). Importantly, biomass accumulation was similar to that of the *matAB* mutant, with a maximum growth rate of $0.36 \pm 0.01 \text{ h}^{-1}$ and $0.35 \pm 0.01 \text{ h}^{-1}$ for PXM1 and PXM2, respectively (Table 1). Conversely, transformant PXM3, which expresses *matAB* from the constitutive *gap* promoter, formed dense pellets and had a growth rate of 0.19 h^{-1} , similar to the parental strain.

The population dynamics over time were then quantified via image analysis. Previous studies used the maximum particle size to describe the morphology distribution found in submerged cultures (Martin & Bushell, 1996, O'Cleirigh *et al.*, 2005, Hobbs *et al.*, 1989). This allows describing the balance between growth and fragmentation. One or two Gaussian curves were fit through the distribution data to describe the particle distribution (Figure 5). Depending on the population, as a combination of spore aggregation, growth and fragmentation, two sub-populations were apparent, which are best described as two separate Gaussian curves (van Veluw *et al.*, 2012). The population with particle sizes below $100 \mu\text{m}$ primarily consists of sheared fragments and clumps while the other population consists of larger pellets. The maximal particle size for PXM1 and PXM2 cultures after 16 h of growth measured as the Ferret diameter, was $169 \mu\text{m}$ and $196 \mu\text{m}$, respectively (Table 1). This is an increase of 1.5-fold for PMX1 and of 2-fold for PMX2 in comparison to the *matAB* mutant. Between 16-20 h the Ferret diameter increased further for PXM1 and PXM2 to an average of $253 \mu\text{m}$ and $258 \mu\text{m}$, respectively, while the diameter of the *mat* null mutant only increased minimally (to $127 \mu\text{m}$) and in fact decreased by the end of exponential growth phase to an average value below $100 \mu\text{m}$. At 25 h the average particle size of PXM1 and PXM2 had increased to around $300 \mu\text{m}$ indicating that aggregation was still progressing. This was still significantly smaller than the average pellet size found for the wild-type strain, which showed averages ranging from $320 \mu\text{m}$ at 16 h, $439 \mu\text{m}$ at 20 h and $518 \mu\text{m}$ at 25 h. This is comparable to transformant PXM3 ($325 \mu\text{m}$, $419 \mu\text{m}$ and $521 \mu\text{m}$ at 16 h, 20 h, and 25 h respectively).

Apart from the maximal particle size, image analysis also allowed the characterization of the morphology based on other visual characteristics. In an earlier study with the filamentous fungus *Aspergillus niger* the ratio of the area and solidity over pellet length and aspect ratio was used to describe the morphology and was named the Morphology Number (Wucherpennig *et al.*, 2011). This ratio could also be used to describe the morphology of *Streptomyces* mycelia, with small fragments and open mycelia having a value close



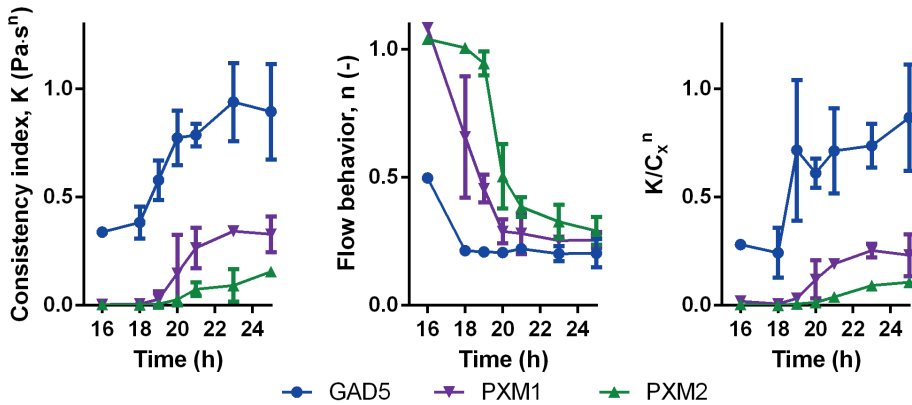


Figure 7. Change of rheology during the batch phase. During the exponential growth phase of GAD5, PXM1 and PXM2 samples were taken for offline viscosity measurements allowing the rheological characterization of the strains over time. Rheological determination of wild-type *S. lividans* 66 and the PXM3 strains were outside the measurement range and were therefore not included. The apparent viscosity determined over a range of shear rates allowed fitting of the Ostwald–de Waele power law model. The values for consistency index K , the flow behaviour index n and the values related to the biomass K/C_x^n are depicted from left to right. Strains with late *matAB* expression showed superior rheological characteristics as compared to the *matAB* null mutant.

Rheological profile

The variation in broth rheology for all strains is presented in Figure 7. *S. lividans* 66 was not included in the comparison because the biomass concentrations remained below the threshold required to allow accurate measurement with a viscometer, with hardly any effect on rheology (Figure 2). Also PXM3, with a morphology similar to wild type, maintained a broth viscosity below the measurement range for the duration of the fermentation. Expectedly, both PXM1 and PXM2 showed an increased culture broth viscosity, but compared to the *matAB* null mutant both transformants showed a reduced average viscosity, illustrated by the consistency indices (K). And while PXM1 and PXM2 showed non-Newtonian characteristics by the end of the exponential growth phase, shown by the Flow behavior index (n), PXM1 and PXM2 attained these later than the *matAB* control strain. This is also reflected in the biomass-specific viscosity index (Riley *et al.*, 2000), which is

nearly 4 fold lower for PXM1 and about 8 fold lower for PXM2. Taken together, our data show that expression of the *mat* locus after initial growth resulted in improved rheological characteristics as compared to the *matAB* mutant, whilst maintaining a high growth rate.

DISCUSSION

Viscosity is one of the key limiting factors that dictates the efficiency of oxygen transfer during aerobic fermentations (Badino *et al.*, 2001). The entangling mycelium of streptomycetes and other filamentous micro-organisms can strongly increase the apparent viscosity, especially in low shear conditions because of the pseudoplastic behavior of the suspension. In many industrial scale fermentations the shear stress isn't that high, which, combined with a high viscose broth, results in a serious reduction of mass transport of among others oxygen (van't Riet & Tramper, 1991). Oxygen transfer suffers twice, because apart from elongated mixing times the higher viscosity increases the average bubble size, decreasing the oxygen transfer rate. As *Streptomyces* are aerobic micro-organisms that produce energy-expensive and thus oxygen-demanding natural products, maintaining a low viscosity should result in an improved process. Similarly, filamentous fungi that grow as pellets result in culture broths with low viscosity, which was for example beneficial for the production of lovastatin by *Aspergillus terreus* (López *et al.*, 2005). However, pellets are also associated with a low maximum growth rate, which extends fermentation times and thus increase operational costs. In particular the long fermentation times represent a bottleneck for *Streptomyces* as a production.

For filamentous fungi the morphology-associated rheology effects have been studied more extensively than for actinomycetes. Although many of the general trends are comparable, it appears that the biomass of *S. lividans* affects its environment differently. Comparing the dependencies of the flow behavior and biomass with values found for *Absidia corbymbifera* (Kim *et al.*, 1983), our work shows that both the dispersed mycelia and pellets of *S. lividans* have non-Newtonian behavior at much lower biomass concentrations than filamentous fungi. Interestingly, on average the consistency index was also lower, suggesting that the same biomass concentration has less effect on the viscosity. A plausible explanation could be sought in the difference at the cellular scale. The smaller *Streptomyces* hyphae are likely more fragile and thus more prone to fragmentation (Celler *et al.*, 2012). Cell damage caused by agitation already occurs at relatively modest agitation rates during *Streptomyces* fermentations (Roubos *et al.*, 2001, Heydarian *et al.*, 1999). Dispersed *Streptomyces* mycelia fragment more readily, resulting in smaller particle sizes and reduced entangling, with less effects on the viscosity. This effect of fragmentation is also visible for wild-type mycelia after 25 h, where numerous particles with a size <100 µm were found, supposedly originating from pellets that underwent fragmentation. It is unclear whether this fragmentation is the result of famine, which induces cell death (Manteca *et al.*, 2008) or the result of an increase in agitation rate required to meet the oxygen demand at the end of exponential growth. This requires further investigation.



To the best of our knowledge only one other study exists that attempted to rationally affect the morphology of a filamentous micro-organism to improve fermentation characteristics. Christian Müller and colleagues put *chsB* under the control of the *niiA* promoter in *Aspergillus oryzae* (Müller *et al.*, 2002b). The *chsB* mutant had an altered cell-wall architecture, showing hyper-branching and lack of pellets as compared to the parental strain (Müller *et al.*, 2002a). However, induction of *chsB* with the addition of nitrate did not result in the desired change in morphology. The positive effect of delayed expression of *matAB* in terms of improving the growth characteristics of *S. lividans* may be explained by the fact that altering *matAB* expression does not lead to radical changes in overall hyphal architecture, but rather to changes in the accumulated of the EPS-like PNAG, which acts as a 'glue' at the outside of the hyphae. In this sense *matAB* act very differently as compared to the *ssgA*, which has a major impact on hyphal differentiation, among others activating septum formation (Jakimowicz & van Wezel, 2012, Traag & Wezel, 2008). Overproduction of SsgA activates mycelial fragmentation in liquid-grown cultures, resulting in highly reduced particle size (van Wezel *et al.*, 2006). However, SsgA affects germination, tip growth, branching frequency and cell division (van Wezel *et al.*, 2000a, Noens *et al.*, 2007), which has major repercussions for hyphal integrity, among others leading to increased cell lysis.

It is currently unclear why late expression of *matAB* only resulted in less dense pellets, instead of fully mature pellets. Perhaps delayed production of PNAG is insufficient for fully mature coalescence. Alternatively, the lack of PNAG during the earliest stages of growth may also affect spore aggregation, another important determinant of pellet morphology (Zacchetti *et al.*, 2016). Spore aggregation depends on *matAB* during germination and the first few hours of growth. Delaying *matAB* transcription during growth likely eliminates spore aggregation and will thus affect population dynamics. Aggregated spores may create a nucleation point for the complex scaffolding needed to form the dense core of pellets, and this will be different from later aggregation events as shown in this study.

Industrial fermentations are often conducted as fed-batch cultures, and the benefits of deregulation of *matAB* expression may be more beneficial in such a system. Studies into the rheology of fed-batch cultures established a further increasing apparent viscosity during the feeding stage, indicating that in fed-batch systems there is more to gain by controlling the morphology (Pamboukian & Facciotti, 2005). Expressing the *mat* locus in actinomycetes that do not have a copy of the *mat* genes on their chromosome and grow dispersed, exemplified by for example the clavulanic acid producer *Streptomyces clavuligerus* or the erythromycin producer *Saccharopolyspora erythraea*, typically induces the formation of mycelial pellets. We therefore expect that our work can be translated to many other systems, thus offering the outlook of tuning the rheology with the aim of improving the productivity of a range of fermentation processes involving filamentous *Actinobacteria*.

ACKNOWLEDGEMENTS

We like to thank Joost Willemse for the support with the automated image analysis. The research was supported by VICI grant 10379 from the Netherlands Technology Foundation STW to GVW.

SUPPLEMENTAL INFORMATION

Table S1: Oligonucleotides

| Primer name | Sequence |
|-------------|---|
| SCO2963_F | CAGTGAATCCATATGGGGGCCGGTTCGGCCGACGAGTGCTC |
| SCO2962_R | ATGCGGATCCTCATCCGACCGGCCTCCCGTCCATGGC |
| pSCO1800_F | AGTGAATTCCTCCACGCCGGGGCACATC |
| pSCO1800_R | AGTCATATGCAACCCCTCCTTGCGATCGCC |
| pSCO1947_F | AGTCGAATTCATCGGTACGTACCGACCC |
| pSCO1947_R | AGTCCATATGCCGATCTCCTCGTTGGTACGCC |
| pSCO1968_F | GATGAATTCGGGCGCCAGGAACGGCTGAC |
| pSCO1968_R | GATCATATGTACTCCTCGCGTCGAACGAT |

Table S2: Strains and vectors used in this study

| Strain name | Genotype | Reference |
|-----------------------|--|-----------------------------------|
| <i>S. lividans</i> 66 | SLP2+ SLP3+ | (Kieser <i>et al.</i> , 2000) |
| GAD5 | <i>S. lividans</i> 66 Δ matAB | (van Dissel <i>et al.</i> , 2015) |
| PXM1 | GAD5 + pSET152-P ^{ChpE} - <i>matAB</i> | this study |
| PXM2 | GAD5 + pSET152-P ^{GlpQ2} - <i>matAB</i> | this study |
| PXM3 | GAD5 + pSET152-P ^{GapA} - <i>matAB</i> | this study |

| Vector name | Construct | Reference |
|-------------|--|-------------------------------------|
| pSET152 | <i>oriT</i> RK2, pUC18 replicon, Apra ^R | Bierman <i>et al.</i> , 1992 |
| pJET1.2 | pUC18 replicon, Amp ^R | CloneJET PCR cloning kit, Fermentas |
| pMAT5 | pSET152- <i>matAB</i> | this study |
| pMAT6 | pSET152-P ^{GlpQ2} - <i>matAB</i> | this study |
| pMAT7 | pSET152-P ^{BppA} - <i>matAB</i> | this study |
| pMAT8 | pSET152-P ^{ChpE} - <i>matAB</i> | this study |



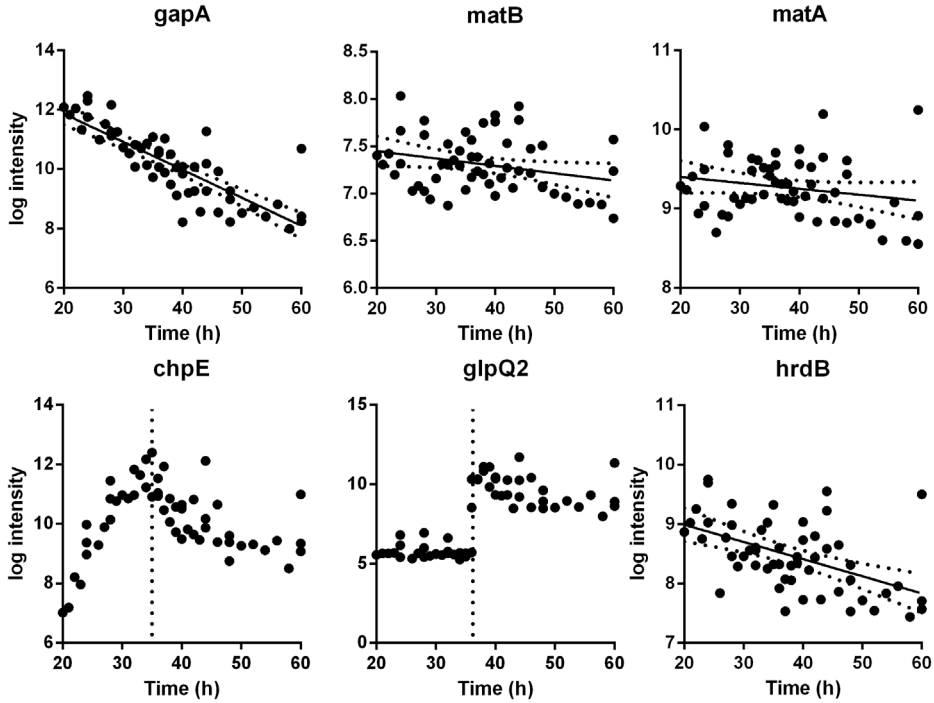


Figure S1: Expression data of *gapA* (SCO1947), *matB* (SCO2962), *matA* (SCO2963), *chpE* (SCO1800), *glpQ2* (SCO1968) and *hrdB* (SCO5820) obtained from GEO GSE18489 and). Depicted here are the mRNA levels from high density sampling of batch fermentation with *Streptomyces coelicolor* performed by (Thomas *et al.*, 2012). From this data can be concluded that *gapA*, *matA* and *matB* have a constitutive expression pattern and the expression levels of *chpE* and *glpQ2* are low early during the batch phase, but increase over time. The principle vegetative sigma factor *hrdB* is depicted as example of a stable household gene.



6

Morphology-driven downscaling of *Streptomyces lividans* to micro cultivation

van Dissel, D. & van Wezel, G.P.

ABSTRACT

Actinomycetes are prolific sources of secondary metabolites and industrially relevant enzymes. Growth of these mycelial microorganisms in small culture volumes is very challenging due to their complex morphology. Since morphology and production are typically linked, scaling down culture volumes requires better control over morphogenesis. In larger scale platforms, ranging from shake flasks to bioreactors, the hydrodynamics play an important role in shaping the morphology and determining product formation.

Here, we report on the effects of agitation on the mycelial morphology of *S. lividans* grown in microtiter plates (MTP). Our work shows that at the proper agitation rate cultures can be scaled down to volumes as small as 100 μl while maintaining the same morphology as seen in larger scale platforms. Using image analysis we compared the morphology of the cultures, which when the MTP was agitated at 1400 rpm approached those observed in shake flasks, while product formation was maintained.

Our study shows that the morphology of actinomycetes in microcultures can be controlled in similar manner as in larger scale cultures by carefully controlling the mixing rate. This could facilitate high-throughput screening and successful upscaling.



INTRODUCTION

The need to screen strains under many conditions increases the demand for optimized high throughput screening (HTS) methods. Downscaling of culture volumes, while maintain key factors like reproducibility and productivity comparable to shake flasks or small scale bioreactors, is necessary to make large screening efforts rapid and economically feasible (Long *et al.*, 2014). Development of an HTS platform for *Streptomyces*, which are multicellular filamentous organisms, is challenging and only a few tries in the literature can be found (Minas *et al.*, 2000, Siebenberg *et al.*, 2010, Sohoni *et al.*, 2012). In submerged cultures the filamentous mycelia manifest a complex morphology that has a profound impact on the regulation of product formation (van Dissel *et al.*, 2014). Successful downscaling of the culture volume therefore includes matching the morphology found in larger scale platforms (i.e. shake flasks or bioreactors).

Streptomycetes typically display a wide range of morphologies in submerged cultures (reviewed in (van Dissel *et al.*, 2014). Perhaps the most difficult morphology to scale down is that of aggregating, pellet forming Streptomycetes. This is exemplified by *Streptomyces coelicolor*, a model for *Streptomyces* growth and antibiotic production (Barka *et al.*, 2016), and by the related *Streptomyces lividans*, the ideal heterologous enzyme production host (Anné *et al.*, 2012). These streptomycetes are characterized by the formation of large multicellular aggregates or pellets. In a liquid culture, depending on the medium, the pellets exist as two distinct populations which differ in size (van Veluw *et al.*, 2012). The core of the pellets undergoes a developmental cycle, which is linked to the regulation of antibiotic production (Manteca *et al.*, 2008, Martin & Bushell, 1996). A mycelial pellet may be considered a self-immobilized biofilm (Petrus & Claessen, 2014), a term borrowed from granular sludge research, which deals with similar morphology dynamics (Liu & Tay, 2002).

The exact morphology, i.e. size, density and shape, is greatly dependent on the characteristics of the environment (Wucherpennig *et al.*, 2010). The hydrodynamics, the characteristics of the agitated medium, seems to be of particular great importance as it influences many parameters associated with morphogenesis (Olmos *et al.*, 2013). Low agitation causes poor distribution of nutrients and reduced oxygen transfer rates, stunting growth and production, while strong agitation can cause cell death (Roubos *et al.*, 2001). The relationship between pellet morphology, hydrodynamics (and oxygen supply) and production has been well studied for bioreactors (Tamura *et al.*, 1997, Roubos *et al.*, 2001, Ohta *et al.*, 1995) and for shake flasks (Mehmood *et al.*, 2012, Dobson *et al.*, 2008), but has not been tried in an HTS setting which necessitates small culture volumes without affecting the growth properties. In this work we sought to match the morphology seen in larger scale platforms by controlling the hydrodynamics of the culture, down to 100 μ l culture scale. The dimensions of microtiter plates (MTP), with small well diameters, requires extensive mixing forces to match the hydrodynamics. We applied an MTP vortex to reach high mixing rates and precise speed control, which allowed a successful scaling down, with native morphology and production found in larger scale platforms.

MATERIALS AND METHODS

Bacterial strains, plasmids

S. lividans 66 was used for morphological analysis and enzyme production and *S. coelicolor* M145 was used for antibiotic production. The plasmid pIJ703 (Katz *et al.*, 1983), which carries the *melC1* and *melC2* genes for heterologous tyrosinase production, was transformed to its host by protoplast transformation (Kieser *et al.*, 2000). Spores were harvested from soy flour mannitol agar plates and stored in 20% glycerol at -20°C as described (Kieser *et al.*, 2000). The spore titer was determined by plating serial dilutions and counting CFUs.

Cultivation conditions

For cultivation in shake flasks, *S. lividans* was grown in 30 mL tryptic soy broth (Difco) with 10% sucrose (TSBS) in a 100 mL Erlenmeyer flasks equipped with a stainless steel spring. The flask was inoculated with 10⁶ CFUs/ml and cultivated at 30°C in an orbital shaker with 1 inch orbit (New Brunswick) at 170 RPM. For the production of tyrosinase 25 µM CuCl₂ was added to the TSBS medium.

For antibiotic production *S. coelicolor* was cultivated in Yeast Extract - Malt Extract (YEME; (Kieser *et al.*, 2000)) but without sucrose (YEMEO) .

100 µl media with 10⁶ cfu/ml spores was added to wells of a V-bottom 96 well MTP (Greiner Bio-One, Germany). To minimize evaporation, the plate was covered with a custom molded silicone sheet made from MoldMax40 (Materion, USA), using the 96 well plate as a mold. An AeraSeal film (Excel Scientific, USA) was added to the top for sterility, while allowing gas exchange. The combined silicone sheet and AeraSeal film were fastened the MTP using masking tape. A Microplate Genie Digital (Scientific Industries, USA) was used for agitation. This microtiter plate vortex has an orbit of 1 mm with accurate speed control. The rotation speed was also checked using a Voltcraft DT-10L digital tachometer (Conrad, Germany). The entire setup was placed in a humidity-controlled incubator set to 70% RH and 30°C. The evaporation rate was around 8 µL per well per day.

Image analysis

Image analysis was performed as described by whole slide imaging combined with automated image analysis using imageJ (Zacchetti *et al.*, 2016). In short, 100 µl sample was transferred to a glass microscope slide and covered by a 24x60 cover slip. The slide was mounted in an Axio Observer (Zeiss, Germany) equipped with an automated XY-stage, which allowed whole slide imaging using a 10x objective. The imageJ plugin for automated image analysis optimized for *Streptomyces* liquid morphology was used to obtain both the maximum Feret length in µm and a shape description with a value between 0 and 1 measured as the circularity, where 1 describes a perfect circle (Stojmenovic *et al.*, 2013) of each mycelial fragment or pellet found in the sample. Incorrectly analyzed pellets (e.g. out-of-focus mycelia) were removed manually. Further data processing and visualizing was done



in Microsoft Excel. The spread of a distribution was calculated as the standard deviation of the population, which indicates how spread out the measured particles are within a measurement. The deviation of the mean of each term was calculated from the differences between analyses of multiple samples.

Tyrosinase activity measurement

Tyrosinase activity was measured by the conversion over time L-3,4-dihydroxyphenylalanine spectrophotometrically at a wavelength of 475 nm, as described (Kieser et al., 2000).

Actinorhodin quantification

The production of actinorhodin by *S. coelicolor* was determined as follows. Culture supernatant (40 μ l) was treated with 0.5 μ l 5 M HCl to pH 2 to 3, extracted with a 0.5 volume of methanol-chloroform (1:1), and centrifuged at 5,000 rpm for 10 min. The concentration was calculated from the A_{542} (ϵ_{542} , 18,600).

RESULTS

The morphology of S. lividans in shake flasks

Submerged cultivations of streptomycetes are typically done in shake flasks, such as in physiological and metabolic studies. To reproducibly cultivate the filamentous mycelia, the shake flasks are equipped with a spring coil, which increases aeration and creates the shear forces in the vessel so as to obtain more favorable growth and promote fragmentation of the mycelial clumps. Fragmentation is the process where pellets or parts thereof are split off, which is needed for pellet multiplication in the culture. Baffled shake flasks or the addition of glass beads are also used for the same purpose.

We wondered if it would be possible to mimic these growth conditions and obtain similar growth characteristics in much smaller cultures volumes. As a reference, the morphological characteristics of shake flask cultures were investigated by image analysis, which allows a large number of pellet particles to be analyzed on multiple morphological relevant parameters. Around 500 aggregates were analyzed from a 24 h shake flask-grown culture, corresponding to the end of the exponential growth phase, which roughly corresponds temporally to the onset of antibiotic production (Nieselt *et al.*, 2010). Previous work comparing the maximum length of pellets revealed two different populations of *S. lividans* (van Veluw *et al.*, 2012). This separation is even more clear when also the circularity is taken into account, showing two distinct clusters of particles, that not only differ in size, but also in shape (Figure 1D, scatter plot). Pellets of population “a” (Figure 1D, falling within the yellow dotter oval) have similar lengths around 200 μ m, but with a wide spread in circularity (Also see figure 1A as example). Most pellets are found in cluster “b” (Figure 1D, purple striped

oval), of which about half of the total pellet population were situated in the centroid around “C”. The “average” pellet had a homogenous density, the majority showing a slightly oval shape (Figure 1, C). Increasing the pellet size was often accompanied by a loss of structural integrity (Figure 1B). Because of the effects of pellets on production and regulation it is important to capture all of these morphological characteristics in our effort to scale down.

Dependency of agitation rate on the morphology in micro-cultures.

The insight that pellet formation is mostly the result of the hydrodynamic forces and/or the supply of sufficient oxygen, often described by the power dissipation (P) and the $k_L a$, prompted new experiments to match the environmental properties with those found in shake flasks. Both of these properties can be changed with (and are linked to) the agitation rate. A digital vortex, designed for microtiter plate (MTP) mixing, enabled setting the mixing

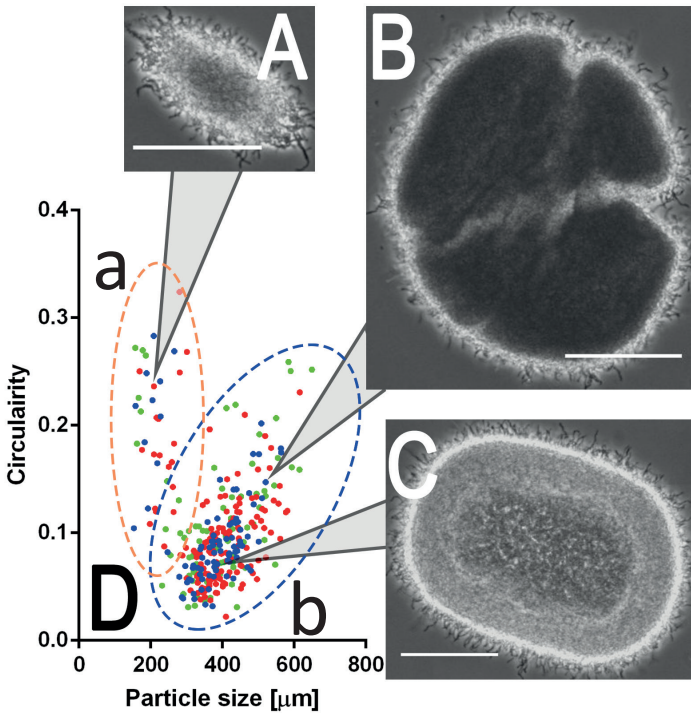


Figure 1. Morphological characterization of *S. lividans* in shake flask cultures. Spores of *S. lividans* 66 were inoculated at 10^6 CFU/ml into a shake flask (equipped with a coiled spring) containing 30 mL TSBS. The culture was grown for 24 h in an orbital shaker set to 30°C. Three 100 μ L samples from two independent cultures were taken at 24 h and subjected to image analysis to obtain the maximum length and circularity of each distinguishable mycelial aggregate. Light micrographs A, B and C represent the three archetypes of the pellet morphologies seen in the culture, and corresponds to the indicated locations in the particle size (x-axes) and circularity (y-axes) scatterplot (D), for which the data was obtained by image analysis, the colors corresponds to data obtained from independent cultures. Bar, 100 μ m.



rate, studying the effects on morphology and thus establishing whether a population could be obtained with morphological characteristics similar to those found in larger scale cultures.

In 100 µl MTP cultures and at low agitation rates, the mycelia failed to aggregate into the dense pellets normally observed in shake flasks, showing a more irregular shaped open morphology (Figure 2A, G). Preliminary experiments suggest that this may at least in part be caused by insufficient oxygen supply (see Discussion). Apart from the lower density, the average length of the mycelia is around 480 µm with a wide spread, indicating how narrow the measured particles are distributed, ranging from 80 µm to large aggregates of up to 1500 µm, likely resulting from fusion of multiple aggregates (Table 1).

At 1000 rpm the mycelia formed denser pellets, typical of *S. lividans* grown in shake flasks or in the fermenter (Figure 2H). However, the average pellet size of around 600 µm and the significantly smaller number of particles per culture volume suggest that the hydrodynamic forces in de micro-cultures were weaker than in shake flask-grown cultures (Figure 2B). At 1200 rpm the average pellet size approached that found in shake flasks, but the pellets had a more elongated, oval-shaped morphology, with an average roundness close to 0.2 (Figure 2C, I). At this agitation rate a few pellets of the vertical cluster appeared, indicating that the shear stress was sufficiently high to induce fragmentation (Figure 2C, inset). Increasing the mixing rate further to 1400 rpm lowered the circularity to the desired value of 0.1, with the average pellet length now closely resembling that found in shake-flask cultures (Figure 2D, J). Also the distribution of the pellet population closely resembled those formed in shake flasks, including the occurrence of the population of smaller oval-shaped pellets (Figure 2D, inset). When the agitation was further increased to 1600 rpm the cultures showed again an increase in length and a decrease in circularity (Figure 2I and J). Also the Feret diameter of the second population pellets decreases drastically, indicating that the mycelia might be exposed to a shear stress high enough to induce substantial cell damage (Figure 2I, picture). Increasing the agitation to 1800 rpm resulted in a similar trend as seen in 1600 rpm where

Table 1. Average length and circularity of the population of mycelial aggregates under different growth conditions for *S. lividans*.

| Culture | Length | | Circularity | |
|--------------|----------|----------|-------------|-------------|
| | Average | Spread | Average | Spread |
| Shake flask* | 372 ± 19 | 104 ± 24 | 0.11 ± 0.02 | 0.07 ± 0.03 |
| 800rpm | 463 ± 58 | 310 ± 2 | 0.22 ± 0.00 | 0.07 ± 0.01 |
| 1000rpm | 623 ± 88 | 189 ± 4 | 0.16 ± 0.00 | 0.06 ± 0.01 |
| 1200rpm | 415 ± 36 | 100 ± 20 | 0.18 ± 0.03 | 0.05 ± 0.00 |
| 1400rpm | 378 ± 51 | 104 ± 22 | 0.10 ± 0.00 | 0.06 ± 0.01 |
| 1600rpm | 412 ± 62 | 170 ± 12 | 0.12 ± 0.02 | 0.08 ± 0.02 |
| 1800rpm | 423 ± 3 | 135 ± 40 | 0.10 ± 0.02 | 0.07 ± 0.00 |

*shake flask was mixed at 170 rpm in a 1inch orbital shaker

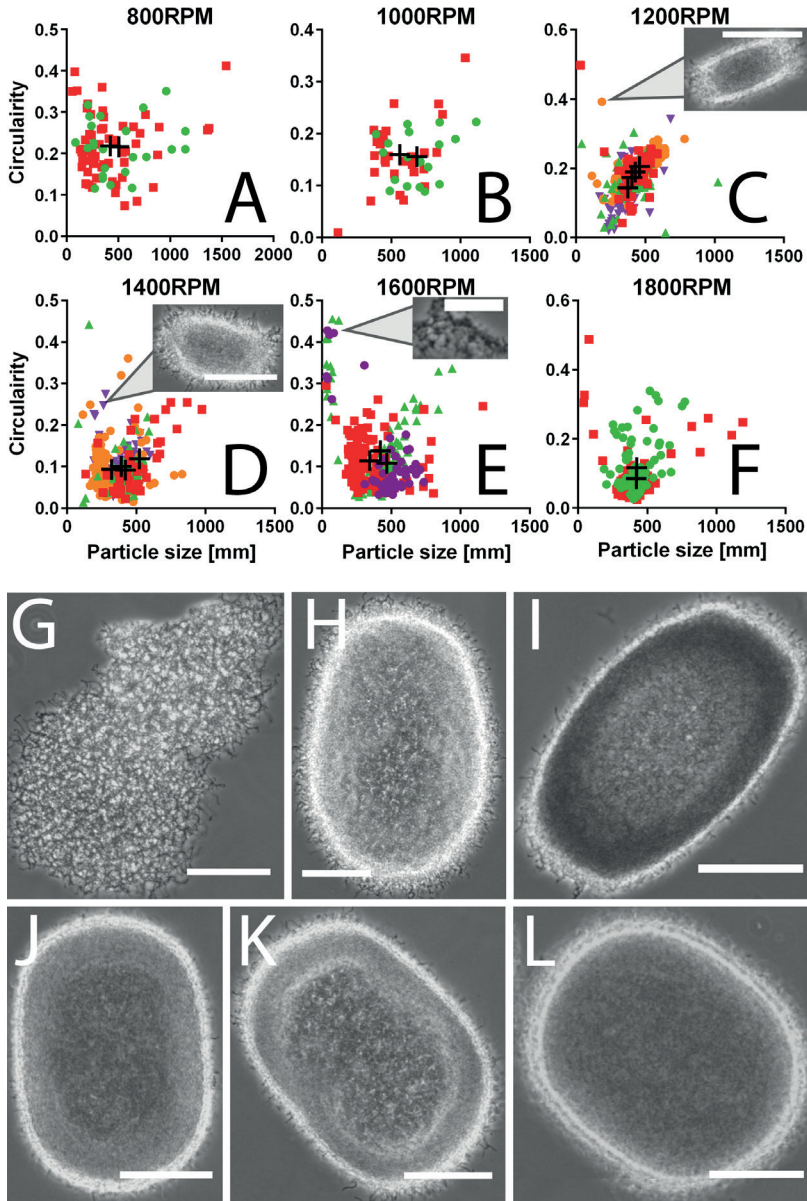


Figure 2. Growth of *S. lividans* in 100 μL MTP cultivation at different agitation rates. Spores of *S. lividans* 66 were inoculated at 10^6 CFU/ml into 100 μL in a 96 well MTP with V-shaped bottom. The MTPs were agitated using a digital MTP vortex, which was set in a humidified incubator with temperature set to 30°C. The agitation rate was changed between experiments ranging from 800 rpm (A,G), 1000 rpm (B,H), 1200 rpm (C,I), 1400 rpm (D,J), 1600 rpm (E,K) and 1800 rpm (F,L) and the effects on morphology of each aggregate after 24 h of cultivation was analyzed in respect to its circularity (y-axes) and maximum length in μm (x-axes) and are displayed in a scatter plot (A,B,C,D,E,F). Agitation rates were analyzed at least twice (replicates presented by different colors) and the centroids calculated (black crosses). C,D,E: image showing an aggregate of the smaller population. G,H,I,J,K,L: examples of a typical pellet found near the centroid. Scale bars: 100 μm or 50 μm (E).



larger pellets again appeared as part of the population. This may be explained by the culture fluid showing “out of phase” characteristics at high rotations speeds (Büchs *et al.*, 2000, Büchs *et al.*, 2001), which would result in a lower power consumption, and thus lower fragmentation rates and increased average pellet size.

Production of heterologous enzymes and antibiotics

Mycelia of 24 h old micro-cultures grown at an agitation speed of 1400 rpm generally had a morphology that was very similar to that observed for mycelia grown in shake-flasks. To analyze how similar the cultures were in terms of their producing capacity, we analyzed the production of tyrosinase, which is a good model system for extracellular enzyme production, and was heterologously expressed in *S. lividans* by the introduction of plasmid pIJ703 (van Wezel *et al.*, 2006). A similar amount of active enzyme was produced in shake flasks and in MTPs, although production started slightly earlier in MTPs (Figure 3). As the morphology appeared comparable, this is most likely the result of evaporation, which increases apparent biomass and substrate concentrations.

To study the effect on antibiotic production, we used *Streptomyces coelicolor* M145 as the model organism, as this strain produces pigmented antibiotics which are readily assessed spectrophotometrically. For this study, we compared the production of the blue-pigmented actinorhodin between shake flasks and micro-cultures (Figure 4). After 48h of growth both cultures had produced comparable amounts of actinorhodin, suggesting that also antibiotic production is very similar in the two cultivation systems.

DISCUSSION

High-throughput screening of actinomycetes for natural products or enzymes typically takes place in micro-scale liquid-grown cultures in an MTP-based setup. The alternative is solid-grown cultures, but it is very difficult to translate growth conditions from solid- to liquid-grown cultures. A drawback of screening of actinomycetes in submerged cultures is the formation of large mycelial networks, which show flocculation or attachment to abiotic surfaces and are associated with slow growth (van Dissel *et al.*,

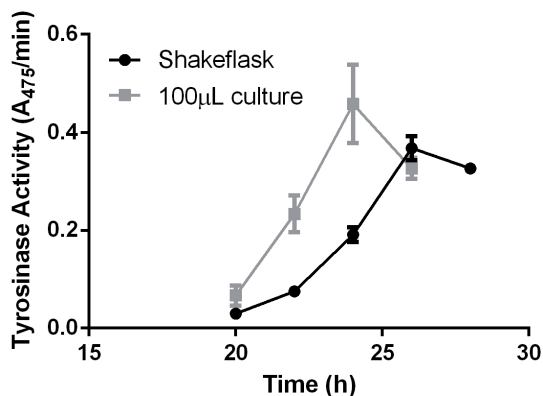


Figure 3. Tyrosinase production by S. lividans in shakeflasks and 100 µL cultures. Transformants of *S. lividans* 66 heterologously expressing the secreted enzyme tyrosinase from plasmid pIJ703 were grown in TSBS in either shake flasks or V-bottom MTPs. The graph represents the conversion rate of l-3,4-dihydroxyphenylalanine by the culture supernatant, which is indicative of tyrosinase activity. The shake flasks were run in duplicate, while the tyrosinase was measured in three different wells in the MTP.

2014). Additionally, cultures tend to be highly heterogeneous due to the large surface area of the mycelial clumps. Recently, we showed that aggregation of germlings increases culture heterogeneity (Zacchetti *et al.*, 2016). Because heterogeneity creates a distribution of morphologies, all contributing to production differently (van Veluw *et al.*, 2012, Martin & Bushell, 1996), a large population is often required to maintain reproducibility. As a lot of heterogeneity is the result of the environment, careful control is needed to mimic the morphology of a shake flask in small-scale cultivation platform.

This study shows that the distribution of a heterogeneous mycelial population is highly dependent on the agitation rate in 96-well MTPs. Especially at insufficient mixing rates the mycelia failed to aggregate into a typical pellet structure. It is likely that this is at least in part the result of insufficient oxygen supply, which is important for antibiotic production (Chen & Wilde, 1991, Yegneswaran *et al.*, 1991). A $k_L a$ of at least 100 h^{-1} is needed for the production of pristinamycins by *Streptomyces pristinaespiralis* (Mehmood *et al.*, 2010).

The relationship between oxygen supply and morphology is less well understood, but preliminary experiments where the oxygen supply was limited in a shake flask by reducing the gas exchange, resulted in pellets with a reduced density similar to what was found in poorly agitated MTPs (DvD and GPvW, unpublished results). Although the $k_L a$ was not measured in this study, initial calculations using equations for orbital mixing (Seletzky *et al.*, 2007) showed that the $k_L a$ could be as low as 40 h^{-1} when mixing at 800 rpm. This low value is suggestive of oxygen limitation as the cause of the morphology observed at low agitation rates and that in part the change in morphology by increased agitation is the result of an increased oxygen supply. While these observations are indicative of oxygen limitation as determining factor for mycelial morphology, oxygen transfer and hydrodynamic stress are coupled processes for orbital shaken cultivation methods (and to some extent also for bioreactors). At least for pristinamycin production hydrodynamic stress, described as the power input, was more descriptive for both pellet morphology and production levels (Mehmood *et al.*, 2012). How precisely agitation affects morphogenesis in MTP plates is as yet unclear and requires further study.

Detailed comparison of mycelial morphologies by image analysis allowed selection of

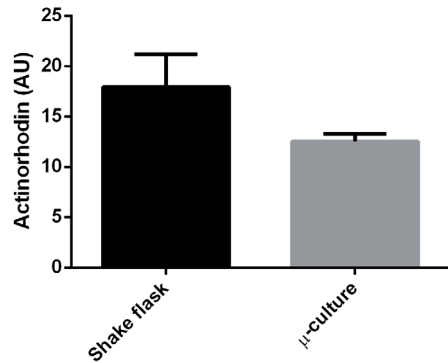


Figure 4. Actinorhodin production by *S. coelicolor* after 48 h of growth. *S. coelicolor* M145 was cultivated in minimal media for 48 h. The shake flasks were run in duplicate, while antibiotic production was measured in three different wells in the MTP. Actinorhodin was extracted by chloroform/methanol and measured spectrophotometrically at 542 nm. The average amount of actinorhodin concentration (in arbitrary units) and the standard deviation of three independent cultures are shown.



the appropriate culturing conditions to obtain a preferred average pellet size and structure. Comparison of maximal pellet length and circularity provided additional insights into the exact morphology of the pellets, which aided the down-scaling process. Besides providing the option of medium- to high throughput screening, the ability to grow *Streptomyces* with a native morphology on a small scale also allows studies that involve for example the addition of expensive or low abundance chemicals or enzymes.

CONCLUSION

The complex morphology displayed by filamentous actinomycetes in liquid-grown cultures greatly influences their productivity. Screening these bacteria for new therapeutic agents in an MTP-based setup without affecting normal growth and morphology would be a major advantage. This is in particular important in the light of the future upscaling, so as to maximize the chance that productivity is maintained. We have been able to translate growth and morphology from shake flasks to 100 μ L microcultures by carefully tuning the rate of agitation. The resulting growth and average pellet size in standard HTS-compatible MTPs was reproducibly comparable to those in larger scale cultures, which is an important contribution to the state of the art.

LIST OF ABBREVIATIONS

- HTS – High throughput screening
- MTP – microtiter plate
- rpm – Rounds per minute
- $k_L a$ – specific oxygen transfer coefficient
- P – Power dissipation

ACKNOWLEDGEMENTS

We like to thank Joost Willemse for the support with the automated image analysis. The research was supported by VICI grant 10379 from the Netherlands Technology Foundation STW to GVW.



7

General discussion

Bacteria are typically seen as individual planktonic cells, dividing by binary fission to achieve rapid growth. However, many bacteria prefer to live in a community, either during a defined stage of their life cycle in the form of a biofilm, or permanently as a full-fledged multicellular organism (Claessen *et al.*, 2014). Living as a community increases fitness by offering better protection and allowing more complex behavior like division of labor (Jefferson, 2004). But in order for neighboring cells to work in unison also more complex structures are required, like adhesion and cell-cell communication.

Streptomycetes are mycelial organisms that grow as hyphae, and they undergo a complex life cycle whereby they propagate via sporulation, involving complex regulatory networks and developmental checkpoints (Flärdh & Buttner, 2009). Different parts of the mycelia take up different roles. The tip of the hyphae grow by extension, and at these apices a wide range of cellulolytic and proteolytic enzymes is secreted, allowing assimilation of dead plant matter (Willemsen *et al.*, 2012). More centrally positioned sections produce a wide variety of antibiotics, for which the species is best recognized (Bibb, 1996). In view of all the complex mechanisms being directed throughout the mycelia we can truly appreciate the multicellularity of this organism. Having said that, from the perspective of commercialization this complex morphogenesis also poses several major issues, which was the driving force behind this thesis.

Streptomyces and Biotechnology

From an applied perspective we are very interested in *Streptomyces* species *because* they produce such a wide chemical variety of compounds that we apply as antibiotics, antifungal,



anticancer and immunosuppressant agents (Hopwood, 2007). Also the large diversity of enzymes are put to good use, finding uses in the washing industry to the pretreatment of lignocellulosic materials for bioethanol production.

Industrial production of these compounds generally occurs in large bioreactors where the micro-organisms are cultivated in a fluid environment. The liquid is mixed vigorously to allow aeration and to secure an even distribution of biomass and nutrients. Although this is an efficient use of space and equipment it is very different from the natural soil habitats. Especially multicellular organisms like filamentous fungi or *Streptomyces* are a poor match for submerged fermentation (Wucherpennig *et al.*, 2010). The mycelial network entangles in the turbulent environment changing the liquid in a non-Newtonian fluid, which increases the apparent viscosity, negatively affecting the mass transfer and mixing times, thereby decreasing the efficiency of the fermentation (Metz *et al.*, 1979). Also the long hyphae themselves are prone to breaking, causing lysis of compartments (Li *et al.*, 2002). Besides growing as a loose mycelial network, many *Streptomyces* species can aggregate into dense pellets. Pellets do not affect the apparent viscosity nearly as much, but also limit the maximal obtainable rates by restricting mass transfer toward the pellet's core. Interestingly pellets also play a regulatory role in production, sometimes impacting product formation in a yet poorly understood mechanism (Wardell *et al.*, 2002, López *et al.*, 2005). Clearly, the efficiency of a fermentation with a filamentous micro-organism depends greatly on its morphology. Work described in this thesis aims at the discovery, understanding and development of novel ways to control morphology of *Streptomyces* species with the goal of improving the fermentability and production. An overview of what is known about the environmental and genetic factors affecting liquid morphogenesis is discussed in Chapter 2.

Reverse engineering as a source of new morphogenes

Our aim to improve the fermentability of *Streptomyces* prompted analysis of *S. lividans* strains PM01 and PM02 that had been selected for their favorable growth behavior in a bioreactor, obtained through evolution in a chemostat (Roth *et al.*, 1985). Over the course of the evolution experiment the strains adapted to the environment, resulting in the stable strains PM01, which makes very small pellets, and PM02, which is unable to make any pellets at all. Both had superior maximum growth rates compared to the parental strain, but were genetically black boxes. As these strains descended from *S. lividans* 66, which is a preferred heterologous enzyme production host because of a low proteolytic activity and the ability of secreting complex enzymes (Anné *et al.*, 2012), we initially considered PM02 as a potential production platform only to find that it was unable to secrete enzymes through the twin arginine transporter (Tat) system. This made this strain a very attractive candidate to reverse engineer. With reverse engineering we aimed to reconstruct the key features of these black box mutants by targeted genomic disruption. Sequencing of PM01 and PM02 revealed a handful of mutations that were sub sequentially recreated in the parent strain leading to the discovery of *matA* and *matB*, two genes that were essential for

mycelial aggregation. We compared the growth of clean knockout mutants and found that the absence of pellets in the *matAB* double mutant increased the growth rate and enzyme production rate by 60%, both most likely the result of an increased surface area exposed to the media, allowing high substrate uptake rates. A major advancement was achieved with this discovery, improving *S. lividans* as a production host for enzymes, but also paving the way to an increased understanding and control of morphogenesis in liquid-grown cultures.

Mechanism of pellet aggregation

The discovery of the mat locus was not our first adventure into genetic morphology engineering. Overexpression of the developmental protein SsgA induces septum formation throughout the vegetative mycelium, which increases the rate at which fragmentation takes place, leading to a reduced particle size (van Wezel et al., 2000a, van Wezel et al., 2006). Similar to the mat mutants, reduction of particle size resulted in increased growth rate of the culture and increased enzyme production rates. Also the *csIA-glxA* gene cluster (Xu et al., 2008, Chaplin et al., 2015) and the recently discovered partner *dtpA* (Petrus et al., 2016) are somehow involved in controlling *Streptomyces* morphology in liquid-grown cultures. These genes are responsible for the production of a cellulose-like polysaccharide that, together with the hydrophobic Chaplin proteins, facilitate adhesion (de Jong et al., 2009b). Beside this there are reports that extracellular DNA (Kim & Kim, 2004), cell wall fusions (Koebisch et al., 2009) and hyaluronic acids (Kim & Kim, 2004) are involved in this process of cellular adhesion. Similar to the surface attachment of a biofilm the *Streptomyces* liquid morphogenesis is a complex process.

In Chapter 4 we showed that the MatB protein produces the exo-polysaccharide poly-1,6- β -N-acetylglucosamine (PNAG), which is well characterized and an essential component of cellular adhesion in *E. coli*, *S. epidermidis* and *B. subtilis* (Wang et al., 2004, McKenney et al., 1998, Roux et al., 2015). The polysaccharide, synthesized by the glycosyltransferase domain of MatB, acts as a bacterial glue; the extracellular carbohydrate esterase domain of MatB most likely partially deacetylated the chain, giving it a positive charge allowing it to stick to the outside of the cell wall. This layer can be seen by high resolution scanning electron microscopy covering the entire cell wall. Interestingly, great similarities exist between the morphology in liquid cultures of null mutants deleted for either the *matAB* or *csIA-glxA* genes. We found that MatA and MatB are required to support adhesion to hydrophilic surfaces like glass (and cells), while CslA is required for adhering to hydrophobic surfaces like polystyrene. This opens the idea that the architecture of a pellet depends on both hydrophilic and hydrophobic adhesive forces. Interestingly, in liquid-grown cultures the expression of the mat genes to non-pelleting strains such as *S. venezuelae*, *S. clavuligerus*, *S. albus* or *Sacch. erythraea* was able to induce pellet formation, which suggest that under non-native conditions the presence of PNAG is enough to induce pellet formation. For now it remains unclear why native aggregation depends on a combination of mechanisms, but possibly it is a matter of robustness.



Gateway to synthetic morphology

Understanding the mechanism by which the *mat* genes act led to the insight that it has a very direct way of facilitating adhesion. This led to the idea that these genes could be employed rationally to improve the fermentability of *Streptomyces*. In Chapter 5 strains were created that expressed *matA* and *matB* from different promoters with the goal of allowing initial fast dispersed growth combined with later aggregation during exponential growth. The promoter regions of *chpE* (Claessen *et al.*, 2003) and *glpQ2* (Thomas *et al.*, 2012) were selected for their expression profile based on previous transcription data (Nieselt *et al.*, 2010) and fusion with the *matAB* locus gave strains that had a growth rate that was on par with the *matAB* null mutant described in Chapter 3, but which limited the rise of apparent viscosity also associated with full dispersed growth. Interestingly, although the viscosity as a function of morphology had been characterized for the filamentous fungus *Absidia corymbifera* (Kim *et al.*, 1983), this had never been done for *Streptomyces*. We found that, compared to the data from filamentous fungi, the dispersed growing *S. lividans matAB* null mutant affected the flow behavior already at biomass concentrations as low as 1 g/L, creating a non-Newtonian fluid, but the rise in apparent viscosity was not as quick during the fermentation process. Most likely this is the result of fragmentation as image analysis showed that particles of the *matAB* null mutant remain small. Pellets on the other hand affect viscosity only at biomass concentrations not readily encountered in fermentations. By analyzing multiple particles through image analysis we could establish that strains with altered *matAB* expression obtain morphologies that are best described as the intermediate between the two extreme morphologies of pelleting and dispersed growth. Over time the strains progress towards a pelleting morphology, but not really aggregating to the same extent as wild-type *S. lividans*. It is an interesting notion that potentially large amounts of PNAG are needed to allow wild-type levels of aggregation. Still we believe that the example of morphology engineering that we describe in this chapter is a major step forward in the fermentability of streptomycetes.

***Streptomyces* in microcultures**

Besides being difficult to control in shake flasks or bioreactors, growth of *Streptomyces* on a small scale is probably even more difficult (Sohoni *et al.*, 2012). The heterogeneity of a population consisting of multicellular aggregates (van Veluw *et al.*, 2012), combined with a complicated interconnectedness of morphology and environment creates difficulties for small scale growth, while growth on such a scale is desirable for high throughput experiments needed for screening thousands of strains under many environmental conditions needed to explore the chemical diversity offered by these strains. As discussed in Chapter 2 morphology is the result of genetic and environmental factors. In Chapter 6 we show that it is possible to modulate the morphology of *Streptomyces lividans* and *Streptomyces coelicolor*, both of which are extreme pellet formers, by cultivating them in microtiter plates on a vortex. This

allowed precise speed control at extreme agitation speeds, matching shear forces found in larger cultivation vessels. Interestingly, at low agitations rates (around 800 rpm) aggregation was absent, and pellet formation could be induced only by increasing the mixing rate to values of at least 1000 rpm. A substantial mixing rate is needed to induce the fragmentation rate, for which purpose coiled springs are routinely added to shake flasks. Increasing the stirring speed further to 1600 rpm fragmentation became more dominant, with abundant lysis seen in the form of small debris. Our data show that the mycelial morphology was optimal for these growth conditions at 1400 rpm mixing rate, which gave morphological characteristics close to those found in shake flasks. It provides important proof of concept that it is feasible to screen for enzyme and antibiotic production in volumes as small as 100 μL , which is an important step forward in the screening of streptomycetes.

OUTLOOK: LINKING MORPHOLOGY AND PRODUCTIVITY

As a result of interdependencies between morphology, environment and genetics, and the interconnection of morphology and productivity, an interdisciplinary out of the box approach is needed to fully elucidate all the actors and understand how they affect production. Therefore this thesis does not only describes multiple perspectives in understanding and controlling *Streptomyces* morphology in liquid cultures, but it can also be set in a larger framework where we aim to understand the morphogenesis on multiple levels, ranging from studying in detail the role of cell division (Celler *et al.*, 2016), following the dynamics of cellular processes in a time-resolved manner (Willemse *et al.*, 2012) and modeling hyphal growth in silico (Celler *et al.*, 2012). The next challenge is to converge the lessons learned from the different approaches and relate it to further optimization of the production process.

From experiments performed on solid media it is known that antibiotic production and programmed cell death in the vegetative mycelium are part of the developmental cycle, hypothetically to create nutrients and a competitor-free environment for the formation of spores (Manteca *et al.*, 2005, Wildermuth, 1970, Miguélez *et al.*, 1999). The core of a pellet has a characteristic; some antibiotics are produced there and cell death is also present (Manteca *et al.*, 2008). This, combined with a limited amount of studies in liquid cultures led to the idea that pellets are beneficial for antibiotic production (van Wezel *et al.*, 2006, Martin & Bushell, 1996, López *et al.*, 2005). As a result of the poor solubility of oxygen in water, it is most likely that this is the cue that orchestrates this. In biofilm systems the absence of oxygen is a trigger for developmental genes (Worlitzsch *et al.*, 2002). Also oxygen-limiting conditions have actually been measured for *Aspergillus niger* in pellets as small as 200 μm (Hille *et al.*, 2005), which makes it likely that *Streptomyces* pellets also possess an anoxic core. Although the link between pellet formation, oxygen limitation and development requires further elucidation there is plenty of evidence that oxygen limitation is a major player in this.

We have performed some initial experiments that showed the effects of oxygen limitation



on the activity of the *mat* genes. The non-aggregating mycelium seen under low mixing conditions in the micro cultures described in Chapter 6 are likely the result of low oxygen conditions as similar morphologies are obtainable by restricting the air flow in a shake flask. Additions of a nitric oxide donor, an important cue for anaerobic metabolism (Barraud *et al.*, 2006, Plate & Marletta, 2012), also inhibited pellet formation and repression of the *mat* promoter. This is again similar to known biofilm systems where it is also known that exopolysaccharide production is inhibited by nitric oxide (Barraud *et al.*, 2009). Interestingly, this regulation is performed through c-di-GMP in other organisms by direct interaction of the glycosyltransferases. Likely in streptomycetes it occurs through a different mechanism as bioinformatics analysis suggest that c-di-GMP binding PilZ domain is absent throughout the genus. In *Streptomyces* c-di-GMP acts as a signaling molecule in development, by modulating the activity of the global developmental regulator BldD (Tschowri *et al.*, 2014). It will be interesting to see if c-di-GMP also affects exo-polysaccharide production.

Work described in this thesis has offered new ways to tune the mycelial morphology, which enable us to resolve the link between morphology and production in the near future, eventual leading towards an optimal morphology for productivity. We are now able to regulate pellet size through *matAB* gene activity, creating populations with altered pellet sizes. Also as discussed in Chapter 4, introduction of the *mat* genes induces pellet formation in non-pelleting species and, although the research is still in progress, initial trials with these strains did result in altered growth profile, associated with pelleted growth, but also a delayed production of antibiotic production. This could mean that in liquid-grown cultures the occurrence of antibiotic production is not necessarily linked to the morphology and that there is still a lot we do not understand in terms of how antibiotic production is regulated.

The work presented in this thesis has provided new insights into the genetic and environmental factors that control the morphology of *Streptomyces* in submerged cultures, and it also offers leads as to how this can be harnessed to fine tune the growth parameters for improved productivity. With that, new paths have been uncovered that may lead towards better understanding of the principles of mycelial growth of streptomycetes, as well as new opportunities for their use as commercial production platform.



N

Nederlandse Samenvatting

Over het algemeen denken wij aan bacteriën als eencellige organismen, die rondzwemmen op zoek naar voedsel en snel vermeerderen via binaire deling. Maar in werkelijkheid leven de meeste bacteriën een groot gedeelte van hun levenscyclus als onderdeel van een gemeenschap in een biofilm of permanent als een volwaardig multicellulair organisme. Bacteriën geven hun rondzwervende, snel groeiende, bestaan op omdat leven in een gemeenschap hun overlevingskansen vergroot. Deze levenswijze biedt bescherming tegen omgevingsfactoren en bevordert complex gedrag zoals samenwerking en specialisatie. Om een dergelijke gemeenschap te kunnen vormen, moeten cellen zich aan elkaar kunnen hechten. Deze rol wordt over het algemeen vervuld door de extracellulaire matrix, die vaak bestaat uit een combinatie van polysachariden, extracellulair DNA en eiwitten. Multicellulaire organismes zijn waarschijnlijk ontstaan doordat rondzwerven onnodig werd en stopte de celdeling voordat er volledige scheiding kon plaatsvinden.

Streptomyceten zijn dergelijke multicellulaire bacteriën; ze groeien als lange draden, ook wel hyfen genoemd, die uitgroeien tot een mycelium netwerk. Ze bezitten een complexe levenscyclus, geregeld via complexe cellulaire regel netwerken met checkpunten in hun ontwikkeling, leidend tot voorplanten via sporen. Verschillende delen van het mycelium zijn gespecialiseerd voor de vervulling van verschillende rollen. De top van een hyfe groeit via tip-extensie, en in deze apex vindt de secretie van een grote verscheidenheid aan cellulolytische en proteolytische enzymen plaats die de assimilatie van dood plantenmateriaal faciliteert. In meer centrale gedeeltes van het mycelium vindt de productie van antibiotica plaats, een vermogen waarmee deze bacteriegroep zijn maatschappelijk nut bewijst. Door alle complexe mechanismen als groter geheel te bestuderen kunnen we de streptomyceet als multicellulair



organisme waarderen. Dat gezegd hebbende, voor biotechnologische industrialisatie zorgt de complexe groeiwijze als gevolg van de morfologie voor tal van problemen. Het verminderen van deze problemen was de drijvende kracht achter deze thesis.

Streptomyces en Biotechnology

Vanuit een industrieel perspectief zijn wij voornamelijk geïnteresseerd in streptomyceten omdat ze een onvoorstelbaar veelzijdig chemisch arsenaal tot hun beschikking hebben, dat we kunnen inzetten als antibiotica, antischimmel, antikanker en immuun-onderdrukkende middelen (Hopwood, 2007). Ook de verschillende enzymen vinden hun toepassing van wasmiddelen tot de voorbereiding van biomassa voor bio-ethanol productie.

Industriële productie vindt over het algemeen plaats in een waterige omgeving in grote bioreactoren. De vloeistof met de micro-organismen en alle benodigde voedingsstoffen voor groei en productie, wordt krachtig gemixt voor een homogene distributie en voldoende zuurstofvoorziening. Groei in bioreactoren is efficiënt, maar de omstandigheden daarin zijn wezenlijk anders dan in aarde, de natuurlijke habitat van streptomyceten. Vooral multicellulaire organismen zoals filament vormende schimmels of streptomyceten zijn een slechte match voor vloeistof-gebaseerde fermentaties (Wucherpfennig *et al.*, 2010). Het netwerk van mycelium raakt verward in de turbulente omgeving, wat de vloeistof in een viskeuze, niet-Newtonische drab verandert. Dit heeft negatieve gevolgen voor het massatransport en de vermeningstijd, wat de efficiëntie van de fermentatie doet afnemen (Metz *et al.*, 1979). In deze omgeving kunnen de individuele hyfen ook gemakkelijk breken, met celdood als gevolg (Li *et al.*, 2002). Sommige streptomyceten aggregeren in dichte pellets als reactie op groei in vloeistof. Deze pellets veranderen de viscositeit van de vloeistof nauwelijks, maar limiteren wel de toevoer van voedingsstoffen richting de kern waardoor een gedeelte van de biomassa in mindere mate kan deelnemen aan het groei- en productieproces. Interessant genoeg lijkt de pellet morfologie ook een effect te hebben op de regulatie van product formatie, met als gevolg dat pellets soms nodig zijn voor efficiënte productie (Wardell *et al.*, 2002, López *et al.*, 2005).

Het moge duidelijk zijn dat de morfologie van een filament vormend organisme een grote invloed heeft op de efficiëntie waarmee geproduceerd kan worden. Het werk dat beschreven is in dit proefschrift richtte zich op het begrijpen hoe de morfologie van streptomyceten zich in vloeistof organiseert en de ontwikkeling van nieuwe manieren om de morfologie te controleren, zodat deze geoptimaliseerd kan worden voor verbetering van de groei en productie in een industriële fermentatie. Een overzicht van de al bestaande kennis over de effecten van de omgeving en de genetische factoren die een rol spelen bij de morfologische ontwikkeling in vloeistof is beschreven in Hoofdstuk 2.

“Reverse engineering” als bron voor nieuwe morfo-genen

Met ons doel om de fermenteerbaarheid van *Streptomyces* te vergroten is gestart met de van *S. lividans* afgeleide stammen PM01 en PM02 te analyseren. Deze twee geëvolueerde

stammen waren geïsoleerd uit een chemostaatexperiment waar ze verbeterde groei eigenschappen vertoonden (Roth *et al.*, 1985). Gedurende het experiment was er selectiedruk voor snelle groei, wat resulteerde in de stabiele stam PM01, welke kleine pellets maakt, en PM02, welke de mogelijkheid tot pellet formatie totaal had verloren. Beide stammen groeiden met superieure snelheid vergeleken met de ouderstam, maar waren ook genetisch gezien een “zwarte doos”. Het was dus onbekend waarom ze zo konden groeien. We beschouwden PM01 en PM02 initieel als een interessante productie stam voor heterologe enzym productie, niet alleen vanwege zijn mooie groei karakter, maar ook omdat zij afstamden van *S. lividans*, een *Streptomyces* soort die aantrekkelijk is voor enzymproductie vanwege lage proteolytische activiteit en efficiënt complexe enzymen kan uitscheiden (Anné *et al.*, 2012). We er achter kwamen dat deze stam de mogelijkheid om enzymen via het twin arganine transport (Tat) systeem te exporteren had verloren. Geen productiestam dus, maar wel een interessante kandidaat om te “reverse engineeren”. Hiermee pogen we de sleutelaspecten van deze “zwarte doos” te ontcijferen door gerichte mutaties te maken in het genoom van de ouderstam. Sequensen van het genoom van PM01 en PM02 legde een handvol mutaties bloot welke werden aangebracht in wild-type *S. lividans*. Dit leidde tot de ontdekking van *matA* en *matB*, twee genen welke essentieel waren voor mycelium aggregatie. In vergelijking met de ouderstam, groeide een stam waar *matA* en *matB* beide waren verwijderd uit het genoom ongeveer 60% sneller en produceerde een heteroloog enzym eveneens met eenzelfde verhoogde snelheid. Dit betekende een grote vooruitgang voor *S. lividans* as productiestam. Ook betekende de ontdekking van de *mat* genen een nieuwe manier om het mechanisme van pellet formatie te besturen en de mogelijkheid om het te proces te controleren.

Het mechanisme van pellet aggregatie

De ontdekking van de *mat* genen was niet onze eerste bezigheid in genetische morfologie manipulatie. Overexpressie van het ontwikkelingseiwit SsgA induceert septumformatie in het vegetatieve mycelium, met een versnelling van fragmentatie tot gevolg, wat de pellet grootte doet afnemen (van Wezel *et al.*, 2000a, van Wezel *et al.*, 2006). Analoog aan de *mat* mutanten, leidt deze morfologieverandering tot een versnelling van groeisnelheid van de cultuur en verhoogt het de enzym productie.

Daarnaast is er ook het *csIA-glxA* gen cluster (Xu *et al.*, 2008, Chaplin *et al.*, 2015), dat geholpen door de recent ontdekte partner *dtpA* (Petrus *et al.*, 2016)2016 ook via een nog niet volledig begrepen mechanisme betrokken is in pelletformatie. Deze genen lijken verantwoordelijk voor de aanmaak van een cellulose-achtige extracellulaire polysacharide die samen met de hydrofobe chaplin eiwitten voor hechting zorgen (de Jong *et al.*, 2009b). Hiernaast zijn er voorbeelden in de literatuur van de betrokkenheid van extracellulair DNA (Kim & Kim, 2004), celwand fusies (Koebsch *et al.*, 2009) en hyaluron zuur (Kim & Kim, 2004) in cel-cel adhesie. Net as een biofilm dat zich op een oppervlakte bevindt, is het mechanisme van adhesie bij *Streptomyces* een ingewikkeld proces.



In Hoofdstuk 4 laten we zien dat het MatB eiwit de extracellulaire polysacharide poly-1,6- β -*N*-acetylglucosamine (PNAG) maakt, een molecuul waarvan al eerder was aangetoond dat het essentieel is voor biofilmformatie in *E. coli*, *S. epidermis* en *B. subtilis* (Wang *et al.*, 2004, McKenney *et al.*, 1998, Roux *et al.*, 2015). De polysacharide wordt geproduceerd door de glycosyltransferase domein van MatB, waarschijnlijk geholpen door het extracellulaire domain van MatB dat een acetylgroep van het polymeer kan verwijderen waardoor het een positieve lading krijgt. Hierdoor zou PNAG gemakkelijk met de celwand kunnen associëren. Dit polymeer is zichtbaar onder de scanning elektron microscoop als een laag die de gehele hyfen bedekt. Interessant genoeg vertonen de mutanten van *matAB* en *csIA-glxA* genen een vergelijkbare morfologie. We ontdekten dat MatA en MatB een functie vervullen bij hechting aan een hydrofiel glazen oppervlak terwijl CslA en GlxA nodig zijn voor de hechting aan een hydrofoob plastic oppervlak. Dit scheidt het idee dat pellets bij elkaar worden gehouden door de combinatie van hydrofiel en hydrofobe interacties. Interessant is echter dat streptomyceetsoorten die normaal niet in staat zijn om pellets in vloeistof te vormen, zoals *S. venezuelae*, *S. clavuligerus*, *S. albus of Sacch. Erythraea*, dit wel kunnen wanneer *matAB* worden geïntroduceerd, wat suggereert dat onder niet native omstandigheden de aanwezigheid van PNAG genoeg is voor pelletformatie. Voor nu is het niet totaal duidelijk waarom *S. lividans* onder natuurlijke omstandigheden op een combinatie van mechanismes vertrouwt voor hechting, maar het draagt ongetwijfeld bij aan de robuustheid van het systeem.

De portaal naar synthetische morfologie

Het doorgronden van het mechanisme van de mat genen leidde tot het inzicht dat dit werkt via een hele directe manier van adhesie. Dit introduceerde het idee dat deze genen ideaal waren voor een rationele manier de proces eigenschappen van *Streptomyces* in een bioreactor te verbeteren. In hoofdstuk 5 staat beschreven hoe we dieper ingaan op de eigenschappen van de open- en pelletmorfologie. Uiteindelijk trachten we de positieve eigenschappen van beiden in één stam te verenigen: zowel snelle groei zonder aggregatie als pelletformatie om de viscositeit te beperken.

Interessant genoeg was de functie van viscositeit ten opzichte van de morfologie nog niet eerder voor streptomyceten bepaald, terwijl dit wel een belangrijke parameter is voor een industriële fermentatie. Wel was dit al gedaan voor de filament vormende schimmel *Absidia corymbifera* (Kim *et al.*, 1983), die toch een totaal ander formaat dan streptomyceten heeft. We ontdekten dat bij een biomassa concentratie van slechts 1 g/l de open groeiende *S. lividans matAB* nul mutant de vloeistof al in een niet-Newtoniaanse vloeistof veranderde. Interessant genoeg leidde bij hogere biomassaconcentraties de filament vormende schimmel wel tot een hogere viscositeit. Dit verschil is waarschijnlijk toe te schrijven aan een grotere fragmentatiesnelheid bij streptomyceten ten opzichte van schimmels, aangezien image analyse aantoonde dat de *Streptomyces* fragmenten klein bleven. Aan de andere kant konden we zien dat pellets de vloeistof eigenschappen alleen beïnvloedden bij concentraties

die normaal niet gehaald worden in een fermentatie.

Vervolgens creëerden we stammen die *matA* en *matB* tot expressie brengen via verschillende promotoren met het doel om initieel open en dus snelle groei te faciliteren, maar later pelletformatie te induceren. De promoterregio's van *chpE* (Claessen *et al.*, 2003) en *glpQ2* (Thomas *et al.*, 2012) werden geselecteerd aan de hand van hun expressie profiel, gemeten in een eerdere studie (Nieselt *et al.*, 2010). Fusies van deze regio's met de *matAB* locus gaf stammen met een vergelijkbare groeisnelheid met de *matAB* nul mutant beschreven in hoofdstuk 3, maar waarbij ook de verhoging van de viscositeit binnen de perken kon worden gehouden in de batchfase te aggregeren. Door grote hoeveelheden cellen automatisch te analyseren met de microscoop konden we aantonen dat stammen met de veranderde *matAB* expressie een morfologie vertoonden die gemiddeld gezien ergens tussen wildtype en de *matAB* nul mutant inzat. Wanneer de cultuur langer groeide, werd de pellet morfologie meer zichtbaar, maar aggregatie vond niet in dezelfde hoedanigheid plaats als bij wild-type *S. lividans*. Het lijkt er dus op dat grote hoeveelheden PNAG aanwezig moeten zijn om wild-type levels van aggregatie te kunnen induceren. Toch tonen wij in dit hoofdstuk een voorbeeld van rationele morfologie engineering welke een grote vooruitgang betekent in het fermenterend vermogen van streptomyceten.

Streptomyceten in microculturen

Ook al zijn streptomyceten moeilijk onder controle te houden in een schudfles of in een bioreactor, het is mogelijk nog moeilijker om dit te bereiken in een zeer klein volume (Sohoni *et al.*, 2012). De heterogeniteit van de populatie, bestaande uit multicellulaire aggregaten van verschillende groottes (van Veluw *et al.*, 2012) gecombineerd met de wederzijdse afhankelijkheid van morfologie en de omgeving zorgt voor veel complicaties bij groei op zeer kleine schaal. Dit is echter wel nodig voor screeningsexperimenten waarbij het gewenst is om duizenden stammen onder vele verschillende omstandigheden te testen om de chemische diversiteit geproduceerd door streptomyceten te verkennen. Zoals beschreven in hoofdstuk 2 is de morfologie het resultaat van genetische en omgevings- factoren. In hoofdstuk 6 laten we zien dat we de morfologie van *S. lividans* en *S. coelicolor*, stammen die grote pellets maken, kunnen moduleren in een microtiterplaat door deze op een vortex te plaatsen. Met de vortex kon de roersnelheid precies worden ingesteld en konden hoge snelheden worden bereikt. Interessant genoeg was aggregatie afwezig bij lage roersnelheden rond de 800 rpm en kon pelletformatie worden gestimuleerd door de roersnelheid te verhogen boven de 1000 rpm. Een hoge roersnelheid was nodig om fragmentatie te induceren. In schudflessen wordt fragmentatie verhoogd door er een veer van roestvrijstaal in te plaatsen. Wanneer de roersnelheid boven de 1600 rpm kwam, namen wij naast fragmentatie ook een substantiële hoeveelheid dood cel materiaal waar. Hierdoor stelden wij vast dat 1400 rpm de ideale conditie was voor groei, waarbij we ook via image analyse konden laten zien dat de eigenschappen van de pellets vrijwel identiek waren met culturen opgegroeid in een schudfles. Deze studie toont aan dat het mogelijk is om streptomyceten te cultiveren in een



volume van slechts 100 µl en te screenen voor enzym- en antibioticaproductie.

Tot Slot

Omdat de morfologie, de omgeving en de genetica elkaar allemaal beïnvloeden en omdat er een nauw verband bestaat tussen de morfologie en de productiviteit, is een interdisciplinaire “out of the box” benadering nodig om alle actoren te ontdekken en te begrijpen hoe deze de productie beïnvloeden. Daarom is er in dit proefschrift niet alleen beschreven hoe wij de vorming van de morfologie van *Streptomyces* vanuit verschillende perspectieven proberen te begrijpen en manipuleren, maar tevens kunnen wij de verkregen kennis plaatsen in een ruimer kader waar we de morfologie op verschillende niveaus willen begrijpen; waar we zowel kijken naar de rol van celdeling (Celler *et al.*, 2016), de dynamische cellulaire processen volgen over de tijd (Willemse *et al.*, 2012) en de morfologie digitaal proberen te modelleren (Celler *et al.*, 2012). De volgende stap zal zijn om al deze kennis te combineren wat verdere inzichten zou moeten geven over het verband tussen morfologie en productie.

Uit experimenten die niet plaats vonden in vloeistof, maar op vast medium, is bekend dat antibioticaproductie en geprogrammeerde celdood plaats vinden in het vegetatief mycelium en deel uit maken van de ontwikkelingscyclus (Manteca *et al.*, 2005, Wildermuth, 1970, Miguélez *et al.*, 1999). In vloeistof zijn in de kern van de pellet vergelijkbare condities waargenomen; sommige antibiotica worden daar geproduceerd en er vindt tevens geprogrammeerde cel dood plaats (Manteca *et al.*, 2008). Deze observaties en een gelimiteerd aantal studies in vloeistof hebben geleid tot het idee dat pellets een positief effect op antibioticaproductie kunnen hebben (van Wezel *et al.*, 2006, Martin & Bushell, 1996, López *et al.*, 2005). Er is nog veel onbekend hoe de processen in de kern van een pellet worden gereguleerd, maar vermoedelijk spelen de nutriënt limiterende condities hierin een grote rol. Met name de toevoer van zuurstof, nodig in grote hoeveelheid, maar slecht oplosbaar in water, zijn vaak aangewezen als belangrijk signaal. In biofilmsystemen van andere organismes is de afwezigheid van zuurstof een bekende trigger voor ontwikkelingsgenen (Worlitzsch *et al.*, 2002). Wanneer de regulatie van de morfologie verder bestudeerd gaat worden moet de toevoer van zuurstof zeker in oogschouw worden genomen.

Met verkennende experimenten hebben we al laten zien dat de expressie van de *mat* genen reageren op oxidatieve stress. De reductie van aggregatie bij mycelium waargenomen in de micro-culturen bij lage roersnelheden, beschreven in Hoofdstuk 6, zijn zeer waarschijnlijk het effect van lage zuurstof concentraties aangezien we dit effect ook konden waarnemen wanneer de zuurstof toevoer was vermindert door een schudfles gedeeltelijk af te sluiten met parafilm. Tevens verminderde de toevoeging van een stikstofoxide donor, een belangrijke signaalstof voor het anaerobe metabolisme (Barraud *et al.*, 2006, Plate & Marletta, 2012), pelletformatie en de expressie van *mat*. Ook dit is vergelijkbaar aan andere biofilmsystemen waar stikstofoxide de productie van extracellulaire polysacchariden onderdrukt (Barraud *et al.*, 2009). In deze systemen vindt de regulatie plaats via het signaal

molecuul c-di-GMP, waarbij het direct met de glycosyltransferase een interactie aangaat via een PilZ domein. Interessant genoeg is dit domein totaal afwezig in streptomyceten. In plaats daarvan bindt c-di-GMP aan bldD, een globale regulator van de ontwikkelingscyclus (Tschowri *et al.*, 2014). Een interessante ontdekking ligt in het verschiet betreft de regulatie van *mat* en een mogelijke link met de ontwikkelingscyclus.

Samenvattend heeft het werk, beschreven in deze thesis, nieuwe inzichten opgeleverd hoe wij de morfologie van streptomyceten kunnen afstellen. In de nabije toekomst zal dit een fantastisch handvat blijken waarmee we de link tussen morfologie en productie verder kunnen bestuderen en zal leiden tot een optimalisatie van de morfologie voor productie. We zijn nu verder in staat om de morfologie aan onze wensen aan te passen, hoofdstuk 5 doet hierin al de eerste stappen, maar we kunnen ook, zoals wordt genoemd in hoofdstuk 4, deze kennis toepassen bij andere streptomyceten. Dit kan leiden tot verbeteringen voor de productie van enzymen en antibiotica, maar mogelijk ook een nuttig gereedschap in de kist kan blijken voor het ontdekken van nieuwe antibiotica.



R

References

Amijee, F., E. Allans, R. Waterhouse, L. Glover & A. Paton, (1992) Non-pathogenic association of L-form bacteria (*pseudomonas syringae* pv. *phaseolicola*) with bean plants (*Phaseolus vulgaris* L.) and its potential for biocontrol of halo blight disease. *Biocontrol Science and Technology* **2**: 203-214.

Anné, J., B. Maldonado, J. Van Impe, L. Van Mellaert & K. Bernaerts, (2012) Recombinant protein production and streptomycetes. *Journal of biotechnology* **158**: 159-167.

Anné, J., K. Vrancken, L. Van Mellaert, J. Van Impe & K. Bernaerts, (2014) Protein secretion biotechnology in Gram-positive bacteria with special emphasis on *Streptomyces lividans*. *Biochimica et Biophysica Acta (BBA)-Molecular Cell Research* **1843**: 1750-1761.

Aoki, Y., D. Matsumoto, H. Kawaide & M. Natsume, (2011) Physiological role of germicidins in spore germination and hyphal elongation in *Streptomyces coelicolor* A3 (2). *The Journal of antibiotics* **64**: 607-611.

Archer, N.K., M.J. Mazaitis, J.W. Costerton, J.G. Leid, M.E. Powers & M.E. Shirtliff, (2011) *Staphylococcus aureus* biofilms: properties, regulation, and roles in human disease. *Virulence* **2**: 445-459.

Atkin, K.E., S.J. MacDonald, A.S. Brentnall, J.R. Potts & G.H. Thomas, (2014) A different path: revealing the function of staphylococcal proteins in biofilm formation. *FEBS letters* **588**: 1869-1872.

Ayazi Shamlou, P., H.Y. Makagiansar, A.P. Ison, M.D. Lilly & C.R. Thomas, (1994) Turbulent breakage of filamentous microorganisms in submerged culture in mechanically stirred bioreactors. *Chemical Engineering Science* **49**: 2621-2631.

Badino, A., M. Facciotti & W. Schmidell, (2001) Volumetric oxygen transfer coefficients (k L a) in batch cultivations involving non-Newtonian broths. *Biochemical engineering journal* **8**: 111-119.

Bagchi, S., H. Tomenius, L.M. Belova & N. Ausmees, (2008) Intermediate filament-like proteins in bacteria and a cytoskeletal function in *Streptomyces*. *Molecular microbiology* **70**: 1037-1050.

Bailey, J.E., A. Sburlati, V. Hatzimanikatis, K. Lee, W.A. Renner & P.S. Tsai, (1996) Inverse metabolic engineering: A strategy for directed genetic engineering of useful phenotypes. *Biotechnology and Bioengineering* **52**: 109-121.

Baltz, R.H., (2007) Antimicrobials from actinomycetes: back to the future. *Microbe-american society for microbiology* **2**: 125.

Baltz, R.H., (2008) Renaissance in antibacterial discovery from actinomycetes. *Current opinion in*



pharmacology **8**: 557-563.

Barraud, N., D.J. Hassett, S.-H. Hwang, S.A. Rice, S. Kjelleberg & J.S. Webb, (2006) Involvement of nitric oxide in biofilm dispersal of *Pseudomonas aeruginosa*. *Journal of bacteriology* **188**: 7344-7353.

Barraud, N., D. Schleheck, J. Klebensberger, J.S. Webb, D.J. Hassett, S.A. Rice & S. Kjelleberg, (2009) Nitric oxide signaling in *Pseudomonas aeruginosa* biofilms mediates phosphodiesterase activity, decreased cyclic di-GMP levels, and enhanced dispersal. *Journal of bacteriology* **191**: 7333-7342.

Bartholomew, W.H., E.O. Karow, M.R. Sfat & R.H. Wilhelm, (1950) Oxygen Transfer and Agitation in Submerged Fermentations. Mass Transfer of Oxygen in Submerged Fermentation of *Streptomyces griseus*. *Ind. Eng. Chem.* **42**: 1801-1809.

Bellgardt, K.-H., (1998) Proces models for production of β -lactam antibiotics. In: Relation Between Morphology and Process Performances. K. Schügerl (ed). Springer Berlin Heidelberg, pp. 153-194.

Belmar-Beiny, M.T. & C.R. Thomas, (1991) Morphology and clavulanic acid production of *Streptomyces clavuligerus*: Effect of stirrer speed in batch fermentations. *Biotechnology and Bioengineering* **37**: 456-462.

Bentley, S.D., K.F. Chater, A.M. Cerdeno-Tarraga, G.L. Challis, N.R. Thomson, K.D. James, D.E. Harris, M.A. Quail, H. Kieser, D. Harper, A. Bateman, S. Brown, G. Chandra, C.W. Chen, M. Collins, A. Cronin, A. Fraser, A. Goble, J. Hidalgo, T. Hornsby, S. Howarth, C.H. Huang, T. Kieser, L. Larke, L. Murphy, K. Oliver, S. O'Neil, E. Rabinowitsch, M.A. Rajandream, K. Rutherford, S. Rutter, K. Seeger, D. Saunders, S. Sharp, R. Squares, S. Squares, K. Taylor, T. Warren, A. Wietzorrek, J. Woodward, B.G. Barrell, J. Parkhill & D.A. Hopwood, (2002) Complete genome sequence of the model actinomycete *Streptomyces coelicolor* A3(2). *Nature* **417**: 141-147.

Beun, J., A. Hendriks, M. Van Loosdrecht, E. Morgenroth, P. Wilderer & J. Heijnen, (1999) Aerobic granulation in a sequencing batch reactor. *Water Research* **33**: 2283-2290.

Bewick, M., S. Williams & C. Veltkamp, (1975) Growth and ultrastructure of *Streptomyces venezuelae* during chloramphenicol production. *Microbios* **16**: 191-199.

Bhattacharjee, A., J.S. Oeemig, R. Kolodziejczyk, T. Meri, T. Kajander, M.J. Lehtinen, H. Iwai, T.S. Jokiranta & A. Goldman, (2013) Structural basis for complement evasion by Lyme disease pathogen *Borrelia burgdorferi*. *Journal of Biological Chemistry* **288**: 18685-18695.

Bhosale, S.H., M.B. Rao & V.V. Deshpande, (1996) Molecular and industrial aspects of glucose isomerase. *Microbiological reviews* **60**: 280-300.

Bi, E. & J. Lutkenhaus, (1991) FtsZ ring structure associated with division in *Escherichia coli*. *Nature* **354**: 161-164.

Bibb, M., (1996) The regulation of antibiotic production in *Streptomyces coelicolor* A3(2). *Microbiology*

142: 1335-1344.

Bibb, M.J., (2005) Regulation of secondary metabolism in streptomycetes. *Current Opinion in Microbiology* **8**: 208-215.

Bibb, M.J., Á. Domonkos, G. Chandra & M.J. Buttner, (2012) Expression of the chaplin and rodlin hydrophobic sheath proteins in *Streptomyces venezuelae* is controlled by σ BldN and a cognate anti-sigma factor, RsbN. *Molecular microbiology* **84**: 1033-1049.

Bibb, M.J., J.M. Ward & D.A. Hopwood, (1978) Transformation of plasmid DNA into *Streptomyces* at high frequency.

Bierman, M., R. Logan, K. O'Brien, E.T. Seno, R.N. Rao & B.E. Schoner, (1992) Plasmid cloning vectors for the conjugal transfer of DNA from *Escherichia coli* to *Streptomyces* spp. *Gene* **116**: 43-49.

Biró, S., I. Békési, S. Vitális & G. Szabó, (1980) A substance effecting differentiation in *Streptomyces griseus*. Purification and properties. *European journal of biochemistry/FEBS* **103**: 359-363.

Bokhove, M., D. Claessen, W. de Jong, L. Dijkhuizen, E.J. Boekema & G.T. Oostergetel, (2013) Chaplins of *Streptomyces coelicolor* self-assemble into two distinct functional amyloids. *Journal of structural biology* **184**: 301-309.

Boyd, A. & A. Chakrabarty, (1995) *Pseudomonas aeruginosa* biofilms: role of the alginate exopolysaccharide. *Journal of industrial microbiology* **15**: 162-168.

Boyle, D.S. & W.D. Donachie, (1998) *mraY* is an essential gene for cell growth in *Escherichia coli*. *J Bacteriol* **180**: 6429-6432.

Branda, S.S., A. Vik, L. Friedman & R. Kolter, (2005) Biofilms: the matrix revisited. *Trends in microbiology* **13**: 20-26.

Braun, S. & S.E. Vecht-Lifshitz, (1991) Mycelial morphology and metabolite production. *Trends in Biotechnology* **9**: 63-68.

Brünker, P., W. Minas, P.T. Kallio & J.E. Baile, (1998) Genetic engineering of an industrial strain of *Saccharopolyspora erythraea* for stable expression of the Vitreoscilla haemoglobin gene (vhb). *Microbiology* **144**: 2441-2448.

Büchs, J., S. Lotter & C. Milbradt, (2001) Out-of-phase operating conditions, a hitherto unknown phenomenon in shaking bioreactors. *Biochemical Engineering Journal* **7**: 135-141.

Büchs, J., U. Maier, C. Milbradt & B. Zoels, (2000) Power consumption in shaking flasks on rotary shaking machines: II. Nondimensional description of specific power consumption and flow regimes in unbaffled flasks at elevated liquid viscosity. *Biotechnology and bioengineering* **68**: 594-601.

Busarakam, K., A.T. Bull, G. Girard, D.P. Labeda, G.P. van Wezel & M. Goodfellow, (2014) *Streptomyces*



leeuwenhoekii sp. nov., the producer of chaxalactins and chaxamycins, forms a distinct branch in *Streptomyces* gene trees. *Antonie Van Leeuwenhoek* **105**: 849-861.

Bush, M.J., M.J. Bibb, G. Chandra, K.C. Findlay & M.J. Buttner, (2013) Genes required for aerial growth, cell division, and chromosome segregation are targets of WhiA before sporulation in *Streptomyces venezuelae*. *MBio* **4**: e00684-00613.

Bushell, M.E., (1988) Growth, product formation and fermentation technology. *Actinomycetes in biotechnology*: 185-217.

Camacho, C., G. Coulouris, V. Avagyan, N. Ma, J. Papadopoulos, K. Bealer & T.L. Madden, (2009) BLAST+: architecture and applications. *BMC bioinformatics* **10**: 421.

Celler, K., R.I. Koning, A.J. Koster & G.P. van Wezel, (2013) Multidimensional view of the bacterial cytoskeleton. *Journal of bacteriology* **195**: 1627-1636.

Celler, K., R.I. Koning, J. Willemsse, A.J. Koster & G.P. van Wezel, (2016) Cross-membranes orchestrate compartmentalization and morphogenesis in *Streptomyces*. *Nature communications* **7**.

Celler, K., C. Picioareanu, M.C. van Loosdrecht & G.P. van Wezel, (2012) Structured morphological modeling as a framework for rational strain design of *Streptomyces* species. *Antonie Van Leeuwenhoek* **102**: 409-423.

Cerca, N., G.B. Pier, M. Vilanova, R. Oliveira & J. Azeredo, (2005) Quantitative analysis of adhesion and biofilm formation on hydrophilic and hydrophobic surfaces of clinical isolates of *Staphylococcus epidermidis*. *Research in microbiology* **156**: 506-514.

Cerri, M.O. & A.C. Badino, (2012) Shear conditions in clavulanic acid production by *Streptomyces clavuligerus* in stirred tank and airlift bioreactors. *Bioprocess and Biosystems Engineering* **35**: 977-984.

Chaplin, A.K., M.L. Petrus, G. Mangiameli, M.A. Hough, D.A. Svistunenko, P. Nicholls, D. Claessen, E. Vijgenboom & J.A. Worrall, (2015) GlxA is a new structural member of the radical copper oxidase family and is required for glycan deposition at hyphal tips and morphogenesis of *Streptomyces lividans*. *Biochemical Journal* **469**: 433-444.

Chater, K. & R. Losick, (1997) Mycelial life style of *Streptomyces coelicolor* A3 (2) and its relatives. *Bacteria as multicellular organisms*: 149-182.

Chater, K.F., (1972) A morphological and genetic mapping study of white colony mutants of *Streptomyces coelicolor*. *Microbiology* **72**: 9-28.

Chater, K.F., S. Biró, K.J. Lee, T. Palmer & H. Schrepf, (2010) The complex extracellular biology of *Streptomyces*. *FEMS Microbiology Reviews* **34**: 171-198.

Chater, K.F., C.J. Bruton, K.A. Plaskitt, M.J. Buttner, C. Méndez & J.D. Helmman, (1989) The developmental fate of *S. coelicolor* hyphae depends upon a gene product homologous with the motility σ factor of *B.*

subtilis. *Cell* **59**: 133-143.

Chatfield, C.H., H. Koo & R.G. Quivey, (2005) The putative autolysin regulator LytR in *Streptococcus mutans* plays a role in cell division and is growth-phase regulated. *Microbiology* **151**: 625-631.

Chen, H.C. & F. Wilde, (1991) The effect of dissolved oxygen and aeration rate on antibiotic production of *Streptomyces fradiae*. *Biotechnology and Bioengineering* **37**: 591-595.

Claessen, D., W. de Jong, L. Dijkhuizen & H.A.B. Wösten, (2006) Regulation of *Streptomyces* development: reach for the sky! *Trends in Microbiology* **14**: 313-319.

Claessen, D., R. Rink, W. de Jong, J. Siebring, P. de Vreugd, F.H. Boersma, L. Dijkhuizen & H.A. Wösten, (2003) A novel class of secreted hydrophobic proteins is involved in aerial hyphae formation in *Streptomyces coelicolor* by forming amyloid-like fibrils. *Genes & development* **17**: 1714-1726.

Claessen, D., D.E. Rozen, O.P. Kuipers, L. Sjøgaard-Andersen & G.P. van Wezel, (2014) Bacterial solutions to multicellularity: a tale of biofilms, filaments and fruiting bodies. *Nature Reviews Microbiology* **12**: 115-124.

Claessen, D., I. Stokroos, H.J. Deelstra, N.A. Penninga, C. Bormann, J.A. Salas, L. Dijkhuizen & H.A. Wösten, (2004) The formation of the rodlet layer of streptomycetes is the result of the interplay between rodlines and chaplins. *Molecular microbiology* **53**: 433-443.

Claessen, D., H.A. Wösten, G.v. Keulen, O.G. Faber, A.M. Alves, W.G. Meijer & L. Dijkhuizen, (2002) Two novel homologous proteins of *Streptomyces coelicolor* and *Streptomyces lividans* are involved in the formation of the rodlet layer and mediate attachment to a hydrophobic surface. *Molecular microbiology* **44**: 1483-1492.

Colson, S., J. Stephan, T. Hertrich, A. Saito, G.P. van Wezel, F. Titgemeyer & S.e.b. Rigali, (2007) Conserved *cis*-Acting Elements Upstream of Genes Composing the Chitinolytic System of Streptomycetes Are DasR-Responsive Elements. *Journal of Molecular Microbiology and Biotechnology* **12**: 60-66.

Colson, S., G.P. van Wezel, M. Craig, E.E. Noens, H. Nothaft, A.M. Mommaas, F. Titgemeyer, B. Joris & S. Rigali, (2008) The chitobiose-binding protein, DasA, acts as a link between chitin utilization and morphogenesis in *Streptomyces coelicolor*. *Microbiology* **154**: 373-382.

Craig, M., S. Lambert, S. Jourdan, E. Tenconi, S. Colson, M. Maciejewska, M. Ongena, J.F. Martin, G. van Wezel & S. Rigali, (2012) Unsuspected control of siderophore production by N-acetylglucosamine in streptomycetes. *Environmental microbiology reports* **4**: 512-521.

Crook, N. & H.S. Alper, (2012) Classical Strain Improvement. In: Engineering Complex Phenotypes in Industrial Strains. R. Patnaik (ed). John Wiley & Sons, Inc., pp. 1-33.

Cruz-Morales, P., E. Vijgenboom, F. Iruegas-Bocardo, G. Girard, L.A. Yanez-Guerra, H.E. Ramos-Aboites, J.L. Pernodet, J. Anne, G.P. van Wezel & F. Barona-Gomez, (2013) The genome sequence of



Streptomyces lividans 66 reveals a novel tRNA-dependent peptide biosynthetic system within a metal-related genomic island. *Genome Biol Evol* **5**: 1165-1175.

Cui, Y.Q., R.G.J.M. van der Lans & K.C.A.M. Luyben, (1997) Effect of agitation intensities on fungal morphology of submerged fermentation. *Biotechnology and Bioengineering* **55**: 715-726.

Dalton, K.A., A. Thibessard, J.I. Hunter & G.H. Kelemen, (2007) A novel compartment, the 'subapical stem' of the aerial hyphae, is the location of a sigN-dependent, developmentally distinct transcription in *Streptomyces coelicolor*. *Molecular microbiology* **64**: 719-737.

Daniel, R.A. & J. Errington, (2003) Control of cell morphogenesis in bacteria: two distinct ways to make a rod-shaped cell. *Cell* **113**: 767-776.

Daza, A., J.F. Martin, A. Dominguez & J.A. Gil, (1989) Sporulation of several species of *Streptomyces* in submerged cultures after nutritional downshift. *Journal of General Microbiology* **135**: 2483-2491.

de Jong, W., A. Manteca, J. Sanchez, G. Bucca, C.P. Smith, L. Dijkhuizen, D. Claessen & H.A.B. Wösten, (2009a) NepA is a structural cell wall protein involved in maintenance of spore dormancy in *Streptomyces coelicolor*. *Molecular Microbiology* **71**: 1591-1603.

de Jong, W., H.A. Wosten, L. Dijkhuizen & D. Claessen, (2009b) Attachment of *Streptomyces coelicolor* is mediated by amyloid fimbriae that are anchored to the cell surface via cellulose. *Molecular Microbiology* **73**: 1128-1140.

de Leeuw, E., B. Graham, G.J. Phillips, C.M. ten Hagen-Jongman, B. Oudega & J. Luirink, (1999) Molecular characterization of *Escherichia coli* FtsE and FtsX. *Mol Microbiol* **31**: 983-993.

Delic, I., P. Robbins & J. Westpheling, (1992) Direct repeat sequences are implicated in the regulation of two *Streptomyces* chitinase promoters that are subject to carbon catabolite control. *Proceedings of the National Academy of Sciences* **89**: 1885-1889.

Dell'Era, S., C. Buchrieser, E. Couvé, B. Schnell, Y. Briers, M. Schuppler & M.J. Loessner, (2009) *Listeria monocytogenes* L-forms respond to cell wall deficiency by modifying gene expression and the mode of division. *Molecular microbiology* **73**: 306-322.

DePas, W.H., D.A. Hufnagel, J.S. Lee, L.P. Blanco, H.C. Bernstein, S.T. Fisher, G.A. James, P.S. Stewart & M.R. Chapman, (2013) Iron induces bimodal population development by *Escherichia coli*. *Proceedings of the National Academy of Sciences* **110**: 2629-2634.

Derouaux, A., D. Dehareng, E. Lecocq, S. Halici, H. Nothaft, F. Giannotta, G. Moutzourelis, J. Dusart, B. Devreese, F. Titgemeyer, J. Van Beeumen & S. Rigali, (2004) Crp of *Streptomyces coelicolor* is the third transcription factor of the large CRP-FNR superfamily able to bind cAMP. *Biochemical and Biophysical Research Communications* **325**: 983-990.

Desveaux, D., J. Allard, N. Brisson & J. Sygusch, (2002) A new family of plant transcription factors

displays a novel ssDNA-binding surface. *Nature Structural & Molecular Biology* **9**: 512-517.

Ditkowski, B., N. Holmes, J. Rydzak, M. Donczew, M. Bezulska, K. Ginda, P. Kędzierski, J. Zakrzewska-Czerwińska, G.H. Kelemen & D. Jakimowicz, (2013) Dynamic interplay of ParA with the polarity protein, Scy, coordinates the growth with chromosome segregation in *Streptomyces coelicolor*. *Open biology* **3**: 130006.

Dobson, L., C. O'Cleirigh & D. O'Shea, (2008) The influence of morphology on geldanamycin production in submerged fermentations of *Streptomyces hygroscopicus* var. *geldanus*. *Applied Microbiology and Biotechnology* **79**: 859-866.

Edwards, D.H. & J. Errington, (1997) The *Bacillus subtilis* DivIVA protein targets to the division septum and controls the site specificity of cell division. *Molecular microbiology* **24**: 905-915.

Ekkers, D.M., D. Claessen, F. Galli & E. Stamhuis, (2014) Surface modification using interfacial assembly of the *Streptomyces* chaplin proteins. *Applied microbiology and biotechnology* **98**: 4491-4501.

El-Enshasy, H., K. Hellmuth & U. Rinas, (1999) Fungal morphology in submerged cultures and its relation to glucose oxidase excretion by recombinant *Aspergillus niger*. *Applied Biochemistry and Biotechnology* **81**: 1-11.

Elibol, M. & F. Mavituna, (1999) A remedy to oxygen limitation problem in antibiotic production: addition of perfluorocarbon. *Biochemical Engineering Journal* **3**: 1-7.

Elliot, M.A., N. Karoonuthaisiri, J. Huang, M.J. Bibb, S.N. Cohen, C.M. Kao & M.J. Buttner, (2003) The chaplins: a family of hydrophobic cell-surface proteins involved in aerial mycelium formation in *Streptomyces coelicolor*. *Genes & development* **17**: 1727-1740.

Erikson, D., (1947) Differentiation of the Vegetative and Sporogenous Phases of the Actinomycetes: 1. The Lipid Nature of the Outer Wall of the Aerial Mycelium. *Microbiology* **1**: 39-44.

Errington, J., (2013) L-form bacteria, cell walls and the origins of life. *Open biology* **3**: 120143.

Fedorushyn, M., E. Welle, A. Bechthold & A. Luzhetskyy, (2008) Functional expression of the Cre recombinase in actinomycetes. *Appl Microbiol Biotechnol* **78**: 1065-1070.

Fernández-Martínez, L.T., R.D. Sol, M.C. Evans, S. Fielding, P.R. Herron, G. Chandra & P.J. Dyson, (2011) A transposon insertion single-gene knockout library and new ordered cosmid library for the model organism *Streptomyces coelicolor* A3(2). *Antonie van Leeuwenhoek* **99**: 515-522.

Fernández, M. & J. Sánchez, (2002) Nuclease activities and cell death processes associated with the development of surface cultures of *Streptomyces antibioticus* ETH 7451. *Microbiology* **148**: 405-412.

Ferrer-Mirallas, N. & A. Villaverde, (2013) Bacterial cell factories for recombinant protein production; expanding the catalogue. *Microb Cell Fact* **12**: 113.



Flårdh, K. & M.J. Buttner, (2009) *Streptomyces* morphogenetics: dissecting differentiation in a filamentous bacterium. *Nature Reviews. Microbiology* **7**: 36-49.

Flårdh, K., D.M. Richards, A.M. Hempel, M. Howard & M.J. Buttner, (2012) Regulation of apical growth and hyphal branching in *Streptomyces*. *Current opinion in microbiology* **15**: 737-743.

Flårdh, K. & G. van Wezel, (2003) Cell division during growth and development in *Streptomyces*. *Recent research developments in bacteriology* **1**: 71-90.

Flinspach, K., L. Westrich, L. Kaysser, S. Siebenberg, J.P. Gomez-Escribano, M. Bibb, B. Gust & L. Heide, (2010) Heterologous expression of the biosynthetic gene clusters of coumermycin A(1), clorobiocin and caprazamycins in genetically modified *Streptomyces coelicolor* strains. *Biopolymers* **93**: 823-832.

Fuchino, K., S. Bagchi, S. Cantlay, L. Sandblad, D. Wu, J. Bergman, M. Kamali-Moghaddam, K. Flårdh & N. Ausmees, (2013) Dynamic gradients of an intermediate filament-like cytoskeleton are recruited by a polarity landmark during apical growth. *Proceedings of the National Academy of Sciences* **110**: E1889-E1897.

Gao, C., D. Mulder, C. Yin & M.A. Elliot, (2012) Crp is a global regulator of antibiotic production in *Streptomyces*. *MBio* **3**: e00407-00412.

Gebbink, M.F., D. Claessen, B. Bouma, L. Dijkhuizen & H.A. Wösten, (2005) Amyloids—a functional coat for microorganisms. *Nature reviews microbiology* **3**: 333-341.

Gerke, C., A. Kraft, R. Süßmuth, O. Schweitzer & F. Götz, (1998) Characterization of the N-acetylglucosaminyltransferase activity involved in the biosynthesis of the *Staphylococcus epidermidis* polysaccharide intercellular adhesin. *Journal of Biological Chemistry* **273**: 18586-18593.

Girard, G., B.A. Traag, V. Sangal, N. Mascini, P.A. Hoskisson, M. Goodfellow & G.P. van Wezel, (2013) A novel taxonomic marker that discriminates between morphologically complex actinomycetes. *Open biology* **3**: 130073.

Glazebrook, M.A., J.L. Doull, C. Stuttard & L.C. Vining, (1990) Sporulation of *Streptomyces venezuelae* in submerged cultures. *Microbiology* **136**: 581-588.

Glazebrook, M.A., L.C. Vining & R.L. White, (1992) Growth morphology of *Streptomyces akiyoshiensis* in submerged culture: influence of pH, inoculum, and nutrients. *Canadian Journal of Microbiology* **38**: 98-103.

Glover, W.A., Y. Yang & Y. Zhang, (2009) Insights into the molecular basis of L-form formation and survival in *Escherichia coli*. *PLoS One* **4**: e7316.

Gottelt, M., S. Kol, J.P. Gomez-Escribano, M. Bibb & E. Takano, (2010) Deletion of a regulatory gene within the cpk gene cluster reveals novel antibacterial activity in *Streptomyces coelicolor* A3(2). *Microbiology* **156**: 2343-2353.

- Götz, F., (2002) *Staphylococcus* and biofilms. *Molecular Microbiology* **43**: 1367-1378.
- Gramajo, H.C., E. Takano & M.J. Bibb, (1993) Stationary-phase production of the antibiotic actinorhodin in *Streptomyces coelicolor* A3 (2) is transcriptionally regulated. *Molecular microbiology* **7**: 837-845.
- Granozzi, C., R. Billella, R. Passantino, M. Sollazzo & A. Puglia, (1990) A breakdown in macromolecular synthesis preceding differentiation in *Streptomyces coelicolor* A3 (2). *Microbiology* **136**: 713-716.
- Gray, D., G. Gooday & J. Prosser, (1990) Apical hyphal extension in *Streptomyces coelicolor* A3 (2). *Microbiology* **136**: 1077-1084.
- Grund, A. & J. Ensign, (1985) Properties of the germination inhibitor of *Streptomyces viridochromogenes* spores. *Journal of general microbiology* **131**: 833.
- Gubbens, J., M. Janus, B.I. Florea, H.S. Overkleeft & G.P. Wezel, (2012) Identification of glucose kinase-dependent and-independent pathways for carbon control of primary metabolism, development and antibiotic production in *Streptomyces coelicolor* by quantitative proteomics. *Molecular microbiology* **86**: 1490-1507.
- Gueiros-Filho, F.J. & R. Losick, (2002) A widely conserved bacterial cell division protein that promotes assembly of the tubulin-like protein FtsZ. *Genes & development* **16**: 2544-2556.
- Gumpert, J., (1982) Growth characteristics and ultrastructure of protoplast type L-forms from *Streptomyces*. *Zeitschrift für allgemeine Mikrobiologie* **22**: 617-627.
- Gumpert, J., (1983) Ultrastructural characterization of core structures and paracrystalline inclusion bodies in L-form cells of streptomycetes. *Zeitschrift für allgemeine Mikrobiologie* **23**: 625-633.
- Gust, B., G.L. Challis, K. Fowler, T. Kieser & K.F. Chater, (2003a) PCR-targeted *Streptomyces* gene replacement identifies a protein domain needed for biosynthesis of the sesquiterpene soil odor geosmin. *Proceedings of the National Academy of Sciences* **100**: 1541-1546.
- Gust, B., S. O'Rourke, N. Bird, T. Kieser & K. Chater, (2003b) Recombineering in *Streptomyces coelicolor*. *Norwich: The John Innes Foundation*.
- Haiser, H.J., M.R. Yousef & M.A. Elliot, (2009) Cell wall hydrolases affect germination, vegetative growth, and sporulation in *Streptomyces coelicolor*. *Journal of bacteriology* **191**: 6501-6512.
- Hall-Stoodley, L., J.W. Costerton & P. Stoodley, (2004) Bacterial biofilms: from the natural environment to infectious diseases. *Nature Reviews Microbiology* **2**: 95-108.
- Hardisson, C., M.-B. Manzanal, J.-A. Salas & J.-E. Suárez, (1978) Fine structure, physiology and biochemistry of arthrospore germination in *Streptomyces antibioticus*. *Microbiology* **105**: 203-214.
- Harriott, O.T. & A. Bourret, (2003) Improving dispersed growth of *Frankia* using Carbopol. *Plant and Soil* **254**: 69-74.



- Hempel, A.M., S. Cantlay, V. Molle, S.-B. Wang, M.J. Naldrett, J.L. Parker, D.M. Richards, Y.-G. Jung, M.J. Buttner & K. Flårdh, (2012) The Ser/Thr protein kinase AfsK regulates polar growth and hyphal branching in the filamentous bacteria *Streptomyces*. *Proceedings of the National Academy of Sciences* **109**: E2371-E2379.
- Heydarian, S.M., A.P. Ison, M.D. Lilly & P.A. Ayazi Shamlou, (2000) Turbulent breakage of filamentous bacteria in mechanically agitated batch culture. *Chemical Engineering Science* **55**: 1775-1784.
- Heydarian, S.M., N. Mirjalili & A.P. Ison, (1999) Effect of shear on morphology and erythromycin production in *Saccharopolyspora erythraea* fermentations. *Bioprocess Engineering* **21**: 31-39.
- Hille, A., T.r. Neu, D.c. Hempel & H. Horn, (2005) Oxygen profiles and biomass distribution in biopellets of *Aspergillus niger*. *Biotechnology and Bioengineering* **92**: 614-623.
- Hobbs, G., C. Frazer, D.J. Gardner, J. Cullum & S. Oliver, (1989) Dispersed growth of *Streptomyces* in liquid culture. *Applied Microbiology and Biotechnology* **31**.
- Hodgson, D.A., (2000) Primary metabolism and its control in streptomycetes: A most unusual group of bacteria. In: *Advances in Microbial Physiology*. Academic Press, pp. 47-238.
- Holmes, N.A., J. Walshaw, R.M. Leggett, A. Thibessard, K.A. Dalton, M.D. Gillespie, A.M. Hemmings, B. Gust & G.H. Kelemen, (2013) Coiled-coil protein Scy is a key component of a multiprotein assembly controlling polarized growth in *Streptomyces*. *Proceedings of the National Academy of Sciences* **110**: E397-E406.
- Hopwood, D.A., (2007) *Streptomyces in nature and medicine: the antibiotic makers*. Oxford University Press New York.
- Hopwood, D.A., H.M. Wright, M.J. Bibb & S.N. COHEN, (1977) Genetic recombination through protoplast fusion in *Streptomyces*.
- Huang, J., C.-J. Lih, K.-H. Pan & S.N. Cohen, (2001) Global analysis of growth phase responsive gene expression and regulation of antibiotic biosynthetic pathways in *Streptomyces coelicolor* using DNA microarrays. *Genes & Development* **15**: 3183-3192.
- Hübscher, J., N. McCallum, C.D. Sifri, P.A. Majcherczyk, J.M. Entenza, R. Heusser, B. Berger-Bachi & P. Stutzmann Meier, (2009) MsrR contributes to cell surface characteristics and virulence in *Staphylococcus aureus*. *FEMS Microbiol Lett* **295**: 251-260.
- Ikeda, M., J. Ohnishi, M. Hayashi & S. Mitsuhashi, (2006) A genome-based approach to create a minimally mutated *Corynebacterium glutamicum* strain for efficient L-lysine production. *J Ind Microbiol Biotechnol* **33**: 610-615.
- Ikeda, M., M. Wachi, H.K. Jung, F. Ishino & M. Mitsuhashi, (1991) The *Escherichia coli* *mraY* gene encoding UDP-N-acetylmuramoyl-pentapeptide: undecaprenyl-phosphate phospho-N-

acetylmuramoyl-pentapeptide transferase. *J Bacteriol* **173**: 1021-1026.

Innes, C. & E. Allan, (2001) Induction, growth and antibiotic production of *Streptomyces viridifaciens* L-form bacteria. *Journal of applied microbiology* **90**: 301-308.

Jakimowicz, D. & G.P. van Wezel, (2012) Cell division and DNA segregation in *Streptomyces*: how to build a septum in the middle of nowhere? *Molecular microbiology* **85**: 393-404.

Jefferson, K.K., (2004) What drives bacteria to produce a biofilm? *FEMS microbiology letters* **236**: 163-173.

Jiang, H. & K.E. Kendrick, (2000) Characterization of *ssfR* and *ssgA*, Two Genes Involved in Sporulation of *Streptomyces griseus*. *Journal of bacteriology* **182**: 5521-5529.

Jonsbu, E., M. McIntyre & J. Nielsen, (2002) The influence of carbon sources and morphology on nystatin production by *Streptomyces noursei*. *Journal of Biotechnology* **95**: 133-144.

Kaplan, J.B., C. Ragunath, N. Ramasubbu & D.H. Fine, (2003) Detachment of *Actinobacillus actinomycetemcomitans* biofilm cells by an endogenous β -hexosaminidase activity. *Journal of bacteriology* **185**: 4693-4698.

Katz, E., C.J. Thompson & D.A. Hopwood, (1983) Cloning and Expression of the Tyrosinase Gene from *Streptomyces antibioticus* in *Streptomyces lividans*. *Journal of General Microbiology* **129**: 2703-2714.

Kawai, Y., J. Marles-Wright, R.M. Cleverley, R. Emmins, S. Ishikawa, M. Kuwano, N. Heinz, N.K. Bui, C.N. Hoyland, N. Ogasawara, R.J. Lewis, W. Vollmer, R.A. Daniel & J. Errington, (2011) A widespread family of bacterial cell wall assembly proteins. *The EMBO Journal* **30**: 4931-4941.

Kawamoto, S. & J.C. Ensign, (1995) Isolation of mutants of *Streptomyces griseus* that sporulate in nutrient rich media: cloning of DNA fragments that suppress the mutations. *Actinomycetologica* **9**: 124-135.

Kawamoto, S., H. Watanabe, A. Hesketh, J.C. Ensign & K. Ochi, (1997) Expression analysis of the *ssgA* gene product, associated with sporulation and cell division in *Streptomyces griseus*. *Microbiology* **143**: 1077-1086.

Kawamoto, S., M. Watanabe, N. Saito, A. Hesketh, K. Vachalova, K. Matsubara & K. Ochi, (2001) Molecular and functional analyses of the gene (*eshA*) encoding the 52-kilodalton protein of *Streptomyces coelicolor* A3 (2) required for antibiotic production. *Journal of bacteriology* **183**: 6009-6016.

Keijsers, B.J., E.E. Noens, B. Kraal, H.K. Koerten & G.P. van Wezel, (2003) The *Streptomyces coelicolor* *ssgB* gene is required for early stages of sporulation. *FEMS Microbiol Lett* **225**: 59-67.

Keijsers, B.J., G.P. van Wezel, G.W. Canters, T. Kieser & E. Vijgenboom, (2000) The ram-dependence of *Streptomyces lividans* differentiation is bypassed by copper. *Journal of Molecular Microbiology and*



Biotechnology **2**: 565-574.

Kelemen, G.H. & M.J. Buttner, (1998) Initiation of aerial mycelium formation in *Streptomyces*. *Current opinion in microbiology* **1**: 656-662.

Kelley, L.A., S. Mezulis, C.M. Yates, M.N. Wass & M.J. Sternberg, (2015) The Phyre2 web portal for protein modeling, prediction and analysis. *Nature protocols* **10**: 845-858.

Kelly-Quintos, C., L.A. Cavacini, M.R. Posner, D. Goldmann & G.B. Pier, (2006) Characterization of the opsonic and protective activity against *Staphylococcus aureus* of fully human monoclonal antibodies specific for the bacterial surface polysaccharide poly-N-acetylglucosamine. *Infection and immunity* **74**: 2742-2750.

Kelly, S., L.H. Grimm, C. Bendig, D.C. Hempel & R. Krull, (2006) Effects of fluid dynamic induced shear stress on fungal growth and morphology. *Process Biochemistry* **41**: 2113-2117.

Kendrick, K.E. & J.C. Ensign, (1983) Sporulation of *Streptomyces griseus* in submerged culture. *Journal of Bacteriology* **155**: 357-366.

Khodakaramian, G., S. Lissenden, B. Gust, L. Moir, P.A. Hoskisson, K.F. Chater & M.C. Smith, (2006) Expression of Cre recombinase during transient phage infection permits efficient marker removal in *Streptomyces*. *Nucleic Acids Res* **34**: e20.

Khweek, A.A., J.D. Fetherston & R.D. Perry, (2010) Analysis of HmsH and its role in plague biofilm formation. *Microbiology* **156**: 1424-1438.

Kieser, T., M.J. Bibb, M.J. Buttner, K.F. Chater & D.A. Hopwood, (2000) *Practical streptomyces genetics*.

Kim, J.-h. & I.C. Hancock, (2000) Pellet forming and fragmentation in liquid culture of *Streptomyces griseus*. *Biotechnology Letters* **22**: 189-192.

Kim, J.H., J. Lebeault & M. Reuss, (1983) Comparative study on rheological properties of mycelial broth in filamentous and pelleted forms. *European journal of applied microbiology and biotechnology* **18**: 11-16.

Kim, Y.-M. & J.-h. Kim, (2004) Formation and dispersion of mycelial pellets of *Streptomyces coelicolor* A3(2). *Journal of Microbiology (Seoul, Korea)* **42**: 64-67.

Koebisch, I., J. Overbeck, S. Piepmeyer, H. Meschke & H. Schrempf, (2009) A molecular key for building hyphae aggregates: the role of the newly identified *Streptomyces* protein HyaS. *Microbial Biotechnology* **2**: 343-360.

Koekman, B. & M. Hans, (2012) The Clavulanic Acid Strain Improvement Program at DSM Anti-Infectives. In: *Engineering Complex Phenotypes in Industrial Strains*. R. Patnaik (ed). John Wiley & Sons, Inc., pp. 169-183.

Kojima, I., Y.R. Cheng, V. Mohan & A.L. Demain, (1995) Carbon source nutrition of rapamycin biosynthesis in *Streptomyces hygroscopicus*. *Journal of Industrial Microbiology* **14**: 436-439.

Komatsu, M., T. Uchiyama, S. Omura, D.E. Cane & H. Ikeda, (2010) Genome-minimized *Streptomyces* host for the heterologous expression of secondary metabolism. *Proc Natl Acad Sci U S A* **107**: 2646-2651.

Kossen, N., (2000) The morphology of filamentous fungi. In: History of Modern Biotechnology II. Springer, pp. 1-33.

Kwak, J. & K.E. Kendrick, (1996) Bald mutants of *Streptomyces griseus* that prematurely undergo key events of sporulation. *Journal of bacteriology* **178**: 4643-4650.

Kwak, J., L.A. McCue, K. Trczianka & K.E. Kendrick, (2001) Identification and characterization of a developmentally regulated protein, EshA, required for sporogenic hyphal branches in *Streptomyces griseus*. *Journal of bacteriology* **183**: 3004-3015.

Labeda, D.P., (1987) Transfer of the type strain of *Streptomyces erythraeus* (Waksman 1923) Waksman and Henrici 1948 to the genus *Saccharopolyspora* Lacey and Goodfellow 1975 as *Saccharopolyspora erythraea* sp. nov., and designation of a neotype strain for *Streptomyces erythraeus*. *International Journal of Systematic and Evolutionary Microbiology* **37**: 19-22.

Large, K.P., A.P. Ison & D.J. Williams, (1998) The effect of agitation rate on lipid utilisation and clavulanic acid production in *Streptomyces clavuligerus*. *Journal of Biotechnology* **63**: 111-119.

Lawlor, E.J., H.A. Baylis & K.F. Chater, (1987) Pleiotropic morphological and antibiotic deficiencies result from mutations in a gene encoding a tRNA-like product in *Streptomyces coelicolor* A3(2). *Genes Dev* **1**: 1305-1310.

Leaver, M., P. Dominguez-Cuevas, J. Coxhead, R. Daniel & J. Errington, (2009) Life without a wall or division machine in *Bacillus subtilis*. *Nature* **457**: 849-853.

Leaver, M. & J. Errington, (2005) Roles for MreC and MreD proteins in helical growth of the cylindrical cell wall in *Bacillus subtilis*. *Molecular Microbiology* **57**: 1196-1209.

Leskiw, B.K., M.J. Bibb & K.F. Chater, (1991) The use of a rare codon specifically during development? *Mol Microbiol* **5**: 2861-2867.

Levin-Karp, A., U. Barenholz, T. Bareia, M. Dayagi, L. Zelcbuch, N. Antonovsky, E. Noor & R. Milo, (2013) Quantifying translational coupling in *E. coli* synthetic operons using RBS modulation and fluorescent reporters. *ACS Synthetic Biology* **2**: 327-336.

Li, Z.J., S. Bhargava & M.R. Marten, (2002) Measurements of the fragmentation rate constant imply that the tensile strength of fungal hyphae can change significantly during growth. *Biotechnology Letters* **24**: 1-7.



- Liman, R., P.D. Facey, G. van Keulen, P.J. Dyson & R. Del Sol, (2013) A laterally acquired galactose oxidase-like gene is required for aerial development during osmotic stress in *Streptomyces coelicolor*. *PLoS ONE* **8**: e54112.
- Liu, G., K.F. Chater, G. Chandra, G. Niu & H. Tan, (2013a) Molecular regulation of antibiotic biosynthesis in *Streptomyces*. *Microbiology and Molecular Biology Reviews* **77**: 112-143.
- Liu, G., M. Xing & Q. Han, (2005) A population-based morphologically structured model for hyphal growth and product formation in streptomycin fermentation. *World Journal of Microbiology and Biotechnology* **21**: 1329-1338.
- Liu, L., H. Yang, H.-d. Shin, J. Li, G. Du & J. Chen, (2013b) Recent advances in recombinant protein expression by *Corynebacterium*, *Brevibacterium*, and *Streptomyces*: from transcription and translation regulation to secretion pathway selection. *Applied Microbiology and Biotechnology* **97**: 9597-9608.
- Liu, Y. & J.-H. Tay, (2002) The essential role of hydrodynamic shear force in the formation of biofilm and granular sludge. *Water Research* **36**: 1653-1665.
- Long, Q., X. Liu, Y. Yang, L. Li, L. Harvey, B. McNeil & Z. Bai, (2014) The development and application of high throughput cultivation technology in bioprocess development. *Journal of biotechnology* **192**: 323-338.
- López, J.C., J.S. Pérez, J.F. Sevilla, E.R. Porcel & Y. Chisti, (2005) Pellet morphology, culture rheology and lovastatin production in cultures of *Aspergillus terreus*. *Journal of biotechnology* **116**: 61-77.
- Low, H.H., M.C. Moncrieffe & J. Löwe, (2004) The crystal structure of ZapA and its modulation of FtsZ polymerisation. *Journal of molecular biology* **341**: 839-852.
- Lucero, H. & H. Kagan, (2006) Lysyl oxidase: an oxidative enzyme and effector of cell function. *Cellular and Molecular Life Sciences CMLS* **63**: 2304-2316.
- Mack, D., W. Fischer, A. Krokotsch, K. Leopold, R. Hartmann, H. Egge & R. Laufs, (1996) The intercellular adhesin involved in biofilm accumulation of *Staphylococcus epidermidis* is a linear beta-1,6-linked glucosaminoglycan: purification and structural analysis. *Journal of Bacteriology* **178**: 175-183.
- MacNeil, D.J., K.M. Gewain, C.L. Ruby, G. Dezeny, P.H. Gibbons & T. MacNeil, (1992) Analysis of *Streptomyces avermitilis* genes required for avermectin biosynthesis utilizing a novel integration vector. *Gene* **111**: 61-68.
- Manteca, A., R. Alvarez, N. Salazar, P. Yagüe & J. Sanchez, (2008) Mycelium Differentiation and Antibiotic Production in Submerged Cultures of *Streptomyces coelicolor*. *Applied and Environmental Microbiology* **74**: 3877-3886.
- Manteca, A., D. Claessen, C. Lopez-Iglesias & J. Sanchez, (2007) Aerial hyphae in surface cultures of *Streptomyces lividans* and *Streptomyces coelicolor* originate from viable segments surviving an early

programmed cell death event. *FEMS Microbiology Letters* **274**: 118-125.

Manteca, A., M. Fernandez & J. Sanchez, (2006a) Cytological and biochemical evidence for an early cell dismantling event in surface cultures of *Streptomyces antibioticus*. *Research in Microbiology* **157**: 143-152.

Manteca, Á., M. Fernández & J. Sánchez, (2005) A death round affecting a young compartmentalized mycelium precedes aerial mycelium dismantling in confluent surface cultures of *Streptomyces antibioticus*. *Microbiology* **151**: 3689-3697.

Manteca, A., H.R. Jung, V. Schwammler, O.N. Jensen & J. Sanchez, (2010) Quantitative proteome analysis of *Streptomyces coelicolor* nonsporulating liquid cultures demonstrates a complex differentiation process comparable to that occurring in sporulating solid cultures. *Journal of proteome research* **9**: 4801-4811.

Manteca, A., U. Mäder, B.A. Connolly & J. Sanchez, (2006b) A proteomic analysis of *Streptomyces coelicolor* programmed cell death. *Proteomics* **6**: 6008-6022.

Manteca, A., J. Ye, J. Sánchez & O.N. Jensen, (2011) Phosphoproteome analysis of *Streptomyces* development reveals extensive protein phosphorylation accompanying bacterial differentiation. *J. Proteome Res.* **10**: 5481-5492.

Marchler-Bauer, A., M.K. Derbyshire, N.R. Gonzales, S. Lu, F. Chitsaz, L.Y. Geer, R.C. Geer, J. He, M. Gwadz & D.I. Hurwitz, (2014) CDD: NCBI's conserved domain database. *Nucleic acids research: gku1221*.

Martin, S.M. & M.E. Bushell, (1996) Effect of hyphal micromorphology on bioreactor performance of antibiotic-producing *Saccharopolyspora erythraea* cultures. *Microbiology* **142**: 1783-1788.

McCormick, J.R., (2009) Cell division is dispensable but not irrelevant in *Streptomyces*. *Current opinion in microbiology* **12**: 689-698.

McCormick, J.R., E.P. Su, A. Driks & R. Losick, (1994) Growth and viability of *Streptomyces coelicolor* mutant for the cell division gene *ftsZ*. *Molecular Microbiology* **14**: 243-254.

McCrate, O.A., X. Zhou, C. Reichhardt & L. Cegelski, (2013) Sum of the parts: composition and architecture of the bacterial extracellular matrix. *Journal of molecular biology* **425**: 4286-4294.

McKenney, D., J. Hubner, E. Muller, Y. Wang, D.A. Goldmann & G.B. Pier, (1998) The *ica* locus of *Staphylococcus epidermidis* encodes production of the capsular polysaccharide/adhesin. *Infect Immun* **66**: 4711-4720.

Medema, M.H., R. Breitling, R. Bovenberg & E. Takano, (2011) Exploiting plug-and-play synthetic biology for drug discovery and production in microorganisms. *Nat Rev Microbiol* **9**: 131-137.

Mehmood, N., E. Olmos, J.-L. Goergen, F. Blanchard, P. Marchal, W. Klöckner, J. Büchs & S. Delaunay, (2012) Decoupling of oxygen transfer and power dissipation for the study of the production of



pristinamycins by *Streptomyces pristinaespiralis* in shaking flasks. *Biochemical Engineering Journal* **68**: 25-33.

Mehmood, N., E. Olmos, P. Marchal, J.-L. Goergen & S. Delaunay, (2010) Relation between pristinamycins production by *Streptomyces pristinaespiralis*, power dissipation and volumetric gas–liquid mass transfer coefficient, kLa. *Process Biochemistry* **45**: 1779-1786.

Mercier, R., Y. Kawai & J. Errington, (2013) Excess membrane synthesis drives a primitive mode of cell proliferation. *Cell* **152**: 997-1007.

Merrick, M., (1976) A morphological and genetic mapping study of bald colony mutants of *Streptomyces coelicolor*. *Microbiology* **96**: 299-315.

Metz, B., N. Kossen & J. Van Suijdam, (1979) The rheology of mould suspensions. In: *Advances in Biochemical Engineering*, Volume 11. Springer, pp. 103-156.

Metz, B. & N.W.F. Kossen, (1977) The growth of molds in the form of pellets—a literature review. *Biotechnology and Bioengineering* **19**: 781–799.

Meyerhoff, J., V. Tiller & K.-H. Bellgardt, (1995) Two mathematical models for the development of a single microbial pellet. *Bioprocess engineering* **12**: 305-313.

Miguélez, E.M., C. Hardisson & M.B. Manzanal, (1999) Hyphal death during colony development in *Streptomyces antibioticus*: morphological evidence for the existence of a process of cell deletion in a multicellular prokaryote. *The Journal of cell biology* **145**: 515-525.

Minas, W., J.E. Bailey & W. Duetz, (2000) Streptomycetes in micro-cultures: Growth, production of secondary metabolites, and storage and retrieval in the 96–well format. *Antonie Van Leeuwenhoek* **78**: 297-305.

Mistry, B.V., R. Del Sol, C. Wright, K. Findlay & P. Dyson, (2008) FtsW is a dispensable cell division protein required for Z-ring stabilization during sporulation septation in *Streptomyces coelicolor*. *Journal of bacteriology* **190**: 5555-5566.

Müller, C., C.M. Hjort, K. Hansen & J. Nielsen, (2002a) Altering the expression of two chitin synthase genes differentially affects the growth and morphology of *Aspergillus oryzae*. *Microbiology* **148**: 4025-4033.

Müller, C., M. McIntyre, K. Hansen & J. Nielsen, (2002b) Metabolic engineering of the morphology of *Aspergillus oryzae* by altering chitin synthesis. *Applied and environmental microbiology* **68**: 1827-1836.

Naeimpoor, F. & F. Mavituna, (2000) Metabolic flux Analysis in *Streptomyces coelicolor* under various nutrient limitations. *Metabolic Engineering* **2**: 140-148.

Nazari, B., M. Kobayashi, A. Saito, A. Hassaninasab, K. Miyashita & T. Fujii, (2013) Chitin-induced gene expression in secondary metabolic pathways of *Streptomyces coelicolor* A3 (2) grown in soil. *Applied*

and *environmental microbiology* **79**: 707-713.

Nielsen, J. & J. Villadsen, (1992) Modelling of microbial kinetics. *Chemical Engineering Science* **47**: 4225-4270.

Nieminen, L., S. Webb, M.C. Smith & P.A. Hoskisson, (2013) A flexible mathematical model platform for studying branching networks: experimentally validated using the model actinomycete, *Streptomyces coelicolor*. *PLoS one* **8**: e54316.

Nieselt, K., F. Battke, A. Herbig, P. Bruheim, A. Wentzel, Ø.M. Jakobsen, H. Sletta, M.T. Alam, M.E. Merlo & J. Moore, (2010) The dynamic architecture of the metabolic switch in *Streptomyces coelicolor*. *BMC genomics* **11**: 10.

Noens, E.E., V. Mersinias, J. Willemse, B.A. Traag, E. Laing, K.F. Chater, C.P. Smith, H.K. Koerten & G.P. Van Wezel, (2007) Loss of the controlled localization of growth stage-specific cell-wall synthesis pleiotropically affects developmental gene expression in an *ssgA* mutant of *Streptomyces coelicolor*. *Molecular Microbiology* **64**: 1244-1259.

Noens, E.E., V. Mersinias, B.A. Traag, C.P. Smith, H.K. Koerten & G.P. Van Wezel, (2005) SsgA-like proteins determine the fate of peptidoglycan during sporulation of *Streptomyces coelicolor*. *Molecular Microbiology* **58**: 929-944.

Nothaft, H., S. Rigali, B. Boomsma, M. Swiatek, K.J. McDowall, G.P. Van Wezel & F. Titgemeyer, (2010) The permease gene *nagE2* is the key to N-acetylglucosamine sensing and utilization in *Streptomyces coelicolor* and is subject to multi-level control. *Molecular Microbiology* **75**: 1133-1144.

Novick, A. & L. Szilard, (1950) Experiments with the Chemostat on Spontaneous Mutations of Bacteria. *Proceedings of the National Academy of Sciences of the United States of America* **36**: 708.

O'Toole, G., H.B. Kaplan & R. Kolter, (2000) Biofilm Formation as Microbial Development. *Annual Review of Microbiology* **54**: 49-79.

O'Cleirigh, C., J.T. Casey, P.K. Walsh & D.G. O'Shea, (2005) Morphological engineering of *Streptomyces hygroscopicus* var. *geldanus*: regulation of pellet morphology through manipulation of broth viscosity. *Applied Microbiology and Biotechnology* **68**: 305-310.

Ohta, N., Y.S. Park, K. Yahiro & M. Okabe, (1995) Comparison of neomycin production from *Streptomyces fradiae* cultivation using soybean oil as the sole carbon source in an air-lift bioreactor and a stirred-tank reactor. *Journal of Fermentation and Bioengineering* **79**: 443-448.

Olano, C., C. Méndez & J.A. Salas, (2009) Antitumor compounds from marine actinomycetes. *Marine drugs* **7**: 210-248.

Olmos, E., N. Mehmood, L.H. Husein, J.-L. Goergen, M. Fick & S. Delaunay, (2013) Effects of bioreactor hydrodynamics on the physiology of *Streptomyces*. *Bioprocess and Biosystems Engineering* **36**: 259-



Oud, B., A.J.A. van Maris, J.-M. Daran & J.T. Pronk, (2012) Genome-wide analytical approaches for reverse metabolic engineering of industrially relevant phenotypes in yeast. *FEMS Yeast Research* **12**: 183–196.

Pamboukian, C.R.D. & M.C.R. Facciotti, (2005) Rheological and morphological characterization of *Streptomyces olindensis* growing in batch and fed-batch fermentations. *Brazilian Journal of Chemical Engineering* **22**: 31-40.

Papagianni, M., (2004) Fungal morphology and metabolite production in submerged mycelial processes. *Biotechnology Advances* **22**: 189-259.

Papagianni, M., M. Matthey & B. Kristiansen, (1999) Hyphal vacuolation and fragmentation in batch and fed-batch culture of *Aspergillus niger* and its relation to citric acid production. *Process Biochemistry* **35**: 359-366.

Park, Y., S. Tamura, Y. Koike, M. Toriyama & M. Okabe, (1997) Mycelial pellet intrastucture visualization and viability prediction in a culture of *Streptomyces fradiae* using confocal scanning laser microscopy. *Journal of Fermentation and Bioengineering* **84**: 483-486.

Paton, A. & C.M. Innes, (1991) Methods for the establishment of intracellular associations of L-forms with higher plants. *Journal of applied bacteriology* **71**: 59-64.

Paul, G.C., C.A. Kent & C.R. Thomas, (1994) Hyphal vacuolation and fragmentation in *Penicillium chrysogenum*. *Biotechnology and Bioengineering* **44**: 655–660.

Paul, G.C. & C.R. Thomas, (1998) Characterisation of mycelial morphology using image analysis. In: *Relation Between Morphology and Process Performances*. K. Schügerl (ed). Springer Berlin Heidelberg, pp. 1-59.

Peterlin, P., V. Arrigler, K. Kogej, S. Svetina & P. Walde, (2009) Growth and shape transformations of giant phospholipid vesicles upon interaction with an aqueous oleic acid suspension. *Chemistry and physics of lipids* **159**: 67-76.

Petrus, M.L., E. Vijgenboom, A.K. Chaplin, J.A. Worrall, G.P. van Wezel & D. Claessen, (2016) The DyP-type peroxidase DtpA is a Tat-substrate required for GlxA maturation and morphogenesis in *Streptomyces*. *Open biology* **6**: 150149.

Petrus, M.L.C. & D. Claessen, (2014) Pivotal roles for *Streptomyces* cell surface polymers in morphological differentiation, attachment and mycelial architecture. *Antonie van Leeuwenhoek*: 1-13.

Pickup, K.M. & M.E. Bushell, (1995) Non-fragmenting variants of *Streptomyces* hyphae have enhanced activity of an enzyme (phospho-N-acetylmuramyl pentapeptide translocase) in peptidoglycan biosynthesis. *Journal of Fermentation and Bioengineering* **79**: 247-251.

Piddock, L.J., (2011) The crisis of no new antibiotics--what is the way forward? *Lancet Infect Dis* **12**: 249-253.

Piette, A., A. Derouaux, P. Gerkens, E.E. Noens, G. Mazzucchelli, S. Vion, H.K. Koerten, F. Titgemeyer, E. De Pauw, P. Leprince, G.P. van Wezel, M. Galleni & S. Rigali, (2005) From dormant to germinating spores of *Streptomyces coelicolor* A3(2): new perspectives from the *crp* null mutant. *J Proteome Res* **4**: 1699-1708.

Plate, L. & M.A. Marletta, (2012) Nitric oxide modulates bacterial biofilm formation through a multicomponent cyclic-di-GMP signaling network. *Molecular cell* **46**: 449-460.

Pogliano, J., K. Pogliano, D.S. Weiss, R. Losick & J. Beckwith, (1997) Inactivation of FtsI inhibits constriction of the FtsZ cytokinetic ring and delays the assembly of FtsZ rings at potential division sites. *Proc Natl Acad Sci U S A* **94**: 559-564.

Pope, M.K., B.D. Green & J. Westpheling, (1996) The *bld* mutants of *Streptomyces coelicolor* are defective in the regulation of carbon utilization, morphogenesis and cell-cell signalling. *Molecular microbiology* **19**: 747-756.

Postma, P., J. Lengeler & G. Jacobson, (1993) Phosphoenolpyruvate: carbohydrate phosphotransferase systems of bacteria. *Microbiological reviews* **57**: 543-594.

Ramey, B.E., M. Koutsoudis, S.B. von Bodman & C. Fuqua, (2004) Biofilm formation in plant-microbe associations. *Current opinion in microbiology* **7**: 602-609.

Ravasi, P., S. Peiru, H. Gramajo & H.G. Menzella, (2012) Design and testing of a synthetic biology framework for genetic engineering of *Corynebacterium glutamicum*. *Microb Cell Fact* **11**: 147.

RayChaudhuri, D., (1999) ZipA is a MAP-Tau homolog and is essential for structural integrity of the cytokinetic FtsZ ring during bacterial cell division. *The EMBO Journal* **18**: 2372-2383.

Reichl, U., R. King & E.D. Gilles, (1992) Characterization of pellet morphology during submerged growth of *Streptomyces tendae* by image analysis. *Biotechnology and Bioengineering* **39**: 164-170.

Richards, D.M., A.M. Hempel, K. Flårdh, M.J. Buttner & M. Howard, (2012) Mechanistic basis of branch-site selection in filamentous bacteria. *PLoS Comput Biol* **8**: e1002423.

Rigali, S., H. Nothaft, E.E.E. Noens, M. Schlicht, S. Colson, M. Müller, B. Joris, H.K. Koerten, D.A. Hopwood, F. Titgemeyer & G.P. Van Wezel, (2006) The sugar phosphotransferase system of *Streptomyces coelicolor* is regulated by the GntR-family regulator DasR and links N-acetylglucosamine metabolism to the control of development. *Molecular Microbiology* **61**: 1237-1251.

Rigali, S., F. Titgemeyer, S. Barends, S. Mulder, A.W. Thomae, D.A. Hopwood & G.P. van Wezel, (2008) Feast or famine: the global regulator DasR links nutrient stress to antibiotic production by *Streptomyces*. *EMBO reports* **9**: 670-675.



- Riley, G., K. Tucker, G. Paul & C. Thomas, (2000) Effect of biomass concentration and mycelial morphology on fermentation broth rheology. *Biotechnology and bioengineering* **68**: 160-172.
- Rioseras, B., M.T. López-García, P. Yagüe, J. Sánchez & Á. Manteca, (2014) Mycelium differentiation and development of *Streptomyces coelicolor* in lab-scale bioreactors: Programmed cell death, differentiation, and lysis are closely linked to undecylprodigiosin and actinorhodin production. *Bioresource Technology* **151**: 191-198.
- Rocha-Valadez, J.A., V. Albiter, M.A. Caro, L. Serrano-Carreón & E. Galindo, (2007) A fermentation system designed to independently evaluate mixing and/or oxygen tension effects in microbial processes: development, application and performance. *Bioprocess and Biosystems Engineering* **30**: 115-122.
- Romero, D., C. Aguilar, R. Losick & R. Kolter, (2010) Amyloid fibers provide structural integrity to *Bacillus subtilis* biofilms. *Proceedings of the National Academy of Sciences* **107**: 2230-2234.
- Romero, J., P. Liras & J.F. Martín, (1984) Dissociation of cephamycin and clavulanic acid biosynthesis in *Streptomyces clavuligerus*. *Applied Microbiology and Biotechnology* **20**: 318-325.
- Rosa, J.C., A.B. Neto, C.O. Hokka & A.C. Badino, (2005) Influence of dissolved oxygen and shear conditions on clavulanic acid production by *Streptomyces clavuligerus*. *Bioprocess and Biosystems Engineering* **27**: 99-104.
- Roth, M., C. Hoffmeier, R. Geuther, G. Muth & W. Wohlleben, (1994) Segregational stability of pSG5-derived vector plasmids in continuous cultures of *Streptomyces lividans* 66. *Biotechnology Letters* **16**: 1225-1230.
- Roth, M., D. Noack & R. Geuther, (1985) Maintenance of the recombinant plasmid pIJ2 in chemostat cultures of *Streptomyces lividans* 66 (pIJ2). *Journal of Basic Microbiology* **25**: 265-271.
- Roubos, J.A., P. Krabben, W.T.A.M.d. Laat, R. Babuška & J.J. Heijnen, (2002) Clavulanic acid degradation in *Streptomyces clavuligerus* fed-batch cultivations. *Biotechnology Progress* **18**: 451-457.
- Roubos, J.A., P. Krabben, R.G.M. Luiten, H.B. Verbruggen & J.J. Heijnen, (2001) A quantitative approach to characterizing cell lysis caused by mechanical agitation of *Streptomyces clavuligerus*. *Biotechnology Progress* **17**: 336-347.
- Roux, D., C. Cywes-Bentley, Y.-F. Zhang, S. Pons, M. Konkol, D.B. Kearns, D.J. Little, P.L. Howell, D. Skurnik & G.B. Pier, (2015) Identification of Poly-N-acetylglucosamine as a Major Polysaccharide Component of the *Bacillus subtilis* Biofilm Matrix. *Journal of Biological Chemistry* **290**: 19261-19272.
- Ruas-Madiedo, P., J. Hugenholtz & P. Zoon, (2002) An overview of the functionality of exopolysaccharides produced by lactic acid bacteria. *International Dairy Journal* **12**: 163-171.
- Rueda, B., E.M. Miguélez, C. Hardisson & M.B. Manzanal, (2001a) Changes in glycogen and trehalose

content of *Streptomyces brasiliensis* hyphae during growth in liquid cultures under sporulating and non-sporulating conditions. *FEMS microbiology letters* **194**: 181-185.

Rueda, B., E.M. Miguélez, C. Hardisson & M.B. Manzanal, (2001b) Mycelial differentiation and spore formation by *Streptomyces brasiliensis* in submerged culture. *Canadian journal of microbiology* **47**: 1042-1047.

Saito, A., T. Fujii & K. Miyashita, (2003a) Distribution and evolution of chitinase genes in *Streptomyces* species: involvement of gene-duplication and domain-deletion. *Antonie Van Leeuwenhoek* **84**: 7-15.

Saito, A., T. Shinya, K. Miyamoto, T. Yokoyama, H. Kaku, E. Minami, N. Shibuya, H. Tsujibo, Y. Nagata & A. Ando, (2007) The *dasABC* gene cluster, adjacent to *dasR*, encodes a novel ABC transporter for the uptake of N, N'-diacetylchitobiose in *Streptomyces coelicolor* A3 (2). *Applied and environmental microbiology* **73**: 3000-3008.

Saito, N., K. Matsubara, M. Watanabe, F. Kato & K. Ochi, (2003b) Genetic and biochemical characterization of EshA, a protein that forms large multimers and affects developmental processes in *Streptomyces griseus*. *Journal of Biological Chemistry* **278**: 5902-5911.

Sambrook, J., E.F. Fritsch & T. Maniatis, (1989) *Molecular cloning: a laboratory manual*. Cold Spring Harbor laboratory press, Cold Spring harbor, N.Y.

Sambrook, J. & D.W. Russell, (2001) *Molecular cloning: a laboratory manual* 3rd edition. *ColdSpring-Harbour Laboratory Press, UK*.

Sanchez, S., A. Chavez, A. Forero, Y. García-Huante, A. Romero, M. Sanchez, D. Rocha, B. Sánchez, M. Ávalos & S. Guzmán-Trampe, (2010) Carbon source regulation of antibiotic production. *The Journal of antibiotics* **63**: 442-459.

Sarrà, M., C. Casas, M. Poch & F. Gòdia, (1999) A simple structured model for continuous production of a hybrid antibiotic by *Streptomyces lividans* pellets in a fluidized-bed bioreactor. *Applied biochemistry and biotechnology* **80**: 39-50.

Savage, G. & M. Vander Brook, (1946) The Fragmentation of the mycelium of *Penicillium notatum* and *Penicillium chrysogenum* by a high-speed blender and the evaluation of blended seed. *Journal of bacteriology* **52**: 385.

Schatz, A., E. Bugle & S.A. Waksman, (1944) Streptomycin, a substance exhibiting antibiotic activity against gram-positive and gram-negative bacteria. *Experimental Biology and Medicine* **55**: 66-69.

Scher, K., U. Romling & S. Yaron, (2005) Effect of heat, acidification, and chlorination on *Salmonella enterica* serovar Typhimurium cells in a biofilm formed at the air-liquid interface. *Applied and environmental microbiology* **71**: 1163-1168.

Schlösser, A., J. Jantos, K. Hackmann & H. Schrepf, (1999) Characterization of the binding protein-



dependent cellobiose and cellotriose transport system of the cellulose degrader *Streptomyces reticuli*. *Applied and environmental microbiology* **65**: 2636-2643.

Scholtmeijer, K., M.L. de Vocht, R. Rink, G.T. Robillard & H.A. Wösten, (2009) Assembly of the fungal SC3 hydrophobin into functional amyloid fibrils depends on its concentration and is promoted by cell wall polysaccharides. *Journal of Biological Chemistry* **284**: 26309-26314.

Schrader, K.K. & W.T. Blevins, (2001) Effects of carbon source, phosphorus concentration, and several micronutrients on biomass and geosmin production by *Streptomyces halstedii*. *Journal of Industrial Microbiology and Biotechnology* **26**: 241-247.

Schumacher, M.A., E. Karamooz, A. Zíková, L. Trantírek & J. Lukeš, (2006) Crystal structures of *T. brucei* MRP1/MRP2 guide-RNA binding complex reveal RNA matchmaking mechanism. *Cell* **126**: 701-711.

Schwedock, J., J.R. McCormick, E.R. Angert, J.R. Nodwell & R. Losick, (1997) Assembly of the cell division protein FtsZ into ladder-like structures in the aerial hyphae of *Streptomyces coelicolor*. *Molecular Microbiology* **25**: 847-858.

Seletzky, J.M., U. Noak, J. Fricke, E. Welk, W. Eberhard, C. Knocke & J. Büchs, (2007) Scale-up from shake flasks to fermenters in batch and continuous mode with *Corynebacterium glutamicum* on lactic acid based on oxygen transfer and pH. *Biotechnology and bioengineering*: 800-811.

Seo, D.-J., Y.-H. Jang, R.-D. Park & W.-J. Jung, (2012) Immobilization of chitinases from *Streptomyces griseus* and *Paenibacillus illinoisensis* on chitosan beads. *Carbohydrate Polymers* **88**: 391-394.

Sheng, G.-P., H.-Q. Yu & X.-Y. Li, (2006) Stability of sludge flocs under shear conditions: roles of extracellular polymeric substances (EPS). *Biotechnology and bioengineering* **93**: 1095-1102.

Shioya, S., M. Morikawa, Y. Kajihara & H. Shimizu, (1999) Optimization of agitation and aeration conditions for maximum virginiamycin production. *Applied Microbiology and Biotechnology* **51**: 164-169.

Siebenberg, S., P.M. Bapat, A.E. Lantz, B. Gust & L. Heide, (2010) Reducing the variability of antibiotic production in *Streptomyces* by cultivation in 24-square deepwell plates. *Journal of bioscience and bioengineering* **109**: 230-234.

Smith, K.M. & J.C. Liao, (2011) An evolutionary strategy for isobutanol production strain development in *Escherichia coli*. *Metabolic engineering* **13**: 674-681.

Smits, W.K., O.P. Kuipers & J.-W. Veening, (2006) Phenotypic variation in bacteria: the role of feedback regulation. *Nature Reviews Microbiology* **4**: 259-271.

Sohoni, S.V., P.M. Bapat & A.E. Lantz, (2012) Robust, small-scale cultivation platform for *Streptomyces coelicolor*. *Microbial Cell Factories* **11**: 9.

Stocks, S.M. & C.R. Thomas, (2001) Viability, strength, and fragmentation of *Saccharopolyspora*

erythraea in submerged fermentation. *Biotechnology and Bioengineering* **75**: 702–709.

Stojmenovic, M., A. Jevremovic & A. Nayak, (2013) Fast iris detection via shape based circularity. In: Industrial Electronics and Applications (ICIEA), 2013 8th IEEE Conference on. IEEE, pp. 747-752.

Świątek, M.A., E. Tenconi, S. Rigali & G.P. van Wezel, (2012a) Functional analysis of the N-acetylglucosamine metabolic genes of *Streptomyces coelicolor* and role in control of development and antibiotic production. *Journal of Bacteriology* **194**: 1136-1144.

Świątek, M.A., M. Urem, E. Tenconi, S. Rigali & G.P. van Wezel, (2012b) Engineering of N-acetylglucosamine metabolism for improved antibiotic production in *Streptomyces coelicolor* A3(2) and an unsuspected role of NagA in glucosamine metabolism. *Bioengineered* **3**: 280-285.

Swinnen, S., K. Schaerlaekens, T. Pais, J. Claesen, G. Hubmann, Y. Yang, M. Demeke, M.R. Foulquie-Moreno, A. Goovaerts, K. Souvereinys, L. Clement, F. Dumortier & J.M. Thevelein, (2012) Identification of novel causative genes determining the complex trait of high ethanol tolerance in yeast using pooled-segregant whole-genome sequence analysis. *Genome Res* **22**: 975-984.

Takano, E., H.C. Gramajo, E. Strauch, N. Andres, J. White & M.J. Bibb, (1992) Transcriptional regulation of the *redD* transcriptional activator gene accounts for growth-phase-dependent production of the antibiotic undecylprodigiosin in *Streptomyces coelicolor* A3(2). *Molecular Microbiology* **6**: 2797–2804.

Tamura, S., Y. Park, M. Toriyama & M. Okabe, (1997) Change of mycelial morphology in tylosin production by batch culture of *Streptomyces fradiae* under various shear conditions. *Journal of Fermentation and Bioengineering* **83**: 523-528.

Tenconi, E., S. Jourdan, P. Motte, M.-J. Virolle & S. Rigali, (2012) Extracellular sugar phosphates are assimilated by *Streptomyces* in a PhoP-dependent manner. *Antonie van Leeuwenhoek* **102**: 425-433.

Thomaides, H.B., M. Freeman, M. El Karoui & J. Errington, (2001) Division site selection protein DivIVA of *Bacillus subtilis* has a second distinct function in chromosome segregation during sporulation. *Genes & development* **15**: 1662-1673.

Thomas, L., D.A. Hodgson, A. Wentzel, K. Nieselt, T.E. Ellingsen, J. Moore, E.R. Morrissey, R. Legaie, W. Wohlleben, A. Rodríguez-García, J.F. Martín, N.J. Burroughs, E.M.H. Wellington & M.C.M. Smith, (2012) Metabolic switches and adaptations deduced from the proteomes of *Streptomyces coelicolor* wild type and *phoP* mutant grown in batch culture. *Molecular & Cellular Proteomics* **11**.

Thompson, J.D., T. Gibson & D.G. Higgins, (2002) Multiple sequence alignment using ClustalW and ClustalX. *Current protocols in bioinformatics*: 2.3. 1-2.3. 22.

Titgemeyer, F., J. Walkenhorst, J. Reizer, M.H. Stuiver, X. Cui & M.H. Saier Jr, (1995) Identification and characterization of phosphoenolpyruvate: fructose phosphotransferase systems in three *Streptomyces* species. *Microbiology* **141**: 51-58.



- Tokiwa, Y. & B. Calabia, (2004) Degradation of microbial polyesters. *Biotechnology letters* **26**: 1181.
- Tough, A.J. & J.I. Prosser, (1996) Experimental verification of a mathematical model for pelleted growth of *Streptomyces coelicolor* A3(2) in submerged batch culture. *Microbiology* **142**: 639-648.
- Traag, B.A. & G.P. Wezel, (2008) The SsgA-like proteins in actinomycetes: small proteins up to a big task. *Antonie van Leeuwenhoek* **94**: 85-97.
- Tschowri, N., M.A. Schumacher, S. Schlimpert, N. babu Chinnam, K.C. Findlay, R.G. Brennan & M.J. Buttner, (2014) Tetrameric c-di-GMP mediates effective transcription factor dimerization to control *Streptomyces* development. *Cell* **158**: 1136-1147.
- Ueda, K., K. Endo, H. Takano, M. Nishimoto, Y. Kido, Y. Tomaru, K. Matsuda & T. Beppu, (2000) Carbon-source-dependent transcriptional control involved in the initiation of cellular differentiation in *Streptomyces griseus*. *Antonie Van Leeuwenhoek* **78**: 263-268.
- van't Riet, K. & J. Tramper, (1991) *Basic bioreactor design*. CRC Press.
- van den Berg, M.A., R. Albang, K. Albermann, J.H. Badger, J.M. Daran, A.J. Driessen, C. Garcia-Estrada, N.D. Fedorova, D.M. Harris, W.H. Heijne, V. Joardar, J.A. Kiel, A. Kovalchuk, J.F. Martin, W.C. Nierman, J.G. Nijland, J.T. Pronk, J.A. Roubos, I.J. van der Klei, N.N. van Peij, M. Veenhuis, H. von Dohren, C. Wagner, J. Wortman & R.A. Bovenberg, (2008) Genome sequencing and analysis of the filamentous fungus *Penicillium chrysogenum*. *Nat Biotechnol* **26**: 1161-1168.
- van Dissel, D., D. Claessen, M. Roth & G.P. van Wezel, (2015) A novel locus for mycelial aggregation forms a gateway to improved *Streptomyces* cell factories. *Microbial Cell Factories* **14**: 44.
- van Dissel, D., D. Claessen & G.P. van Wezel, (2014) Morphogenesis of *Streptomyces* in submerged cultures. *Adv Appl Microbiol* **89**: 1-45.
- van Keulen, G., H.M. Jonkers, D. Claessen, L. Dijkhuizen & H.A. Wösten, (2003) Differentiation and anaerobiosis in standing liquid cultures of *Streptomyces coelicolor*. *Journal of bacteriology* **185**: 1455-1458.
- van Veluw, G.J., M.L. Petrus, J. Gubbens, R. de Graaf, I.P. de Jong, G.P. van Wezel, H.A. Wosten & D. Claessen, (2012) Analysis of two distinct mycelial populations in liquid-grown *Streptomyces* cultures using a flow cytometry-based proteomics approach. *Appl Microbiol Biotechnol* **96**: 1301-1312.
- van Wezel, G.P., P. Krabben, B.A. Traag, B.J.F. Keijser, R. Kerste, E. Vijgenboom, J.J. Heijnen & B. Kraal, (2006) Unlocking *Streptomyces* spp. for use as sustainable industrial production platforms by morphological engineering. *Appl. Environ. Microbiol.* **72**: 5283-5288.
- van Wezel, G.P. & K.J. McDowall, (2011) The regulation of the secondary metabolism of *Streptomyces*: new links and experimental advances. *Natural product reports* **28**: 1311-1333.
- van Wezel, G.P., N.L. McKenzie & J.R. Nodwell, (2009) Applying the genetics of secondary metabolism

- in model actinomycetes to the discovery of new antibiotics. *Methods in enzymology* **458**: 117-141.
- van Wezel, G.P., J. van der Meulen, S. Kawamoto, R.G.M. Luiten, H.K. Koerten & B. Kraal, (2000a) *ssgA* is essential for sporulation of *Streptomyces coelicolor* A3(2) and affects hyphal development by stimulating septum formation. *J. Bacteriol.* **182**: 5653-5662.
- van Wezel, G.P., J. White, G. Hoogvliet & M.J. Bibb, (2000b) Application of *redD*, the transcriptional activator gene of the undecylprodigiosin biosynthetic pathway, as a reporter for transcriptional activity in *Streptomyces coelicolor* A3(2) and *Streptomyces lividans*. *Journal of Molecular Microbiology and Biotechnology* **2**: 551-556.
- Vara, J., M. Lewandowska-Skarbek, Y.G. Wang, S. Donadio & C.R. Hutchinson, (1989) Cloning of genes governing the deoxysugar portion of the erythromycin biosynthesis pathway in *Saccharopolyspora erythraea* (*Streptomyces erythreus*). *J Bacteriol* **171**: 5872-5881.
- Vecht-Lifshitz, S.E., S. Magdassi & S. Braun, (1989) Effects of surface active agents on pellet formation in submerged fermentations of *Streptomyces tendae*. *Journal of Dispersion Science and Technology* **10**: 265-275.
- Vecht-Lifshitz, S.E., S. Magdassi & S. Braun, (1990) Pellet formation and cellular aggregation in *Streptomyces tendae*. *Biotechnology and Bioengineering* **35**: 890-896.
- Vlamakis, H., Y. Chai, P. Beauregard, R. Losick & R. Kolter, (2013) Sticking together: building a biofilm the *Bacillus subtilis* way. *Nature Reviews Microbiology* **11**: 157-168.
- Vrancken, K. & J. Anne, (2009) Secretory production of recombinant proteins by *Streptomyces*. *Future Microbiology* **4**: 181-188.
- Vuong, C., S. Kocianova, J.M. Voyich, Y. Yao, E.R. Fischer, F.R. DeLeo & M. Otto, (2004) A crucial role for exopolysaccharide modification in bacterial biofilm formation, immune evasion, and virulence. *Journal of Biological Chemistry* **279**: 54881-54886.
- Walker, R., C. Ferguson, N. Booth & E. Allan, (2002) The symbiosis of *Bacillus subtilis* L-forms with Chinese cabbage seedlings inhibits conidial germination of *Botrytis cinerea*. *Letters in applied microbiology* **34**: 42-45.
- Wang, C.-M. & D.E. Cane, (2008) Biochemistry and molecular genetics of the biosynthesis of the earthy odorant methylisoborneol in *Streptomyces coelicolor*. *Journal of the American Chemical Society* **130**: 8908-8909.
- Wang, X., J.F. Preston, 3rd & T. Romeo, (2004) The *pgaABCD* locus of *Escherichia coli* promotes the synthesis of a polysaccharide adhesin required for biofilm formation. *J Bacteriol* **186**: 2724-2734.
- Wardell, J.N., S.M. Stocks, C.R. Thomas & M.e. Bushell, (2002) Decreasing the hyphal branching rate of *Saccharopolyspora erythraea* NRRL 2338 leads to increased resistance to breakage and increased



antibiotic production. *Biotechnology and Bioengineering* **78**: 141–146.

Wargenau, A., A. Fleißner, C.J. Bolten, M. Rohde, I. Kampen & A. Kwade, (2011) On the origin of the electrostatic surface potential of *Aspergillus niger* spores in acidic environments. *Research in microbiology* **162**: 1011-1017.

Wargenau, A., I. Kampen & A. Kwade, (2013) Linking aggregation of *Aspergillus niger* spores to surface electrostatics: a theoretical approach. *Biointerphases* **8**: 1-12.

Waterhouse, R., H. Buhariwalla, D. Bourn, E. Rattray & L. Glover, (1996) CCD detection of lux-marked *Pseudomonas syringae* pv. *phaseolicola* L-forms associated with Chinese cabbage and the resulting disease protection against *Xanthomonas campestris*. *Letters in applied microbiology* **22**: 262-266.

White, S., M. McIntyre, D.R. Berry & B. McNeil, (2002) The Autolysis of Industrial Filamentous Fungi. *Critical Reviews in Biotechnology* **22**: 1-14.

Wildermuth, H., (1970) Development and organization of the aerial mycelium in *Streptomyces coelicolor*. *Microbiology* **60**: 43-50.

Wilking, J.N., V. Zaburdaev, M. De Volder, R. Losick, M.P. Brenner & D.A. Weitz, (2013) Liquid transport facilitated by channels in *Bacillus subtilis* biofilms. *Proceedings of the National Academy of Sciences* **110**: 848-852.

Willemse, J., J.W. Borst, E. de Waal, T. Bisseling & G.P. van Wezel, (2011) Positive control of cell division: FtsZ is recruited by SsgB during sporulation of *Streptomyces*. *Genes & Development* **25**: 89 -99.

Willemse, J., B. Ruban-Ośmiałowska, D. Widdick, K. Celler, M.I. Hutchings, G.P. van Wezel & T. Palmer, (2012) Dynamic localization of Tat protein transport machinery components in *Streptomyces coelicolor*. *Journal of bacteriology* **194**: 6272-6281.

Wimpenny, J., W. Manz & U. Szewzyk, (2000) Heterogeneity in biofilms. *FEMS Microbiology Reviews* **24**: 661-671.

Winter, N., J.A. Triccas, B. Rivoire, M.C.V. Pessolani, K. Eiglmeier, E.M. Lim, S.W. Hunter, P.J. Brennan & W.J. Britton, (1995) Characterization of the gene encoding the immunodominant 35 kDa protein of *Mycobacterium leprae*. *Molecular microbiology* **16**: 865-876.

Wolński, M., R. Wali, E. Tilley, D. Jakimowicz, J. Zakrzewska-Czerwińska & P. Herron, (2011) Replisome trafficking in growing vegetative hyphae of *Streptomyces coelicolor* A3 (2). *Journal of bacteriology* **193**: 1273-1275.

Wood, P.J., (1980) Specificity in the interaction of direct dyes with polysaccharides. *Carbohydrate research* **85**: 271-287.

Worlitzsch, D., R. Tarran, M. Ulrich, U. Schwab, A. Cekici, K.C. Meyer, P. Birrer, G. Bellon, J. Berger & T. Weiss, (2002) Effects of reduced mucus oxygen concentration in airway *Pseudomonas* infections of

cystic fibrosis patients. *The Journal of clinical investigation* **109**: 317-325.

Wösten, H.A., (2001) Hydrophobins: multipurpose proteins. *Annual Reviews in Microbiology* **55**: 625-646.

Wösten, H.A. & J.M. Willey, (2000) Surface-active proteins enable microbial aerial hyphae to grow into the air. *Microbiology* **146**: 767-773.

Wu, L.J. & J. Errington, (2012) Nucleoid occlusion and bacterial cell division. *Nature Reviews Microbiology* **10**: 8-12.

Wucherpennig, T., T. Hestler & R. Krull, (2011) Morphology engineering-Osmolality and its effect on *Aspergillus niger* morphology and productivity. *Microbial cell factories* **10**: 1.

Wucherpennig, T., K.A. Kiep, H. Driouch, C. Wittmann & R. Krull, (2010) Morphology and rheology in filamentous cultivations. In.: Academic Press, pp. 89-136.

Xu, H., K.F. Chater, Z. Deng & M. Tao, (2008) A cellulose synthase-like protein involved in hyphal tip growth and morphological differentiation in *Streptomyces*. *J Bacteriol* **190**: 4971-4978.

Xu, Q., B.A. Traag, J. Willemse, D. McMullan, M.D. Miller, M.-A. Elslinger, P. Abdubek, T. Astakhova, H.L. Axelrod, C. Bakolitsa, D. Carlton, C. Chen, H.-J. Chiu, M. Chruszcz, T. Clayton, D. Das, M.C. Deller, L. Duan, K. Ellrott, D. Ernst, C.L. Farr, J. Feuerhelm, J.C. Grant, A. Grzechnik, S.K. Grzechnik, G.W. Han, L. Jaroszewski, K.K. Jin, H.E. Klock, M.W. Knuth, P. Kozbial, S.S. Krishna, A. Kumar, D. Marciano, W. Minor, A.M. Mommaas, A.T. Morse, E. Nigoghossian, A. Nopakun, L. Okach, S. Oommachen, J. Paulsen, C. Puckett, R. Reyes, C.L. Rife, N. Sefcovic, H.J. Tien, C.B. Trame, H. van den Bedem, S. Wang, D. Weekes, K.O. Hodgson, J. Wooley, A.M. Deacon, A. Godzik, S.A. Lesley, I.A. Wilson & G.P. van Wezel, (2009) Structural and functional characterizations of SsgB, a conserved activator of developmental cell division in morphologically complex actinomycetes. *The Journal of Biological Chemistry* **284**: 25268-25279.

Yagüe, P., A. Rodríguez-García, M.T. López-García, B. Rioseras, J.F. Martín, J. Sánchez & A. Manteca, (2014) Transcriptomic analysis of liquid non-sporulating *Streptomyces coelicolor* cultures demonstrates the existence of a complex differentiation comparable to that occurring in solid sporulating cultures. *PLoS ONE* **9**: e86296.

Yamazaki, H., Y. Ohnishi & S. Horinouchi, (2003) Transcriptional switch on of *ssgA* by A-factor, which is essential for spore septum formation in *Streptomyces griseus*. *Journal of bacteriology* **185**: 1273-1283.

Yang, H., R. King, U. Reichl & E.D. Gilles, (1992) Mathematical model for apical growth, septation, and branching of mycelial microorganisms. *Biotechnology and Bioengineering* **39**: 49-58.

Yegneswaran, P.K., M.R. Gray & B.G. Thompson, (1991) Effect of dissolved oxygen control on growth and antibiotic production in *Streptomyces clavuligerus* fermentations. *Biotechnology Progress* **7**: 246-250.



Yikmis, M. & A. Steinbüchel, (2012) Historical and recent achievements in the field of microbial degradation of natural and synthetic rubber. *Applied and environmental microbiology* **78**: 4543-4551.

Yin, P., Y.-H. Wang, S.-L. Zhang, J. Chu, Y.-P. Zhuang, N. Chen, X.-F. Li & Y.-B. Wu, (2008) Effect of mycelial morphology on bioreactor performance and avermectin production of *Streptomyces avermitilis* in submerged cultivations. *Journal of the Chinese Institute of Chemical Engineers* **39**: 609-615.

Zacchetti, B., J. Willemse, B. Recter, D. van Dissel, G. van Wezel, H. Wosten & D. Claessen, (2016) Aggregation of germlings is a major contributing factor towards mycelial heterogeneity of *Streptomyces*. *Scientific reports*: In press.

Zhu, H., J. Swierstra, C. Wu, G. Girard, Y.H. Choi, W. van Wamel, S.K. Sandiford & G.P. van Wezel, (2014) Eliciting antibiotics active against the ESKAPE pathogens in a collection of actinomycetes isolated from mountain soils. *Microbiology* **160**: 1714-1725.

Zogaj, X., W. Bokranz, M. Nimtz & U. Römling, (2003) Production of cellulose and curli fimbriae by members of the family *Enterobacteriaceae* isolated from the human gastrointestinal tract. *Infection and immunity* **71**: 4151-4158.



C

Curriculum vitae

Marius Dino van Dissel was born on the 5th of March 1985 in Amsterdam, the Netherlands. In 2003 he graduated from the Barlaeus Gymnasium in Amsterdam. In September of the same year he started his Life Science & Technology study, a shared program of the Leiden University and Delft University of Technology focused on genomics and biotechnology. He finished his Bachelor program in 2008 with a research internship on competitive chemostats with yeast in the group of Prof. dr. J. Pronk under the supervision of dr. L. Hazelwood. After obtaining his bachelor's degree he continued with the master program of Life Science & Technology with a major in bioprocess engineering. As part of his program he conducted an industrial internship at Mascoma, NH, USA where he developed a screening method for cellulase secretion in baker's yeast. A second internship under the supervision of dr. T. Veiga took place in the group of Prof. dr. J. Pronk, where he investigated the response of *Penicillium chrysogenum* in co-cultivation with *B. subtilis*. He obtained his Master degree in March 2011. The same year in June he started his PhD under the supervision of Prof. dr. G.P. van Wezel. The work done as PhD student is described in this thesis. Currently Dino is continuing to work with streptomycetes as a Postdoc in the same group, within the frame work of the EU project SysterAct.



P

Publications

van Dissel, D., Claessen, D., Roth, M. and van Wezel, G.P., 2015. A novel locus for mycelial aggregation forms a gateway to improved *Streptomyces* cell factories. *Microbial cell factories*, **14**(1), p.1.

van Dissel, D., Claessen, D. and van Wezel, G.P., 2014. Morphogenesis of *Streptomyces* in submerged cultures. *Adv. Appl. Microbiol*, **89**, pp.1-45.

Zacchetti, B., Willemse, J., Recter, B., van Dissel, D., van Wezel, G.P., Wösten, H.A.B. and Claessen, D., 2016. Aggregation of germlings is a major contributing factor towards mycelial heterogeneity of *Streptomyces*. *Scientific reports*, **6**, p.27045.

Bajaj, I., Veiga, T., van Dissel, D., Pronk, J.T. and Daran, J.M., 2014. Functional characterization of a *Penicillium chrysogenum* mutanase gene induced upon co-cultivation with *Bacillus subtilis*. *BMC microbiology*, **14**(1), p.1.

